

**SELF-ASSEMBLING MULTIENZYME SYSTEMS AT OIL-  
WATER INTERFACE FOR BIPHASIC  
BIOTRANSFORMATIONS**

**A DISSERTATION  
SUBMITTED TO THE FACULTY OF GRADUATE SCHOOL  
OF THE UNIVERSITY OF MINNESOTA  
BY**

**RAVINDRABHARATHI NARAYANAN**

**IN PARTIAL FULFILLMENT OF THE REQUIREMENTS  
FOR THE DEGREE OF  
DOCTOR OF PHILOSOPHY**

**PING WANG, ADVISER**

**NOVEMBER 2008**

**© RAVINDRABHARATHI NARAYANAN, NOVEMBER 2008**

## ACKNOWLEDGEMENTS

I would like to acknowledge faculty, friends and family members that have helped me during my doctoral work. Firstly, I would like to thank my adviser, Dr. Ping Wang, for his elaborate guidance and commitment. Throughout my doctoral work he encouraged me to develop independent thinking and research skills. He continually stimulated my analytical thinking and greatly assisted me with financial support for the entire period of my Ph.D. work.

I am very grateful for having an exceptional doctoral committee and wish to thank Dr. Romas Kazlauskas, Dr. Shri Ramaswamy, and Dr. Roger Ruan for their continual support, encouragement and valuable suggestions. I am also indebted to the department of Chemical Engineering and Dr. Darrell Reneker at The University of Akron, where part of my Ph.D. work involving enzyme stability and nanofibers were carried out, before our lab moved to University of Minnesota.

I wish to thank Dr. Benjamin Stottrup for allowing me to use his lab and equipment for the surface pressure analysis work, Mr. Mark Sanders, Dr. John Thomas, and Dr. Bruce Maskowitz for helping with different characterization studies. I am extremely grateful for the assistance of Mr. Geoffrey Harms and Mr. Al Knutson for helping me with construction of different reactors and equipments.

I owe a special note of gratitude to all my colleagues and friends, especially Dr. Guangyu Zhu, Ms. Liang Liao, Mr. Songtao Wu and Dr. Xiaodong Tong for their assistance in different projects. I extend many thanks to Ms. Dorit Hafner and Ms. Lisa Wiley for their assistance throughout my graduate studies.

## **ABSTRACT**

Living cells are highly organized with many functional units or organelles separated by membranes. The membrane is comprised of specific proteins and lipid components that enable it to perform its unique roles for that cell or organelle. At cellular membranes, lipid bilayers are stabilized laterally with the help of integral proteins. This stability is provided through a clustering of the hydrophobic core of both the lipid bilayer and the integral protein. Surface and interfacial phenomenon involving the activities of enzymes are wide spread in cellular systems and occur within the interfacial constraints of substrate accessibility, distribution and partitioning. Similar mechanisms can be used to enhance productivity of industrial biotransformations at oil-water interface. Detailed study and manipulation of interfacial enzyme catalysis is of great interest for biotechnology, chemical technology, biology, and offers new opportunities in protein and polymer chemistry, separation science, bio-renewable products, environmental science and waste minimization.

Herein, novel self-assembling enzyme systems were developed by manipulation of microenvironment of the enzymes for interfacial biotransformations at oil-water interface. The enzyme molecules were modified to self-assemble at oil-water interface by conjugation with hydrophobic moieties like polymers. The present work focused on (i) characterization of enzyme assembly morphology, (ii) stabilizing the enzymes at the interface, (iii) broadening the scope of interfacial biocatalysis with multienzyme-cofactor system and developing method to assemble cofactors at the interface, (iv) investigating the kinetic parameters of the interfacial reaction, (v) improving the activity of interfacial

enzyme by interfacial mobility enhancement and (vi) extending the hydrophobic manipulation of enzyme's microenvironment for development of biosensors based on nanofibers containing organic soluble enzymes. Four sets of model reactions system, a single enzyme system and three multiple enzyme system was employed for interfacial biocatalysis study and oxidation of glucose by glucose oxidase was chosen as a model system for biosensor development.

In a previous study, it was demonstrated that interface-assembled enzymes improved the reaction rate by two orders of magnitude. As a part of the present work, the important role of mobility and the assembly morphology of the interface-assembled enzyme on regulating the enzymatic liquid membrane fluidity at the interface were investigated. To characterize the surface assembly morphology of the interface-assembled enzyme by surface pressure analysis, Langmuir film balance was used. The resulting surface pressure isotherm exhibited monolayer assembly, with intramolecular rearrangement of the interface-assembled enzymes. The mobility of the novel interface-assembled enzymes was evaluated by using fluorescence recovery after photobleaching technique that gave the diffusion coefficient of  $6.7 \times 10^{-10} \text{ cm}^2/\text{sec}$ , three orders of magnitude less than that of native enzymes in aqueous solution, due to localization of the modified enzyme at the interface.

Though modification of enzymes with polymer for interfacial assembly reduced its mobility, the conjugation of polymer to enzyme stabilized the enzymes against interfacial denaturation. The polymer stabilizes the three dimensional structure of enzymes and prevent it from unfolding at hydrophobic interfaces. Apart from the

interfacial stabilization of interface-assembled enzyme by polymer, the localization of enzymes at the interface offered a unique opportunity to enhance the stability of the enzymes against the deactivation effect of compounds in bulk phase. Chloroperoxidase (CPO) was chosen as a model enzyme to explore the factors that determine the stability of interface-assembled enzymes. Although the interface-assembled CPO showed improved stability as compared to native CPO, enzyme deactivation by peroxide reactants like hydrogen peroxide ( $\text{H}_2\text{O}_2$ ) in the bulk phase, still limited the overall productivity of the enzyme. Two approaches to further improve the stability of interface-assembled CPO were examined in this work. In one approach, several chemical stabilizers were used to prevent highly reactive intermediates from oxidizing the porphyrin ring active site of CPO; polyethylene glycol (PEG) was found exceptional in that it increased both the operational and storage stability of CPO with a productivity increase of 57%, an operational stability improvement by almost 2 folds and a storage stability of 60% activity retention after 24 hours incubation in 1 mM  $\text{H}_2\text{O}_2$ . On the other hand, glucose enhanced the operational stability by 2 folds, but exhibited no significant effect on storage stability. While in a second approach, *in situ* generation of hydrogen peroxide ( $\text{H}_2\text{O}_2$ ) by using glucose oxidase (GOx) to keep  $\text{H}_2\text{O}_2$  concentration low was applied. It was found that the combined effect of presence of glucose and lowered concentration of  $\text{H}_2\text{O}_2$ , extended operational lifetime to 60 minutes for CPO with *in situ* generation of  $\text{H}_2\text{O}_2$  by GOx.

To expand the scope of interfacial enzyme catalysis, multienzyme oxidoreductases-cofactor systems were employed. The structure of cofactors involves

unique combination of functional groups that are required by oxidoreductases enzymes to carry out biotransformations and any modification to cofactor for interfacial assembly should not affect the enzyme-cofactor interaction. The challenge of modifying cofactors to assemble at the interface was overcome by structural manipulation of the adenine group of nicotinamide cofactor. The synthesis of interface-assembled cofactor gave a process yield of 67%, the modified cofactor was highly stable with a continuous operation of 2150 hours and turnover number of 2617 for a biphasic reaction involving reduction of acetophenone in organic phase and oxidation of glucose in aqueous phase. The Damkohler number that gives the ratio between reaction rate and mass transfer rate was obtained to be 0.12 with interface assembled cofactor, compared to 87.5 with native enzymes and free cofactor, indicating mass transfer limitations with interface assembled cofactor. The kinetic analysis of interface-assembled cofactor gave the binding resistance of enzyme to cofactor at the interface,  $K_c$ , as 0.18 mM compared to 0.03 mM of native enzyme and free cofactor, which indicated that limited interfacial interaction between molecules and two-dimensional mobility of the enzymes contributed significant resistance towards interfacial reaction.

A novel mechanism of nanostirring was developed to improve the two-dimensional mobility of interface-assembled enzymes. Iron oxide ( $\text{Fe}_3\text{O}_4$ ) superparamagnetic nanoparticles were coupled with polymer conjugated enzymes for interfacial assembling and applied to improve the mobility of the interface-assembled enzyme under external electromagnetic field. The enhanced mobility of the interface-assembled enzymes was quantified through fluorescent microscopic visualization, and

enabled over 600% of improvement in the observed reaction rate for both single enzyme and multienzyme systems as compared to reactions in the absence of the magnetic field.

The combination of slow reactions and denaturation of dehydrogenase enzymes due to stirring posed a major constraint for realizing reactions with configuration of both cofactor and enzymes assembled at the interface. This limitation was overcome by development of a unique interfacial biotransformation with interface assembled cofactor and interface-assembled multiple enzymes was realized by employing relatively shear resistant dehydrogenase, ADH RS1, coupled with GluDH for faster NADH turnover. A maximum NADH turnover of 13 was achieved by optimizing the reaction conditions enzyme ratio, organic phase and aqueous phase substrates concentrations, and polymer modifier concentration added during modification of enzymes.

In another effort, the manipulation of microenvironment of enzymes for enhanced hydrophobicity was extended to develop completely organic-soluble enzymes. The organic soluble enzymes were utilized in the development of polymer-enzyme composite nanofibers for biosensing applications. Polyurethane nanofibers of diameters of 100-140 nm containing up to 20% (w/w) protein were prepared via electrospinning. The enzyme, glucose oxidase (GOx), was complexed with an ionic surfactant and was thus transformed into organic soluble prior to electrospinning. When examined for biosensor applications, such prepared nanofibers showed a sensitivity of up to  $66 \text{ A M}^{-1} \text{ mg-enzyme}^{-1}$  (or  $0.39 \text{ A M}^{-1} \text{ cm}^{-2}$ ), 100 times improvement from previous studies. The high enzyme loading coupled with the high specific surface area of the nanofibers enhanced the reaction kinetics and thus enabled strong responses for small changes in glucose



concentration. The confinement of the enzyme within the body of nanofibers also stabilized the enzyme, such that the biosensor retained 80% of its sensitivity after 70 days.

The interface-assembled enzymes with their improved interfacial stability can substitute soluble enzymes that are presently used for many industrial applications with biphasic systems. Also, Interface-assembled enzymes offer simultaneous access to reactants in both the bulk phases across the interface and thus improve the overall efficiency for the biotransformations between immiscible chemicals. The novel polymer-enzyme conjugates and functional materials that were developed through this research with their unique structural, magnetic and mechanical properties can be used in broad range of applications like sensors, membrane technology, generate alternative strategies for encapsulation and delivery of therapeutic agents, and will enable minimum downstream processing for specialty chemical synthesis. The present work is of great interest in the search for production of different important industrial chemicals including bio-renewable products and for sustainable environmental quality.

# TABLE OF CONTENTS

	<b>Page</b>
LIST OF TABLES.....	xii
LIST OF FIGURES.....	xiii
<b>CHAPTER</b>	
I INTRODUCTION .....	1
1.1 Research objectives .....	7
1.2 Approach .....	7
1.3 Outline .....	14
II BACKGROUND .....	15
2.1 Enzymatic biocatalysis .....	15
2.2 Non-traditional enzyme catalysis .....	16
2.2.1 Immobilization of enzymes.....	18
2.2.2 Chemical modifications of enzymes.....	20
2.3 Enzymatic catalysis in biphasic system.....	23
2.4 Interfacial biocatalysis.....	24
2.5 Multi enzyme biocatalysis with cofactor regeneration.....	26
2.6 Electrospun nanofibers for biosensors .....	28
III INTERFACIAL ASSEMBLY AND CHARACTERIZATION OF ENZYMES AT OIL-WATER INTERFACE.....	33
3.1 Introduction .....	33
3.2 Materials and Methods .....	34
3.2.1 Chemicals.....	34
3.2.2 Enzyme modification.....	35
3.2.3 Protein Content Measurement .....	35
3.2.4 Interfacial Surface Pressure Analysis.....	36
3.2.5 Fluorescence Recovery after Photobleaching .....	37
3.3 Results and Discussions .....	38
3.3.1 Interfacial assembly of the enzyme .....	38
3.3.2 Surface pressure analysis of interface assembled enzyme.....	39

3.3.3	Molecular diffusion measurements using fluorescence recovery .....	43
3.4	Conclusion.....	46
IV	STABILIZATION OF INTERFACE-BINDING CHLOROPEROXIDASE FOR INTERFACIAL BIOTRANSFORMATION.....	47
4.1	Introduction .....	47
4.2	Materials and Methods .....	49
4.2.1	Chemicals.....	49
4.2.2	Modification of enzymes.....	50
4.2.3	Styrene epoxidation by chloroperoxidase.....	51
4.2.4	GC analysis of styrene epoxides .....	52
4.2.5	Pretreatment for stabilizer addition.....	53
4.3	Results and Discussions .....	53
4.3.1	Effect of stabilizers on operation stabilities of native and PS- conjugated CPO.....	53
4.3.2	Effect of stabilizers on storage stabilities of native and PS-conjugated CPO.....	56
4.3.3	Enzyme stabilization via <i>in situ</i> generation of H <sub>2</sub> O <sub>2</sub> .....	59
4.4	Conclusion.....	62
V	SYNTHESIS OF INTERFACE-BINDING COFACTORS FOR BIOTRANSFORMATIONS ACROSS OIL-WATER INTERFACES.....	63
5.1	Introduction .....	63
5.2	Materials and Methods .....	65
5.2.1	Chemicals.....	65
5.2.2	Preparation of interface assembled Cofactor.....	66
5.2.3	Interfacial reactions.....	67
5.2.4	GC analysis .....	67
5.3	Results and Discussions .....	68
5.3.1	Interfacial assembly of cofactors .....	69
5.3.2	Characterization of interface-assembled cofactors.....	72
5.3.3	Activity and stability of interface-assembled cofactors .....	74
5.3.4	Kinetic study of cofactor turnover at the interface .....	85

5.4	Conclusion.....	96
<b>VI</b>	<b>NANOSTIRRING OF MAGNETIC INTERFACIAL ENZYME FOR ENHANCEMENT OF INTERFACIAL BIOTRANSFORMATIONS.....</b>	<b>97</b>
6.1	Introduction .....	97
6.2	Materials and methods.....	99
6.2.1	Chemicals.....	99
6.2.2	Synthesis of magnetic nanoparticles.....	100
6.2.3	Interface assembly of magnetic nanoparticles.....	100
6.2.4	Epoxidation of styrene.....	101
6.2.5	Multienzyme reaction system with cofactor regeneration .....	102
6.2.6	GC analysis .....	102
6.2.7	External magnetic field production.....	103
6.2.8	Optical microscopy for enzyme mobility visualization .....	103
6.2.9	Characterization of MLM .....	104
6.3	Results and Discussion.....	104
6.3.1	Interfacial assembly of bioactive magnetic nanoparticles .....	104
6.3.2	Characterization of MLM .....	105
6.3.3	Fabrication of alternating electromagnetic field generator.....	109
6.3.4	Visualization of mobility of MLM at interface.....	112
6.3.5	Nanostirring effect on interface-assembled enzyme's activity .....	115
6.3.6	Effect of nanostirring on native enzyme's activity .....	122
6.4	Conclusion.....	124
<b>VII</b>	<b>MULTIENZYMATIC REACTIONS AT THE INTERFACE WITH BOTH ENZYME AND COFACTOR ASSEMBLED AT THE INTERFACE.....</b>	<b>125</b>
7.1	Introduction .....	125
7.2	Materials and Methods .....	126
7.2.1	Chemicals.....	126
7.2.2	Enzyme modification for interfacial assembly.....	127
7.2.3	Cofactor modification for interfacial assembly.....	127
7.2.4	Interfacial reaction .....	127

7.2.5 GC analysis .....	128
7.3 Results and Discussions .....	128
7.3.1 Reaction system.....	128
7.3.2 Effect of polymer modifier .....	130
7.3.3 Effect of substrate concentrations .....	132
7.3.4 Effect of enzyme ratio .....	134
7.4 Conclusion.....	135
VIII ENZYME-POLYMER COMPOSITE NANOFIBERS WITH HIGH ENZYME LOADINGS FOR USE AS BIOSENSORS .....	136
8.1 Introduction .....	136
8.2 Materials and materials .....	138
8.2.1 Chemicals.....	138
8.2.2 Solubilization of Glucose Oxidase in organic solvent .....	138
8.2.3 Electrospinning.....	139
8.2.4 Enzyme Activity.....	139
8.2.5 Enzyme Stability in Organic Solvent .....	140
8.2.6 Electrochemical experiments.....	140
8.3 Results and Discussions .....	141
8.3.1 Solubilization of GOx in organic solvent .....	141
8.3.2 Electrospinning of solubilized GOx .....	143
8.3.3 Use of NEM as biosensor.....	147
8.4 Conclusion.....	153
IX CONCLUSIONS AND PATH AHEAD .....	154
9.1 Summary .....	154
9.2 Future work .....	161
BIBLIOGRAPHY.....	163
APPENDIX.....	187

## List of Tables

<b>Table</b>		<b>Page</b>
Table 2-1	Historical landmarks in the development of glucose biosensors .....	31
Table 4-1	Effect of stabilizer on native CPO productivity.....	54
Table 4-2	Effect of stabilizer on Interface-binding CPO productivity.....	56
Table 5-1	Kinetic parameters of reaction system involving ADH LB and GluDH with NADPH as cofactor. ....	95
Table 8-1	Effect of enzyme loading and weight (based on electrospinning time) of nanofibrous enzyme activity .....	148
Table 8-2	Performance of NEM with 20 % (w/w) enzyme as glucose biosensor. ....	151

## List of Figures

Figure		Page
Figure 3-1	Interfacial assembly of PS-ADH conjugate .....	39
Figure 3-2	Schematic of Langmuir trough set-up for surface pressure analysis .....	40
Figure 3-3	Surface pressure isotherm of interface-assembled ADH RS1 .....	41
Figure 3-4	Effect of varying degree of rinse on interface-assembled ADH RS1's surface pressure isotherm. ....	42
Figure 3-5	FRAP analysis on interface assembled ADH RS1 .....	44
Figure 3-6	Quantitative FRAP data for evaluating diffusion coefficient .....	45
Figure 4-1	Storage stability of native CPO with 1 mM H <sub>2</sub> O <sub>2</sub> .....	58
Figure 4-2	Storage stability of PS-CPO with 1 mM H <sub>2</sub> O <sub>2</sub> .....	59
Figure 4-3	Time course of styrene epoxidation catalyzed by native CPO with <i>in situ</i> generation of H <sub>2</sub> O <sub>2</sub> .....	61
Figure 4-4	Time course of styrene epoxidation catalyzed by PS-CPO with <i>in situ</i> generation of H <sub>2</sub> O <sub>2</sub> .....	61
Figure 5-1	Synthesis of interface-assembled cofactor .....	71
Figure 5-2	X-ray photoelectron spectroscopy spectral analysis .....	73
Figure 5-3	Multienzymatic reactions with potential importance for interface- assembled cofactors .....	75
Figure 5-4	Theoretical predicted Gibbs free energy .....	77
Figure 5-5	pH dependency of enzyme's activity in reaction system 1 with NADH/NAD <sup>+</sup> as cofactor .....	78
Figure 5-6	Initial reaction rate of reduction of acetophenone by ADH RS1 with simultaneous oxidation of glycerol by GDH .....	79
Figure 5-7	Cofactor turnover for the multienzyme reaction system involving reduction of acetophenone by ADH RS1 with simultaneous oxidation of glycerol by GDH .....	80

Figure 5-8	pH dependency of enzyme's activity in reaction system 2 with NADPH/NADP <sup>+</sup> as cofactor .....	81
Figure 5-9	Initial reaction rate of reduction of acetophenone by ADH LB with simultaneous oxidation of glucose by GluDH.....	82
Figure 5-10	Sustainable reuse of interface assembled NADPH.....	83
Figure 5-11	Cofactor turnover or number of regeneration for the multienzyme reaction system involving reduction of acetophenone by ADH LB with simultaneous oxidation of glucose by GluDH.....	84
Figure 5-12	General scheme of interfacial reaction .....	85
Figure 5-13	Relations of a complete set of equilibriums that define the primary parameters of the catalytic turnover cycle at the interface. ....	85
Figure 5-14	Schematic of diffusion limited interfacial reaction.....	89
Figure 5-15	Concentration of substrate dependent reaction rate in mass transfer controlled regime .....	92
Figure 5-16	Double reciprocal plot of reaction system involving native ADH LB and native GluDH with free NADPH at four fixed levels.....	93
Figure 5-17	Double reciprocal plot of reaction system involving interface-assembled ADH LB and interface-assembled GluDH with free NADPH at four fixed levels.....	94
Figure 5-18	Double reciprocal plot of reaction system involving native ADH LB and native GluDH with interface-assembled NADPH at four fixed levels .....	94
Figure 6-1	Fabrication of MLM to form thin film phase at oil-water interface. ....	105
Figure 6-2	Amount of nanoparticles assembled at the interface .....	107
Figure 6-3	TEM images of MLM.....	107
Figure 6-4	Magnetization curves .....	109
Figure 6-5	Alternating magnetic field generator for nanostirring. ....	111
Figure 6-6	Effect on frequency and field strength of nanostirring on interface-assembled chloroperoxidase activity. ....	112



Figure 6-7	Visualization of mobility of MLM at interface.....	114
Figure 6-8	Correlation of actual mobility of MLM with the improvement in reaction rate on increasing the frequency. ....	114
Figure 6-9	Effect of nanoparticles on reaction rate .....	116
Figure 6-10	Enzymatic activity as function of surface coverage by nanoparticles at the interface. ....	117
Figure 6-11	Effect of nanoparticles on interface-assembled enzyme's activity.....	118
Figure 6-12	Effect of nanoparticles on interface-assembled CPO's activity. ....	120
Figure 6-13	Effect of interface-assembled enzyme concentration. ....	121
Figure 6-14	Effect of nanoparticles on native enzyme's activity. ....	123
Figure 7-1	Reaction system used with multienzymes and cofactor modified at the interface.....	130
Figure 7-2	Effect of polymer added during enzyme modification on reaction rate with both enzymes and cofactor assembled at the interface .....	131
Figure 7-3	Effect of Acetophenone concentration on reaction rate with both enzymes and cofactor assembled at the interface. ....	132
Figure 7-4	Effect of Glucose concentration on reaction rate with both enzymes and cofactor assembled at the interface. ....	133
Figure 7-5	Effect of enzyme ratio on reaction rate with modified enzymes and modified cofactor .....	134
Figure 8-1	Effect of aqueous phase pH on extraction efficiency of GOx. ....	142
Figure 8-2	Effect of solvent on organic-soluble GOx stability .....	144
Figure 8-3	Effect of different parameters on nanofiber quality.....	145
Figure 8-4	Nanofibrous enzyme material (NEM) .....	147
Figure 8-5	Specific activity of different forms of GOx .....	149
Figure 8-6	Current response of the NEM electrode.....	150
Figure 8-7	Effect of storage at 4 <sup>0</sup> C on sensitivity of NEM .....	152

# CHAPTER I

## INTRODUCTION

The membranes and the interfaces of a living cell separate one micro-environment of the cell from another providing the functional identities to individual organelles. These subcellular interfaces act as a workbench for about half of the cellular proteins[1]. Enzymes are proteins that catalyze chemical reactions in biological systems. Almost all processes in a living cell need enzymes in order to occur at significant rates. Interface-active enzymes present at interfaces like cell membranes and subcellular interfaces play an important role in many biological processes[2].

In nature, interface binding enzymes can interact with the surface in great number of ways. This is mainly due to the complexity of the protein molecule which comprises positive and negative charges, groups with hydrogen bond capacity and as well as hydrophobic/ hydrophilic regions. Interface binding can thus occur via electrostatic interactions, hydration forces, acid-base interactions, hydrogen bonding, hydrophobic and the van der Waals interactions[3-6]. The oil-water interface or the lipid-aqueous interface allows hydrophobic residue of the enzyme to be dissolved in, and interact favorably with the oil phase. The hydrophobic and ionic interactions with the gain in entropy due to conformational changes are often regarded as the driving forces for enzymes presence at the interface[7]. The interface-binding enzymes are responsible for important biological processes and function within the interfacial biophysical constraints. The degradation of lipids by lipases is an example of the biological process that occurs at the lipid-aqueous

interface[8, 9]. The properties of the interface formed strongly affect the enzyme activity. Furthermore, the interface is not constant, but as the enzymatic process proceeds the inclusion of the degradation products at the interface changes its properties. The pulmonary surfactant system is another example where the interfacial properties of the complex mixture of proteins and lipids are essential for the proper function of lungs. Alterations of the interfacial behavior of the pulmonary surfactants might affect their ability to promote lung expansion on inspiration, prevent lung collapse during expiration, balance the pulmonary fluids and stabilize small airways.

Traditionally, enzymes as biocatalysts have been developed for aqueous reaction systems. It has been known that enzymes do not require living cell to be active[10]. This opened many applications for enzymes in varied fields like in food technology, in the production of textiles and paper, in diagnostics and food analysis, and in the production of specialty chemicals[11]. Enzymatic reactions result in products free of any unwanted byproducts, this property is widely exploited in many industrial processes. Apart from this huge advantage enzymes also save in energy and waste treatment cost owing to mild reaction condition. Presence of non-aqueous environments like oil phase has detrimental effect on enzyme's activity and stability. However, many important industrial reactions involve both oil and aqueous phase. Methods to engineer enzymes to adapt to the new environments for effective biotransformations will help in realizing the goal of manufacturing bio-renewable products with sustainable environmental quality. The spatial structure of enzymes molecules governs their activity. Native enzymes have a unique structure of molecules that are energetically balanced and created due to

principles of structure hierarchy with optimal use of hydrogen bonds, dispersion, electrostatic, as well as hydrophobic interactions to stabilize the tertiary structure of the polypeptide chains[12]. Enzymes are macro molecules that contain both hydrophobic and hydrophilic groups. In aqueous soluble enzymes, the core of the enzyme molecule consists mainly of hydrophobic groups, while the hydrophilic residues are predominantly on the surface. The solubility of enzymes in organic solvent is determined by the overall surface hydrophobicity of the enzyme.

Enzymes that are active at cell membrane interfaces such as lipases often contain large fractions of hydrophobic moieties present at the surface which have low solubility in water[13, 14]. In enzymes that are not interface active, hydrophilic moieties at surface induces surface change and denaturation on exposure to oil-water interface. Thus, hydrophobic moieties should be introduced onto the surface of the enzymes to change the overall hydrophobicity of the enzymes and protect the enzymes while assembled at the interface. Interface-binding enzymes are desirable for many important industrial biotransformations that involve biphasic reactions. Enzymes at interface are easily accessed by substrates dissolved in both phases across the interface. Surface and interfacial tension measurements and interfacial dilation and shear rheology are methods to characterize such layers at liquid interfaces. The stabilization of enzymes at interface and the stability of the enzymatic membrane itself at the interface are critical in many interfacial processes. Besides hydrodynamic conditions the local events of the interface are controlled by the dynamic interfacial properties, modified by the presence of enzymes and polymer.

In this work, enzymes were modified to work efficiently at oil-water interface, the parameters and mechanisms to enhance the interfacial assembly of enzymes and their performance were investigated. The enzyme molecules were conjugated with polymers like polystyrene that are soluble in oil phase, which gave the modified enzyme an amphiphilic structure similar to a protein-based surfactant. When put in an aqueous oil system, the polymeric part of the polymer-enzyme conjugate stretched out into oil phase and the body of the enzyme is embedded in the aqueous phase. This anchors the enzyme molecule at the interface. However, any modification to enzymes requires a systematic and careful study that involves improving the stability and activity of the modified enzymes in the new environment. Model reactions systems involving, a single enzyme system and three multiple enzyme systems were employed to evaluate interface-assembled enzyme's activity and stability.

The single reaction system involved oxidation of styrene to styrene oxide by the enzyme chloroperoxidase. This enzyme requires two reactants, a water-insoluble styrene and the water-soluble hydrogen peroxide. This system is therefore ideally suited for interfacial catalysis. Other reaction systems involved multiple enzymes that require small molecules called cofactors for carrying out the reaction. The cofactors like Nicotinamide Adenine Dinucleotide ( $\text{NAD}^+$ ) are expensive molecules. In reaction systems that require cofactors, the major costs are the enzymes and the cofactor. Advances in recombinant technology and the development of high level expression systems have the potential to cut the cost of enzymes production. In the case of cofactor, efficient methods for regeneration and recovery are required. Therefore, methods were explored to modify the

cofactors to assemble at the interface for reuse. The multienzyme-cofactor reaction kinetics and mechanism that control the interfacial reaction were investigated by reduction of ketones to chiral alcohols by organic synthesis in the oil phase and oxidation of another set of alcohols to ketones in aqueous phase by multiple enzymes assembled at the interface.

The interfacial biocatalysis research focused on production of specialty chemicals like pharmaceutical compounds in an economical and environmental friendly way. Most of the industrial processes involved in manufacturing important chemicals, releases hazardous byproducts into the environment. Use of enzymes in manufacturing these important chemicals will make the whole process environment friendly. However, enzymes are very expensive catalysts and are evolved in nature to work mostly in aqueous phase. Many industrial reactions involve reactants dissolved in non-compatible phases like oil and water. This result in high production cost for these important chemicals. In the present research, a novel method of engineering enzymes to make it self-assemble at the aqueous oil interface was developed.

In another effort, the modification of enzymes was extended to achieve organic-soluble enzymes that were used for development of sensitive biosensors. A biosensor consists of two components: a bioreceptor and a transducer. The bioreceptor is a biomolecule that recognizes the target analyte whereas the transducer converts the recognition event into a measurable signal. The uniqueness of a biosensor is that the two components are integrated into one single sensor. This combination enables measurement of the target analyte without using reagents. For example, the glucose concentration in a

blood sample can be measured directly by a biosensor by simply dipping the sensor in the sample. This is in contrast to the conventional assay in which many steps are used and each step may require a reagent to treat the sample. The simplicity and the speed of measurement are the main advantages of a biosensor. Diagnostics represent a very large and well-established market that is continually expanding[15]. Particularly in the current climate of prevention rather than remedy, the need for detection at increasingly lower limits is increasing in many diverse areas.

Development of bioactive functional materials for use in highly sensitive biosensors requires presence of high amount of compatible bioactive substances like enzymes within it. Apart from biosensors, such materials have been pursued actively for applications such as catalysts, biomedical applications, coatings and paints and drug delivery. Among the various bioactive materials, polymeric nanofibers functionalized with enzymes have been the subject for many recent studies. One challenge encountered in this area is the incompatibility between the enzymes and polymeric materials. The current work presents the development of high protein content polymer-enzyme composite nanofibers through the use of enzymes with enhanced hydrophobicity. The electrospun enzyme carrying nanofibers has huge advantages over the conventional biosensors. The nanofibers contain enzymes that are water insoluble; this eliminates the requirement of outer membrane in a biosensor to hold the enzymes, thereby reducing the size of the sensor. The use of nanofiber as sensing element increases the surface area that is available for enzyme substrate contact. The high loading of enzyme that is achieved by

employing direct electrospinning of enzyme and polymer, facilitated in accurate and faster detection of analyte in low concentration.

## **1.1 Research objectives**

The research focused on hydrophobic modification of the microenvironment of enzymes for the development of enzyme conjugates and functional materials that had applications in interfacial biotransformations and biosensing respectively. The specific research objectives include:

- (i) Evaluation of assembly morphology and diffusion coefficient of interface-assembled enzyme.
- (ii) Improving the stability of interfacial assembled enzyme under emulsion condition by different approaches like addition of stabilizers and use of multiple enzyme system.
- (iii) Realizing an interfacial self-assembly of cofactor and evaluate the kinetics of interfacial reaction that involves interface-assembled cofactor regeneration.
- (iv) Enhancing the dispersion and mobility of enzyme at the interface by employing external magnetic field.
- (v) Accomplishing the interfacial reaction with both multiple enzymes and cofactors assembled at the interface.
- (vi) Developing sensitive biosensors by electrospinning enzyme carrying nanofibers.

## **1.2 Approach**

Novel interface-assembled multienzyme systems were developed by covalent attachment of the hydrophilic protein head to a hydrophobic polymer tail, resulting in a protein based surfactant structure. This polymer-enzyme conjugate self-assembled at



liquid-liquid or liquid-air interfaces to form a liquid membrane similar to that of lipid monolayers. However, the surface packing and the morphology of the interface-assembled enzymes play important roles in regulating the membrane fluidity, which in turn influences the enzyme mobility, mass transfer of substrates and products to the interface and interfacial interaction of these molecules. Langmuir film balance was used to characterize the surface assembly morphology of the interface-assembled enzymes. Lateral compression of the interface-assembled enzymes in Langmuir film balance resulted in several surface pressures, corresponding to different molecular surface densities of the interface-assembled enzymes. The morphology of the monolayer and different phase transition in its fluidity was observed by fluorescence microscopy. The mobility of the novel interface-assembled enzymes was further evaluated by using fluorescence recovery after photobleaching technique that facilitated the evaluation of diffusion coefficient of the enzymes at the interface.

An important consideration in enzymatic interfacial biocatalysis is the loss of activity of enzyme at the interface. At a liquid-liquid interface, the protein comes into contact with a hydrophobic environment, and will tend to unfold and place the hydrophobic groups in the non-aqueous layer while maintaining as much charge as possible in the water layer. Any change in conformation of the three dimensional structure of enzyme that yields a higher energy state will spontaneously go back to the state of lowest energy. If a hydrophobic group is exposed while a protein is in contact with the interface, it enters into the solvent phase and assumes lower energy state. This will continue to occur until random fluctuations in protein structure can no longer yield a

configuration of lower free energy, ultimately leading to denaturation of enzyme at the interface. Stabilization the enzymes from interfacial unfolding and denaturation is major challenge in the field of interfacial biocatalysis. The presence of polymer at the interface prevents this unfolding to some extent by protecting the hydrophobic groups from exposure to the interface. Chloroperoxidase (CPO) was used to examine the effects of different approaches for stabilizing the enzyme at the interface. However, a major shortcoming in the synthetic use of CPO is their low stability, resulting from irreversible inactivation from hydrogen peroxide ( $H_2O_2$ ). The reason for  $H_2O_2$  inactivation is the oxidative degradation of the porphyrin ring. Exposure of CPO to low levels of  $H_2O_2$  during reaction can improve the stability of interface assembled CPO. The localization of CPO at the interface improved the stability of the interface-binding CPO against the deactivation effect of  $H_2O_2$  in the bulk phase.

Two approaches to further improve the stability of CPO were examined in this work. In one approach, several stabilizers were applied that can either form a solvent layer around the enzyme surface to keep the local  $H_2O_2$  concentration low near the enzyme surface or interact with the oxidative intermediates and prevent CPO from denaturation. The chemical stabilizers included polyethylene glycol (PEG), polyethyleneimine (PEI), polyvinyl alcohol (PVA), polyacrylonitrile (PAN), ethylene glycol, glycerol, glucose and sucrose monododecanoate; while in the second approach, *in situ* generation of hydrogen peroxide ( $H_2O_2$ ) by using glucose oxidase (GOx), from glucose and oxygen to improve the operational stability of CPO was applied. The study

was conducted with both native enzymes in solution and interface-assembled preparations of GOx and CPO at liquid-liquid interface.

To broaden the applications of interfacial enzyme catalysis for complex industrial reaction systems that involve multiple interdependent reactions catalyzed by different enzymes, multienzyme-cofactor systems assembled at oil-water interface with in situ regeneration of cofactors were investigated. In an interfacial enzymatic reaction system involving multienzymes and cofactors, retaining the cofactors inside the reactor is necessary for successful process economy. Therefore, cofactors like NAD(P)H were also modified to self-assemble at oil-water interface. The modification of cofactor molecule for interfacial assembly without interfering with enzyme-cofactor interaction left few functional groups available on the cofactor for modification. Crystallographic information for several dehydrogenases indicated that the adenine ring lies in the hydrophobic pocket and is exposed to the solvent. The most studied positions of N<sup>6</sup> and C8 on the adenine ring for NAD(P)H modification was considered. However, the N<sup>6</sup> modified NAD(P)H derivatives exhibit a better activity by maintaining a more favorable access to the adenine binding site in the enzyme. Therefore, this position of the adenine group of nicotinamide cofactors was used for modification to yield macromolecular derivatives of cofactor that self-assembled at oil-water interface. The N<sup>6</sup> position of nicotinamide cofactors like NAD(P)H was functionalized in the presence of 1-(3-Dimethyl-aminopropyl)-3-ethylcarbodiimide hydrochloride and the subsequent stabilization of amine reactive O-acylisourea intermediate by N-hydroxysuccinimide resulted in a stable and active interface-assembled cofactor. The activities of interface-

binding cofactors were evaluated with two sets of multienzyme reaction systems. One reaction system involved alcohol dehydrogenase RS1 (ADH RS1) and glycerol dehydrogenase (GDH) with NADH as cofactor for reduction of acetophenone in organic phase to S-1-phenylethanol with simultaneous oxidation of glycerol to dihydroxyacetone in aqueous phase. Another reaction system involved alcohol dehydrogenase from *Lactobacillus brevis* (ADH LB) and glucose dehydrogenase (GluDH) with NADPH as cofactor for reduction of acetophenone in organic phase to R-1-phenylethanol with simultaneous oxidation of glucose to  $\beta$ -glucono lactone in aqueous phase. A kinetic study was performed to check for the dominant resistance towards interfacial reaction. Damkohler numbers for different form of the cofactors were evaluated for comparison of different configurations of multienzyme-cofactor system. However, it was observed that the limited mobility of enzymes at the interface contributed significantly towards the resistance for interfacial reaction.

To improve the mobility of interface-assembled enzymes at the interface, a novel mechanism of nanostirring was developed. Iron oxide ( $\text{Fe}_3\text{O}_4$ ) superparamagnetic nanoparticles were directed onto liquid-liquid interface by covering it with polymer conjugated enzymes, realizing a self-assembling magnetic enzymatic liquid membrane (MLM) for interfacial biocatalysis. The aspect of limited mobility of enzyme at the interface was addressed by nanostirring of MLM with an external alternating magnetic field. Epoxidation of styrene by CPO and multienzyme reaction system involving ADH LB and GDH for reduction of acetophenone and oxidation of glucose with NADPH as cofactor was chosen as model reactions for this study. The mobility of interface-

assembled enzymes was quantified through fluorescent microscopic visualization. The improvement in the observed reaction rate was compared to change in intensity due to mobility of enzymes at the interface.

An ideal configuration for interfacial enzyme catalysis would be to have both enzymes and the cofactor assembled at the interface with removal of products from either phase. This will reduce the downstream operations to a great extent and also with elimination of membranes, increase the process flow conditions. High yields can be achieved in such reaction systems with efficient regeneration and reuse of enzymes and cofactors inside the reactor. However, major constraints in employing such configuration are high sensitivity of dehydrogenases for stirring and interfacial binding of cofactor and the enzyme. The limited interaction of enzyme and cofactor at the interface possesses a major hurdle in sustainable cofactor regeneration. Dehydrogenases are very susceptible and are easily denatured by shear caused by the conditions inside a process reactor. To overcome these limitations a fast multienzyme reaction system involving ADH RS1 and GluDH with NADH as cofactor was employed with reduction of acetophenone to S-1-phenylethanol in the organic phase and oxidation of glucose to  $\beta$ -glucono lactone in aqueous phase. ADH RS1 and GluDH are relatively stable dehydrogenases against stirring. This combination of factors resulted in multiple turnover of cofactor at the interface with both cofactor and enzymes assembled at the interface.

The manipulation of microenvironment of enzymes was further extended to develop organic soluble enzymes by ion-pairing with surfactants for fabrication of biosensor. Stable, sensitive and reproducible nanofibrous biosensors were developed by

co-electrospinning polymer and organic soluble enzymes. To detect gases and biological substances at low concentration, a high surface area to mass ratio of membrane material is desirable. This provided an opportunity for polymeric nanofibers to be used as biosensors. Polyurethane (PU) presents a class of polymers that possess a range of very desirable properties for use in biosensors: they are elastomeric, resistant to microorganisms and abrasion, biocompatible and have excellent hydrolytic stability. PU can be electrospun with low concentration of polymer in the electrospinning solution. Therefore, PU was chosen as the polymeric material for the fabrication of biosensor. The parameters like pH, surfactant concentration, enzyme concentration, nature of solvent and phase ratio that affected the process of GOx extraction into organic phase by ion pairing with a surfactant was optimized to result in maximum extraction. The nanofibers consisting of enzyme–polymer composites that are prepared by directly electrospinning a homogenous solution of surfactant-stabilized, organic-soluble enzyme and polymer in an organic solvent led to very high loading of enzymes on the nanofibers. These nanofibers with very high enzyme content per unit mass were ideal candidates for use in biosensors to detect very low concentration of analytes. The surfactant-stabilized enzymes being water insoluble did not leach into aqueous solutions. This highly enzyme loaded biocatalytic nanofibers were evaluated for biosensing applications by employing a cyclic voltammetry analysis in an electrochemical cell.

### **1.3 Outline**

Chapter 2 reviews literature about enzyme catalysis, enzyme reactions with non-conventional methods, interfacial biocatalysis, multienzyme reaction systems and biosensor development. The development and characterization of interface-assembled enzyme is depicted in Chapter 3. Chapter 4 involves stabilization of interface-assembled enzyme by different approaches. Chapter 5 explores the methods to modify cofactor molecules for interfacial assembly and evaluation of kinetics of interface-assembled cofactor. Chapter 6 reveals a mechanism of nanostirring to improve the mobility of interface-assembled enzyme at oil-water interface. Chapter 7 describes the feasibility of reaction system with interface-assembled enzymes and interface-assembled cofactor with multiple turnover of cofactor at the interface. Chapter 8 discusses the development of sensitive biosensors by co-electrospinning an enzyme-polymer solution. The conclusions are summarized in chapter 9.

# CHAPTER II

## BACKGROUND

### 2.1 Enzymatic biocatalysis

Enzymes are biocatalyst that regulate and enable all the biological transformations in living organisms. Each reaction in the biological world occurs with either one or a combination of multiple enzymes. Their exceptional functional properties like activity, selectivity and specificity enables enzymes to catalyze the most complex chemical processes in a benign experimental and environmental conditions[16]. Functioning in controlled *in vitro* environments, enzymes are also capable for production of great variety of valuable products. Enzyme as valuable biocatalyst has broad application in human's daily life, as in the fields of analytical medicine, pharmaceuticals, food, animal feed, crop protection, pulp and paper, chemicals and mining [11]. Compared with other kinds of catalysis, enzymatic catalysis offers the greatest advantage of unsurpassed selectivity and regioselectivity especially with differentiation between enantiomeric substrates.

Enzymes have been traditionally used for drug development, detergents, food processing in chemical industries. A major driving force in the application of enzymatic processes in the chemical process industry is environmental concern and regulation. There is a rapidly growing demand for cleaner, alternative technologies that produce less waste, less energy intensive and avoid the use of toxic reagents and solvents. The characteristic feature of enzymatic processes is high selectivity under mild reaction



condition. This makes them ideal catalyst in the synthesis of biologically active chiral substances like pharmaceuticals, herbicides, fungicides, flavors and fragrances.

Traditionally enzyme catalysis has involved aqueous solutions, with water being a natural, safe and cheap media for biocatalysis. However, many industrial biotransformations involve hydrophobic substrates and products. Currently several challenges are faced in improving the performance of enzymes for industrial biocatalysis: 1) Screening of enzymes for suitable properties [17]. 2) Modification of properties via techniques of molecular biology[18]. 3) Enhance enzyme stability and activity under a range of conditions such as extreme temperatures or pH values, or physical forces[19-21]. 4) Improvement of enzyme properties via reaction and reactor engineering[22-24]. Such successful improvement of enzyme properties should be one of key solutions for the development of a much more sustainable chemical industry that is able to synthesize very complex and useful compounds under very mild and cost-effective conditions.

## **2.2 Non-traditional enzyme catalysis**

Enzymes have traditionally been viewed as a biocatalyst functioning only in aqueous environment since their origin is living organisms. However, it was found that in nearly anhydrous conditions enzyme can still maintain its catalytic activity [10]. This observation has a breakthrough impact on the application of enzymes in a broader field. It is of great benefit to many important biotransformations involving organic substances not soluble in aqueous solutions, since the stability of the enzyme and the enzymatic efficiency of the catalytic processing are always the major concerns for enzymatic applications, especially for industrial scale production.

Numerous recent advances have focused on nonaqueous enzymology for the development of active and stable homogeneous (soluble) biocatalysts [25-29] with lot of interest directed towards organic synthesis[16, 30-32]. Enzymatic reactions in organic solvents can avoid undesired side-reactions and in some cases realize reactions that hardly occur in aqueous solutions. For instance, water, as a by-product generated from esterification/transesterification reaction, tends to retard the reaction and the conversion is very low in aqueous solutions. On the contrary, when the same reaction is carried out in anhydrous environment by applying modified/immobilized enzyme the conversion can be improved dramatically [33-35]. Some reactions, when carried out in aqueous solutions, have concomitant undesired background reactions, which may cause low efficiency of reaction and contamination of product. While in anhydrous environment these side reactions can be effectively suppressed and high conversion and high purity of product often can be achieved [36].

When used directly in organic solvents, native enzyme molecules tend to aggregate leading to greatly reduced surface area and consequently unfavorable catalytic efficiency. The advances in genetic and protein engineering have generated more stable and active enzymes. At the same time, enzyme modification and immobilization have become the commonly applied methods to tailor enzymes in different reaction configurations[37-42]. Solubilization of enzymes in organic solvents requires modification of the native enzyme to prevent it from aggregation or denaturation. Covalent techniques are well described in the literature (e.g. attachment of polyethylene glycol chains to enzymes) [43]. Noncovalent modifications are much less common; however, they are capable of

providing highly active and soluble enzyme forms that can be studied spectroscopically in the nonaqueous milieu [44].

### **2.2.1 Immobilization of enzymes**

Immobilization refers to the incorporation of biocatalysis with insoluble carriers. Generally, immobilized enzymes are known to be useful for establishment of enzyme reuse system or continuous reaction processes. Immobilization is also pursued for enzyme stabilization. Methods for immobilization have usually been classified as physical adsorption [45], ionic bonding, physical entrapment [46, 47], crosslinking of the enzymes [48, 49] and covalent bonding to the carriers. [50, 51] Industrial applications of immobilized enzymes include production of sugars from starch, analysis of various pharmaceutical and drug-related products, affinity chromatography and immunoassay procedures [52-55].

The modern history of enzyme immobilization can be traced to late 1940s but much of the early work was largely ignored by biochemists because it was published in journals of other disciplines [56]. The basis of present technologies was developed in the 1960s and there was an explosive increase in publications [57]. Initially only single enzymes were used for immobilization but by 1970s more complex systems, including two-enzyme reactions with cofactor regeneration were developed [58]. The first industrial use of immobilized enzymes was reported in 1966 by Chibata and coworkers [57], who developed the immobilization of *Aspergillus oryzae* aminoacylase for resolution of synthetic racemic D-L amino acids. In some industrial processes whole

microbial cells containing the desired enzymes are immobilized and used as catalyst [59]. In the past three or four decades, immobilization technology has developed rapidly and has become a matter of rational design, but there is still need for further improvement. The major components of an immobilized enzyme system are the enzyme, the matrix and the mode of attachment of the enzyme to the matrix. The term solid phase, support, modifier and matrix are used synonymously with respect to immobilization of enzymes.

However, mass transfer limitation associated with the solid support is the main drawback of immobilized enzymes system. Comparing with native enzyme dissolved in aqueous solution, immobilized enzyme reaction system is heterogeneous. Diffusion of the substrate from bulk phase to reach the enzyme active sites on the surface of the support is an important factor which affects the product efficiency. Mechanisms like stirring can help the mass transfer in the process but may cause corruption of the support. Other than mass transfer limitation, the interactions between enzymes and support materials, the interaction between support materials and water also may affect the efficiency and the stability of immobilized enzyme [60]. For both small- and large-scale applications, it is important to choose a suitable support and method for immobilization. The support material should be insoluble in solution and permeable to substrates and products, rigid and has suitable size and shape, better be hydrophilic to retain enough water for enzyme. Porous supports are widely used while their morphological (particle size, pore size, and specific surface area) and chemical characteristics (water partition characteristics, substrate/product partition characteristics and direct effects of the support on the enzyme) are both important characters inside. Recent studies revealed that the great potential for the

use of nanoporous, nanofibrous and nanoparticle materials can provide really high loading of enzyme and better efficiency [61, 62]. Immobilized enzyme can be used widely for reaction requiring single enzyme. For multiple enzyme systems that requiring interactions among catalytic components like the system to be examined, this immobilization is not a feasible configuration.

### **2.2.2 Chemical modifications of enzymes**

Chemical modification implies altering the side groups of amino acid or attaching additional chemical groups to the enzymes. It is also an effective way to alter the properties of the enzyme molecules. Typical reagents such as small molecules, bifunctional reagents, and polymeric materials have always been utilized to increase the stability of enzyme in organic phase or mutagenesis direct to specific-site used mostly in protein engineering [63]. Enzyme can also be altered leading to new catalytic features by chemical modification. The redesign of enzyme activity through the chemical modification of amino acid side chains is currently a common technique. It is an intriguing approach for catalyst development because chemical modification altered both physical properties and catalytic efficiency and provides the enzyme enormous range of functionality [38, 63, 64], which was needed in pharmaceuticals, food processing and detergent applications.

Chemical modification of certain side chain on enzyme molecule contributes to the change of catalytic behavior. Chemical modification has been practiced widely both in protein chemistry studies [65] and enzyme manipulation [66]. In the recent exploration of

nonaqueous biocatalysis, various modification methods have been examined to improve the organic-compatibility of enzymes. Another interesting example obtained from the non-specific modifications of amines in *Candida rugosa* lipase (CRL) with benzyloxycarbonyl, lauroyl and acetyl that enhanced enantioselectivity of lipase in esterification of 2-(4-substituted phenoxy)propanoic acids with n-BuOH in isopropyl ether [67]. Based on the proof of circular dichroism and electron spin resonance studies, the authors made the assumption that because of the acylation of charged lysine sidechains, CRL accepts less flexible conformation which means although the reaction rates for both enantiomers, the effect on unfavoured S enantiomer would be more pronounced.

One of the challenges for biocatalysts application in industry is to increase their stability especially in nonaqueous media. And with the surprising result obtained by Levashov in 2001 [68], the introduction of both hydrophobic and hydrophilic groups into  $\alpha$ -chymotrypsin led the enzyme to withstand a broader range of organic solvent concentration in water-organic mixture, exhibiting comparable activity as that of the unmodified enzyme in biphasic system. The chemical modification may also lead to enhanced thermostability and autolytic stability of enzymes. For example, 1-ethyl-3-(3-diethylaminopropyl) carbodiimide(EDC) was used to modify trypsin which introduced almost two monoamino  $\alpha$ ,  $\beta$  or  $\gamma$  cyclodextrins into trypsin.. The modified trypsins showed up to five- to eightfold enhanced autolytic stability and thermostability.

Chemical modifications also take an important part in redefining the existing enzymes' catalytic efficiency and substrate specificity. As reported, synthetic reagent

brought a broad range of functionality that abnormally present in proteins. Alkyl, aryl, anionic and cationic groups have been used by Jones and co-workers who gained significant results in this area [69]. Based on the study of Subtilisin Bacillus lentus(SBL), the resulting semisynthetic enzymes varied both catalytic efficiency and specificity comparing with the wild-type enzyme. According to the X-ray structure of SBL, some positions in the S1, S1' and S2 binding pockets were mutated to cysteine and derivatized with a number of reagents which probably account for changing the specificity of SBL by filling up the S1 pocket with a bulky cyclohexyl group. Thus, the preference of wild-type SBL with large hydrophobic P1 residues changed to small P1 residues [70].

Glutaraldehyde is another common modifier used for enzyme crosslinking [71]. Cross-linked enzyme crystals was proven to be highly stable under otherwise denaturing conditions such as varying pH values, high temperatures, proteolytic degradation, and organic solvents compared with native enzymes. Furthermore, cross-linking via covalent bonds (CLECs) have made enzymes highly active and stable in organic media which is an inexpensive method for enzyme to improve thermal and proteolytic stability. Attachment of chemical groups, such as alkyl, phenyl, and poly(ethylene glycol) (PEG) groups, was applied to increase the enzymes' solubility, and thus their activity in organic media[43, 72-80]. Bifunctional and polyfunctional modifier have been employed for enzyme crosslinking such as the stabilizing effects of Penicillin G asylase, which is used in pharmaceutical to produce precursors, crosslinking with dextran dialdehydes [49]. Other methods like incorporation of enzymes to polymer networks have been developed [81-84]. Other protein manipulation technologies such as surfactant coating [85] and

deglycosylation [78] have also been developed or reexamined to enhance enzymes' nonaqueous activity. However, the number of residual viable enzyme active sites remaining is hard to determined, so the data from each paper is not comparable. Poly (ethylene glycol) (PEG) is the most commonly used polymer to generate organic solvent-soluble enzymes [86-88], and it has been also applied extensively in drug delivery systems [89]. Because of the amphiphilic nature of PEG, the modified enzyme can be easily solubilized in organic solvents.

### **2.3 Enzymatic catalysis in biphasic system**

Though the reaction efficiency in an nonaqueous environment is improved to a certain extent, mass transfer resistance still remains as a considerable limitation [90] gaining more importance in biotransformations that involve water-soluble substances and organic compounds that are incompatible to each other. Traditionally, biphasic reaction systems have been employed to carry out biotransformation that involves immiscible reactants [91, 92]. A lot of reactions involving organic chemicals have been investigated with biphasic systems like enzymatic resolution of epoxides in octane-buffer system using enantioselective epoxide hydrolases [93]. Biphasic system offer several desired advantages. In addition to increased substrate presence in the reactor, the biphasic configuration can also simplify product purification, and sometimes make thermodynamically unfavorable reactions become possible [94-96]. It is also used to extract product to another phase to avoid side reactions like product hydrolysis. Pencilin G acylase was immobilized on porous supports to synthesize antibiotics in two-phase



system [97]. The product was continuously extracted into another phase to improve the yield. The same reaction resulted in 55% lower yield in a monophasic reaction system due to product hydrolysis.

The aqueous phase was almost unexceptionally used as a biocatalyst container in all the previously studied biphasic processes. An alternative approach is to use reverse micellar solutions [98, 99]. This involves essentially the same reaction configuration as in bulk biphasic systems, since enzyme molecules were contained in the water pools surrounded by a surfactant layer. Even with the great R&D efforts made in this area, several inherent drawbacks have made the traditional biphasic reactions largely inefficient due to reactions are strongly mass-transfer limited [90, 100, 101]. The major disadvantage being that only enzyme molecules near the interface may be effectively involved in the reaction, while the majority of the enzyme in the bulk aqueous phase does not participate in the reaction [100, 101].

## **2.4 Interfacial biocatalysis**

In nature, certain enzymes have been observed to get adsorbed onto interfaces (air-water, liquid-liquid, and water-solid) [102-104] due to electrostatic interactions, hydration forces, acid-base interactions, hydrogen bonding and the van der Waals interactions. The oil-water interface or the lipid-aqueous interface allows hydrophobic residue of the enzyme to be dissolved in, and interact favorably with the oil phase. In fact, in the biological world, considerable amount of enzymes are associated with various membranes, which are composed of hydrophobic lipid bilayers [105]. Adsorption of

proteins at interfaces is accompanied by conformational changes that may influence their catalytic or biological function that is of importance to a wide range of application. This includes industrial biocatalysis, and delivery and stabilization of therapeutic proteins. Enzymes assembled at an organic-aqueous interface could provide the maximum accessibility to chemicals dissolved in both phases across the interface. Interfacial enzymes act on insoluble substrates. Phospholipases and lipases are two important examples from this group of enzymes. For example, lipase shows its majority activity at the hydrophobic interfaces, which induces the exposure of the active sites [106, 107]. Lipases hydrolyze the ester bond of triacylglycerols, which are insoluble in aqueous media. The triacylglycerols are emulsified by bile salts, forming emulsion droplets. Lipase binds to these oil droplets and catalyzes the reaction at oil/water interface. It has also been reported that hydroxynitrile lyase catalyzes the production of benzaldehyde from mandelonitrile at the diisopropyl ether/water interface [92]. Some research showed that enzymes, upon being adsorbed at the interface or put into organic solvents, tend to lose catalytic activity due to the conformation change caused by the hydrophobic interactions [108, 109]. On the other hand, evidence also showed that chemical modification is an effective way to improve enzyme functionality and stability [34, 70, 110], and can even generate new enzymes [111]. These previous works proved that by chemical modification, some of the properties of the native can be changed toward better performance and it is feasible to assemble enzyme at the organic-aqueous interface by chemically tailoring its surface hydrophobicity.

Zhu and Wang [112] developed an interfacial biocatalysis, in which enzymes were modified to achieve highly selective interfacial assembling with access to substrates in both the phases. The surface of the enzyme molecules was attached with hydrophobic moieties like polystyrene to increase the overall hydrophobicity, leading to a structure similar as the protein-based surfactant [113]. When put into an organic-aqueous biphasic system, the hydrophobic part of the modified enzyme stretches out into organic phase with enzymes embedded in the aqueous side that anchors the enzyme molecule at the interface. The polymer-enzyme conjugate enabled a unique interfacial biocatalysis. This increased enzyme stability against physical inactivation by interfacial stress. Typically, polystyrene (PS), a hydrophobic and easily produced polymer, was used as the modifier and a proteolytic enzyme,  $\alpha$ -chymotrypsin (CT) was selected as the model enzyme for the interfacial assembly.

## **2.5 Multi enzyme biocatalysis with cofactor regeneration**

Multi enzyme reactions have been employed as a one-pot synthesis for multi step reaction sequences and for cofactor regeneration [114]. Many enzymes involved in biochemical pathways associate to form multi-enzyme complexes. The main advantage associated with the multi enzyme reaction with cofactor regeneration is their high yield. There are different methods available for in situ cofactor regeneration. The electrochemical regeneration, applied with electrode-biosensor, is one such method [115]. The in situ cofactor regeneration is generally conducted in aqueous environment due to hydrophilicity of cofactors.

The study of multi enzyme system with cofactor regeneration has been developed for different applications. For example, this approach has been used in conversion of adenosine to ATP using three enzymes, adenosine kinase, adenylate kinase and acetate kinase entrapped in a cross-linked polyacrylamide gel [116], and the regeneration of NADH and NADP using lactate dehydrogenase and glutamate dehydrogenase on polymeric beads [117]. However, free cofactors are difficult to recover from reaction media for reuse. To facilitate the reuse of the cofactors, immobilization of cofactors had been achieved by different methods like physical entrapment of NADH in PEG to enlarge its physical size so that it could be retained in the reactor by ultra filtration films [118]. Alternatively, NADH was attached to the dehydrogenase for enhanced retention through the same film-entrapment methodology [119]. In another study, NADH was entrapped in polyacrylamide hydrogel along with formate and malate dehydrogenase [120]. An interfacial biocatalysis system that enabled the long-term continuous flow reaction system was developed with alcohol dehydrogenase and glucose dehydrogenase and NADH as cofactor, resulted in a cofactor turnover number of 261 [121]. In efforts to develop electrode- based biosensors, cofactors including FAD and NADH have been covalently immobilized onto electrodes [122]. Such sensors were built with the immobilized cofactor interacting with one dehydrogenase immobilized on the same electrodes, with the cofactor being regenerated by reacting with oxygen. Although these efforts have been made for different purposes, they reflect the needs, interests and possibilities in enabling multienzyme biotransformations.

The general scheme of manufacturing specialty chemicals with multi enzyme reactions involves substrates that are soluble in different phases. Interfacial biocatalysis with multi enzymes that are assembled at the oil/water interface provides accessibility for contact with substrates from both phases. However, the main obstacle for the wider use of interfacial assembled enzymes as industrial biocatalysts is the lack of understanding of their adsorption behavior and possible conformational changes at the liquid-liquid interfaces.

## **2.6 Electrospun nanofibers for biosensors**

Recent breakthroughs in nanotechnology have made various nanostructured materials more affordable for a broader range of applications. Nanomaterials' excellent unique material properties along with rapid growth in the synthesis methods are extending their applications enormously. Fabrication of these materials for various applications has been showing significant commercial impact, and will be having larger impact in the future [123]. The use of these materials for biocatalysis is still being explored; various nanostructures have been examined as hosts for enzyme immobilization via approaches including enzyme adsorption, covalent attachment, enzyme encapsulation, and sophisticated combinations of methods [124, 125].

The novel nanostructured materials are considered promising biocatalyst supports due to their unique structural, electronic and mechanical properties [126]. Investigators proved that the nanostructured supporters performed well for NO<sub>x</sub> reduction [127], hydrogen storage [128], hydrogenation [129], hydroformylation [130], electrocatalysis

[131] and biocatalysis [132]. Many researchers have been focusing on the synthesis of graphite nanofibers and their applications. Some of the downsides for the synthesis of carbon nanofibers are the high treatment temperatures and low yields ~ 2 %. Because of these concerns the production of carbon nanofibers are expensive. Less expensive alternative technique, such as electrospinning is therefore needed for the production of nanofibers containing catalytic materials.

Electrospinning provides a simple and highly versatile method for the large-scale fabrication of nanofibers in the range of few nanometers [133, 134]. The standard setup for electrospinning consists of a spinneret with a metallic needle, a high-voltage power supply, a syringe pump, and a grounded collector. In order to obtain a continuous sheet of nanofibers, the collector can be replaced using a rotating cylinder. Polymer, sol gel or composite solution is loaded into the syringe and driven to the needle tip using the syringe pump at constant flow rate. An electric field is applied to the needle tip using the high voltage power supply. When the electric field overcomes the surface tension of the droplet, the droplet is stretched into an electrified jet. The jet is then elongated by electrostatic repulsion until it is deposited on the grounded collector. The elongation by bending instability results in the formation of uniform fibers with nanometer-scale diameters [135].

Enzymes are highly specific catalyst that can be used to detect very small amount of the substrate. This makes them ideal candidate as sensing element with polymer nanofibers as solid support in a biosensor. Conventionally, enzymes are immobilized on the electrospun fibers. This method has a drawback of enzyme immobilization only on

the external surface of the fiber without utilizing the vast inside volume of the nanofibers. To overcome this disadvantage, a direct method of electrospinning enzyme containing polymer solution have been used [136, 137], but most of these studies involved enzyme with water soluble polymers. This leads to leaching of enzymes and the polymer in aqueous solutions, which severely limits the use of these biocatalytic nanofibers as biosensors for clinical applications. Recently, Herricks et. al. [138] solved the leaching problem with solubilized enzyme in organic solvent by forming ion pair complex with a surfactant [85] and electrospinning a homogenous mixture of solubilized enzyme and water insoluble polymer. However, the highest enzyme loading achieved was 6.3 %, which is lower than that reported for immobilization of enzyme on electrospun fibers.

Biosensors have been widely used for clinical, food and environmental purposes. Parameters that affect the performance of a sensor include sensitivity, selectivity, response time, reproducibility and aging, all of which are dependent directly on the property of sensing membrane used [139]. To detect gases and biological substances at low concentration, a high surface area to mass ratio of membrane material is desirable. This provides an opportunity for polymer nanofibers to be used as biosensors. The high surface area to mass ratio in nanofibers increases the loading of sensing element like enzymes on the nanofibers. Wang et. al. [140] reported that the sensors made from electrospun nanofiber membranes containing fluorescent poly(acrylic acid)-poly(pyrene methanol) for detecting metal ions ( $\text{Fe}^{3+}$  and  $\text{Hg}^{2+}$ ) and 2,4-dinitrotulene exhibited a sensitivity of almost three orders of magnitude higher than that of thin films of the same material. A glucose sensor represents the class of biosensor that is widely used for

diagnostic purposes. Table 2-1 gives the historical landmarks in the development of glucose biosensors.

Table 2-1 Historical landmarks in the development of glucose biosensors

<b>Date</b>	<b>Event</b>	<b>References</b>
1962	First Glucose enzyme electrode	[141]
1973	Glucose enzyme electrode based on peroxide detection	[142]
1975	Launch of first commercial glucose sensor system	YSI Inc.
1982	Demonstration of in vivo glucose monitoring system	[143]
1984	Development of ferrocene mediators	[144]
1987	Launch of first personal glucose meter	Medisense Inc.
1987	Electrical wiring of enzymes	[145]
1999	Launch of commercial in vivo glucose sensor	Minimed Inc.
2000	Introduction of a wearable noninvasive glucose monitor	Cygnus Inc.

The noninvasive glucose sensor (GlucoWatch) developed by cygnus Inc. consist of two hydrogel electrolyte disks that serve as the glucose collection reservoirs and contain the GOx enzyme, along with two sets of biosensor electrodes. Each electrode set includes a platinum-graphite-composite sensing electrode, a silver–silver chloride reference electrode, and a third that acts alternately as the counter electrode for the biosensor and the iontophoresis electrode. Iontophoresis current is passed for few minutes by the transdermal monitor to sample and measure glucose. The glucose is collected at the iontophoretic cathode where it reacts with GOx in the hydrogel, producing hydrogen peroxide. At the end of the collection period, the iontophoresis current is stopped, and the biosensors are biased at a potential relative to the silver–silver chloride reference electrode. The current obtained from the detection of hydrogen peroxide is integrated over few minutes. The iontophoretic current polarity then is reversed, and a second sample and measurement cycle is performed. The two measurements are averaged using



a rolling-average scheme and the result is used to calculate glucose level. However, the GlucoWatch is not reliable at very low level of glucose. The sensitivity of GlucoWatch is also hindered by bodily fluids like sweat. To overcome these shortcomings a biosensor that is not affected by aqueous solution and have high enzyme loading to detect low level of glucose should be substituted for the bioreceptor in a new generation biosensor.

## **CHAPTER III**

# **INTERFACIAL ASSEMBLY AND CHARACTERIZATION OF ENZYMES AT OIL-WATER INTERFACE**

### **3.1 Introduction**

The activity of an enzyme primarily depends on the three-dimensional structure of the protein, which is determined by its amino acid sequence. Covalent modification of enzymes always target at the functional groups that are on the side chain of the amino acid at the surface of the enzyme. Generally, chemical modification involves the linkage of a carboxyl groups of the backbone or to reactive groups in the side chains of internal residues to the terminal amino acid. Modification conditions are important to maintaining enzyme activity. Suitable modification methods should be under mild conditions that do not reduce the activity of the enzyme. The nature of the reaction and the choice of the modifier determine the possibility and efficiency of the modification. The parameters that affect the modification include pH, ionic strength of the buffer, temperature, the agents that are present in the media and the mechanical stress while modification are also very important which should be controlled to minimize loss of enzyme activity during modification.

Enzymes are macro molecules that contain both hydrophobic and hydrophilic groups. The solubility of enzymes in organic solvent is determined by the overall surface hydrophobicity of the enzyme. Enzymes that are active at cell membrane interfaces such as lipases often contain large fractions of hydrophobic moieties present at the surface

which have low solubility in water. Aqueous soluble enzymes, covered by hydrophilic moieties at surface, are easily deactivated by unfolding at the interface. Thus, hydrophobic moieties should be introduced onto the surface of the enzymes to change the overall hydrophobicity of the enzymes and protect the enzymes while assembled at the interface. This can be achieved by attaching a hydrophobic tail to the hydrophilic enzyme head through covalent bond, generating a structure similar to a protein based surfactant.

In this work, to characterize the surface assembly morphology of the interface-assembled enzyme, Langmuir film balance was used. The response of modified enzymes at the interface to expansion and compression is a key factor in determining the ease of formation and stability of liquid membrane formed by the modified enzymes at the interface. The resultant interfacial tension kinetics can be interpreted in terms of adsorption/desorption, aggregation/ disaggregation, and intramolecular rearrangement of the interface-assembled enzymes. The mobility of the novel interface-assembled enzymes was further evaluated by using fluorescence recovery after photobleaching technique.

## **3.2 Materials and Methods**

### **3.2.1 Chemicals**

Alcohol Dehydrogenase (ADH RS1) from *Rhodococcus* species (EC 1.1.1.1, 444 IU/ml) was obtained from Julich Chiral Solutions (Julich, Germany). Bovine Serum Albumin (BSA) standard was purchased from Sigma-Aldrich (St. Louis, MO). Carboxyl chloride terminated polystyrene (PS-COCl, Mw 2020) was purchased from Polymer Source, Inc. (Canada). Toluene was purchased from J.T.Baker (Philipsburg, NJ). Protein

assay dye reagents were purchased from Bio-Rad laboratories (Hercules, CA).  $\text{CuSO}_4$  ( $5\text{H}_2\text{O}$ ) and NaOH were purchased from VWR Sci. (PA). Ascorbic acid was purchased from Mallinckrodt, KY. Texas Red dye for FRAP analysis was obtained from Invitrogen.

### **3.2.2 Enzyme modification**

Alcohol Dehydrogenase (ADH RS1) from *Rhodococcus* species was chosen as model enzyme to investigate assembly morphology of interface-binding enzyme. The modification of ADH RS1 was done by adding 10 ml of toluene containing 10 mg of PS- $\text{COCl}$  into 1 ml of buffer (0.1 M Tris, pH 7.8) solution with enzyme concentration of 0.3  $\mu\text{g}/\text{ml}$ . The mixture was shaken at room temperature for 1 hour in dark. After modification, the mixture was centrifuged and the modified enzyme was obtained from the interface. The interface was purified by rinsing with toluene and buffer for three times to remove any unreacted polymer and native enzyme. The modified enzyme was stored at 4  $^{\circ}\text{C}$  for future use.

### **3.2.3 Protein Content Measurement**

The protein content of the enzyme solution and modified enzyme was measured by Bradford Protein Assay. The concentration of enzyme in aq. solution, both before and after the modification, was measured using Coomassie blue reagent[146]. A differential color change occurs in response to various concentrations of protein by binding to primarily basic and aromatic amino acid residues. In a typical measurement, 2.5 ml of reagent was put into cuvette followed by 50  $\mu\text{l}$  of enzyme solution. The solution was incubated at room temperature for 5 minutes and then the absorbance at 595 nm was

measured on a UV-Vis spectrophotometer (Varian, Cary 50 Bio). BSA was used as the standard protein.

The amount of protein content in the modified enzyme conjugate obtained from the interface was also verified by reverse biuret method[147]. Two analytical reagent were first prepared: reagent A was prepared by dissolving 15 mg  $\text{CuSO}_4 \cdot 5\text{H}_2\text{O}$ , 45 mg of potassium sodium tartrate and 2.4 mg NaOH into 100 ml DI water. While, reagent B was prepared by dissolving 25 mg ascorbic acid and 37 mg bathocuproinedisulfonic acid disodium salt in 100 ml DI water. Typically 1 mg of modified enzyme conjugate and 10  $\mu\text{l}$  of water were added to 200  $\mu\text{l}$  of reagent A and the mixture was incubated at 37  $^\circ\text{C}$  for 5 minutes. Then 1000  $\mu\text{l}$  of reagent B was added and the incubation continued for another 30 seconds. The solution was filtered through 0.2  $\mu\text{m}$  syringe filters and the absorbance at 485 nm was measured with the UV-Vis spectrophotometer. The BSA standard was used with the same procedure but with replacing the 10  $\mu\text{l}$  water with protein solution of the same volume.

### **3.2.4 Interfacial Surface Pressure Analysis**

A Nima 612 Langmuir film balance (Coventry, England) was first filled with DI water with a maximum surface area of 425  $\text{cm}^2$ . A block of Teflon with 75  $\text{cm}^2$  area was placed in the center of the trough to reduce the compression ratio. 300 ng of interface-assembled enzyme was spread on the water surface along with hexane and water. The system was then left for 20 min to allow the solvent to evaporate and modified enzymes to disperse throughout the interface. The system was then compressed and expanded for

two times to get a homogenous spreading of the modified enzymes at the interface. The experiment was monitored with a Retiga EXi digital camera (Tuscon, AZ). The barriers were compressed at a speed of 50 cm<sup>2</sup>/min. A Wilhemy plate made of paper was positioned in the interface at the center of the trough with its length parallel to the long dimension of the barrier. A commercial Wilhelmy plate (Nima Technologies) was used to monitor the surface pressure. Readings were collected at a rate of 5 per second with an error of  $\pm 1$  mN/m.

### **3.2.5 Fluorescence Recovery after Photobleaching**

The enzyme was dyed with Texas red dye. Typically 300 ng of enzyme in 1 ml of 7.8 pH tris buffer was reacted with 50  $\mu$ g of Texas Red for 1 hour in dark. This dyed enzyme was modified to assemble at the oil-water interface as outlined by the procedure above. FRAP experiments were performed on a Nikon C1 spectral imaging confocal microscope (Nikon Instruments Inc, Melville, NY) with 10 X objective. The modified enzyme was applied at a hexane-water interface in glass cell with cover slip bottom with water layer less than 1 mm in height from the bottom. Bleaching was performed for six seconds with a circular spot using the 20 mW 408 solid state laser, 15 mW 440 diode laser, 40 mW Argon laser of 457, 488, 514nm lines and 10 mW 561 diode laser at 100% laser power. Fluorescence recovery was monitored with low laser intensity (20% of a 10mW laser) of 561 nm line at 60 seconds intervals.

### **3.3 Results and Discussions**

#### **3.3.1 Interfacial assembly of the enzyme**

A number of classes of enzymes are membrane bound, including phospholipases, peptidases, lactases, and glutaminases [105]. Most of these enzymes contain hydrophobic side chains that interact with fatty acid groups of the membrane phospholipids, thus anchoring the enzymes to the membrane. The most frequently studied interfacial enzyme is lipase, which acts on the carboxyl ester bond in acylglycerols to liberate organic acids and glycerol. Studies have shown that the active site of lipase is covered by a lid like hydrophobic polypeptide chain, which upon binding to a lipid interface, opens and becomes exposed to the lipid phase leading to fully accessible active site [13, 14, 148]. The hydrophobic lid enhances the hydrophobic interaction between enzyme and the lipid surface, resulting in the interesting interfacial activation phenomenon. However, for enzymes with high hydrophilicity, it is relatively hard for them to be adsorbed at the hydrophobic interfaces.

In this research, hydrophobic polystyrene was deliberately attached to the ADH RS1 to enhance the surface hydrophobicity in order for the polymer-enzyme conjugate to assemble at oil-water interface. The protein content estimation by both Bradford analysis and reverse biuret method gave comparable efficiency of the modification procedure. An average yield of 53% of enzymes was obtained on modification by functionalized polystyrene. The resulting polystyrene-enzyme conjugate self-assembled at oil-water interface as seen from Figure 3-1. Oregon Green dye was used to label the enzymes. The

green color observed at the oil-water interface for modified enzyme, indicates a selective interfacial assembly, in contrast to native enzyme that remained in the aqueous phase.

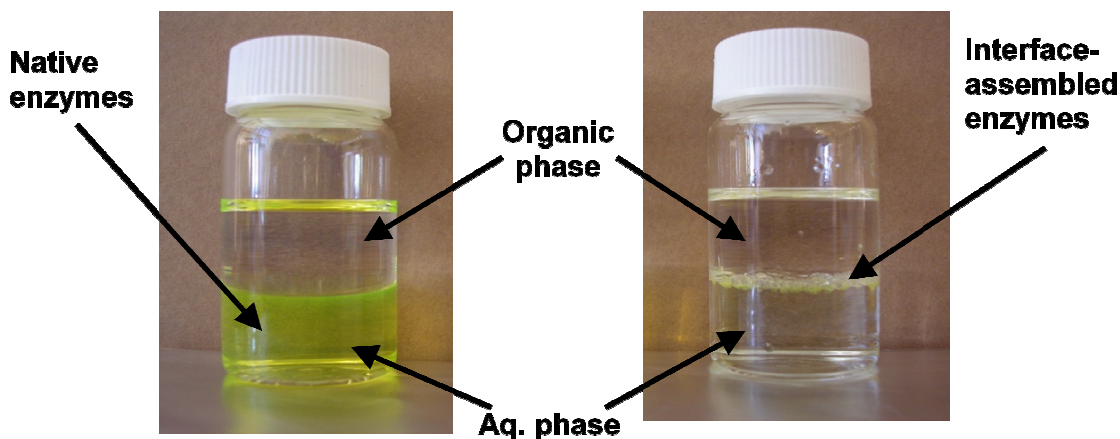


Figure 3-1 Interfacial assembly of PS-ADH conjugate  
Left – Native ADH RS1 dyed with Oregon Green in water phase, Right – Polymer-enzyme dyed conjugate at hexane-water interface

### 3.3.2 Surface pressure analysis of interface assembled enzyme

When an amphiphile is spread on water at low surface concentration, the initial molecular organization is random. As the barrier is drawn across the trough, the surface area available to the amphiphiles is reduced and the molecules are pushed closer together. The surface pressure ( $\pi$ ) will increase, provided the molecules remain on the surface and do not form bulk aggregates. As the pressure increases and the amphiphiles are compressed into a smaller area, the molecular organization increases as molecules make contact and begin to interact. An increase in pressure is observed as the area decreases. The first such inflection is typically from the liquid expanded phase to the liquid-condensed phase. On further reduction of area, a point is reached at which structural



collapse occurs and molecules are forced out of the two-dimensional plane. A schematic of Langmuir trough set-up is shown in Figure 3-2.

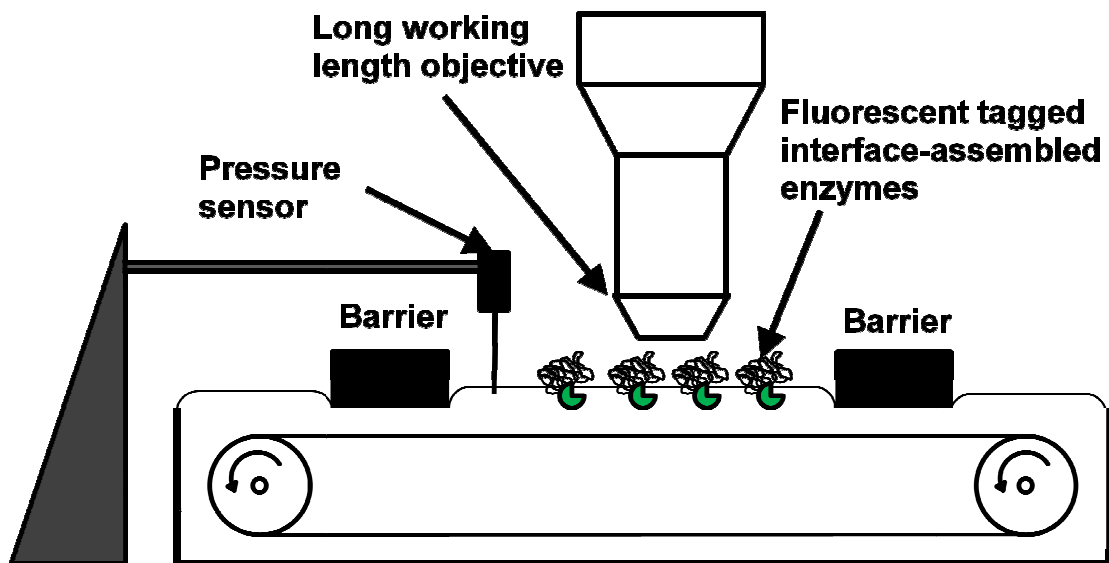


Figure 3-2 Schematic of Langmuir trough set-up for surface pressure analysis

The Langmuir trough or film balance study for observing the assembly behavior of modified enzyme clearly indicates a potential for monolayer assembly of the enzymes at the interface (Figure 3-3). The isotherm indicates that initially when the barriers are wide apart, the monolayer has a relatively weak attraction between molecules does very little to change the surface tension of the subphase. In this region the monolayer is commonly considered to behave as a “gas phase”. On compression at the first transition point the monolayer takes the form of expanded liquid. The kink in the isotherm or the transition point suggests that the monolayer can be further compressed without appreciably changing the pressure. This relatively flat plateau strongly suggests a phase transition and a well purified sample. The monolayer transition in its fluidity was

confirmed using fluorescence microscopy. Because of the large size of the molecule the polymer-enzyme conjugate it is difficult to suggest an exact molecular structural reason for this transition. One possibility is that the enzyme may be lying about its axis at the interface but on further compression the polymer is pushed out of the interface forcing the modified enzyme to take a more upright configuration at the interface. The small kink shown in Figure 3-3 did not appear to be the result of some impurity. This was concluded by rinsing the sample various times and the kink still remained.

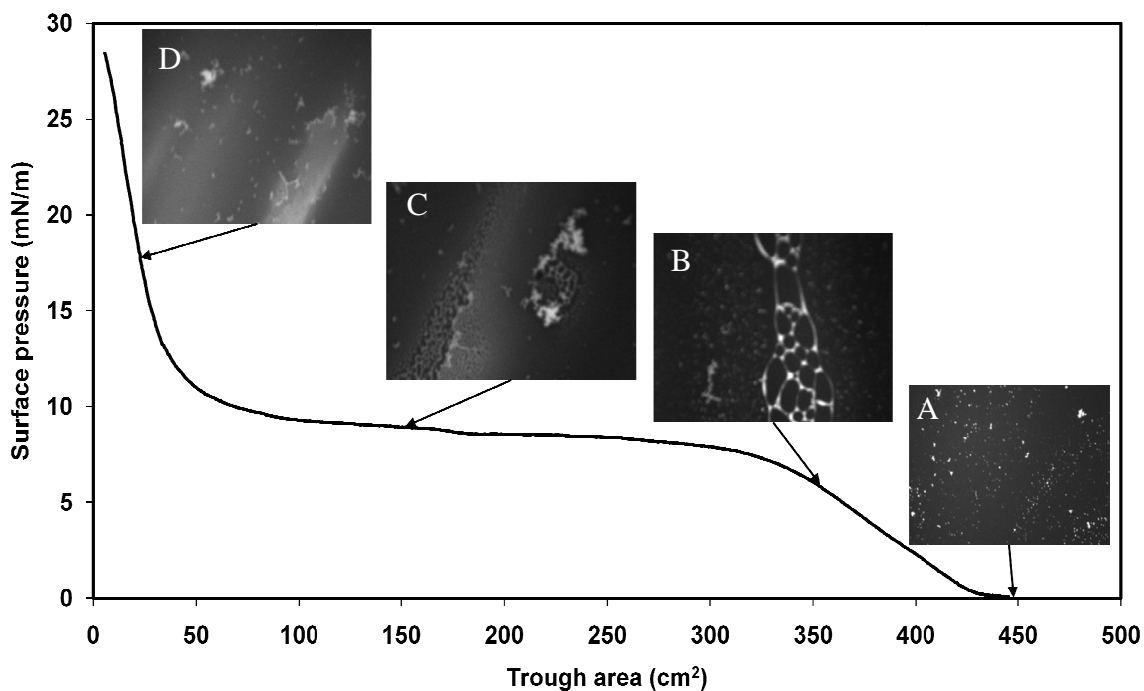


Figure 3-3 Surface pressure isotherm of interface-assembled ADH RS1  
On compression the monolayer behaves like (A) gas phase (B) liquid expanded phase (C) transition phase (D) liquid condensed phase.

The observation of small but significant transition in the plateau region of the surface pressure isotherm may be due to entanglement of the pushed out polymers forming a compressed liquid phase or fluid gel phase, or the change in the amount of

interfacial water hydrating the enzyme. The final transition observed in the monolayer looks typical of a liquid expanded to liquid condensed transition. In Figure 3-4 the purity of the modified enzyme was verified by comparing the surface pressure isotherms of different preparations of interface assembled enzyme with varying degree of rinse of organic and aqueous phase. To verify if that transition is due to presence of impurities, a study was performed with treating the modified enzyme with varying degree of rinse in both aqueous and organic phase. Any unmodified molecule at the interface will be eventually taken out of the interface by repeated rinse with toluene and buffer. However, Figure 3-4 indicates that increase of rinse more than three times does not appreciably change the isotherm behavior, indicating that the small kink in the plateau region is real and corresponds to a physical change within the monolayer.

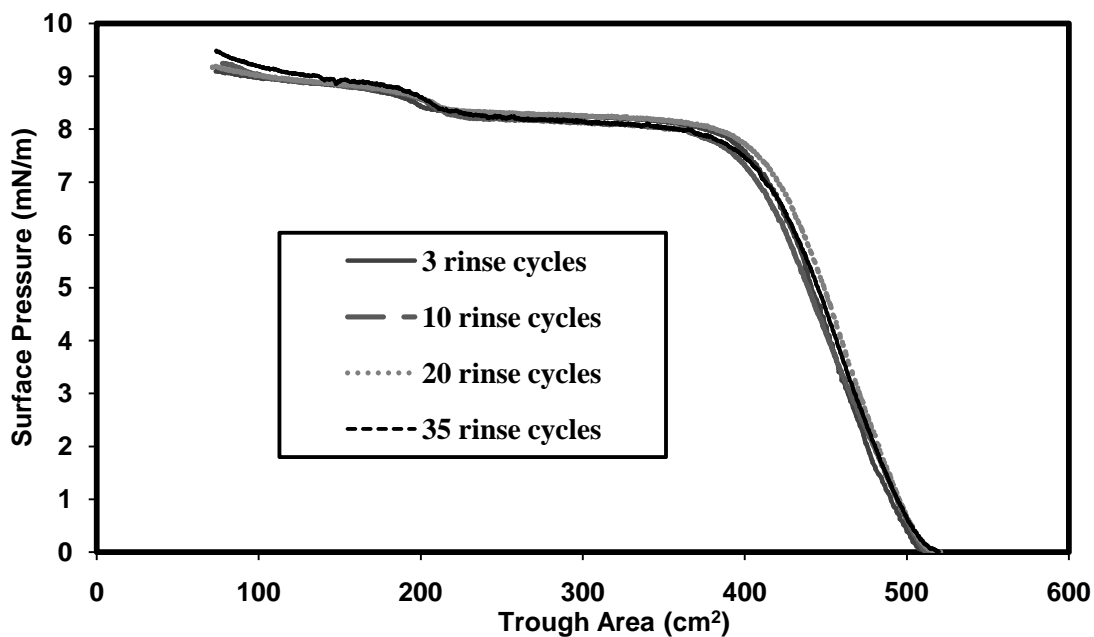


Figure 3-4 Effect of varying degree of rinse on interface-assembled ADH RS1's surface pressure isotherm.

### **3.3.3 Molecular diffusion measurements using fluorescence recovery**

FRAP is a technique used in cellular imaging and has been employed since the early 1970s to study molecular mobility in the plasma membrane, other organellar membranes, and the cytoplasm[149-151]. FRAP involves selective destruction of fluorescent molecules within a region of interest with a high-intensity laser, followed by monitoring of the recovery of new fluorescent molecules into the bleached area over time with low-intensity laser light. As photobleaching irreversibly damages fluorophores, the recovery of the fluorescence within the photobleached region is due to random motion or diffusion of the unbleached fluorescent molecules from the surroundings over time. The kinetics of recovery can be empirically determined by the time  $t_{1/2}$  required to reach 50% of complete recovery. The resulting information can be used to determine kinetic properties, including the diffusion coefficient, mobile fraction, and transport rate of the fluorescently labeled molecules[152, 153].

FRAP experiments were performed on a confocal microscope (Nikon C1 series, NY). A 561 nm helium–argon laser was used for excitation (Figure 3-5). Three prebleach measurements of fluorescence intensity were taken with the 20% laser power, after which a circular area with a diameter of 0.046 mm was photobleached for six seconds using a fast scan rate at 100% laser power. Recovery of fluorescence within the region was imaged at a laser power of 20% of 561 nm line for 180 frames consecutively with a time delay of 60 seconds. The data obtained were corrected using fractional recovery. The

obtained fractional recovery curves were fitted with a model for uniform-disk illumination conditions[154].

$$f(t) = e\left(\frac{-2\tau_D}{t}\right)\left[I_0\left(\frac{2\tau_D}{t}\right) + I_1\left(\frac{2\tau_D}{t}\right)\right] \quad 3-1$$

Where  $I_0$  and  $I_1$  are modified Bessel functions. The diffusion coefficient can be calculated using equation (3-2) from the diffusion time  $\tau_D$  obtained from fitting the equation.

$$D = \frac{\omega^2}{4\tau_D} \quad 3-2$$

Where  $\omega$  is the radius of the bleached ROI. This equation assumes unrestricted two-dimensional (2D) diffusion in a bleached area with no recovery from above and below the focal plane.

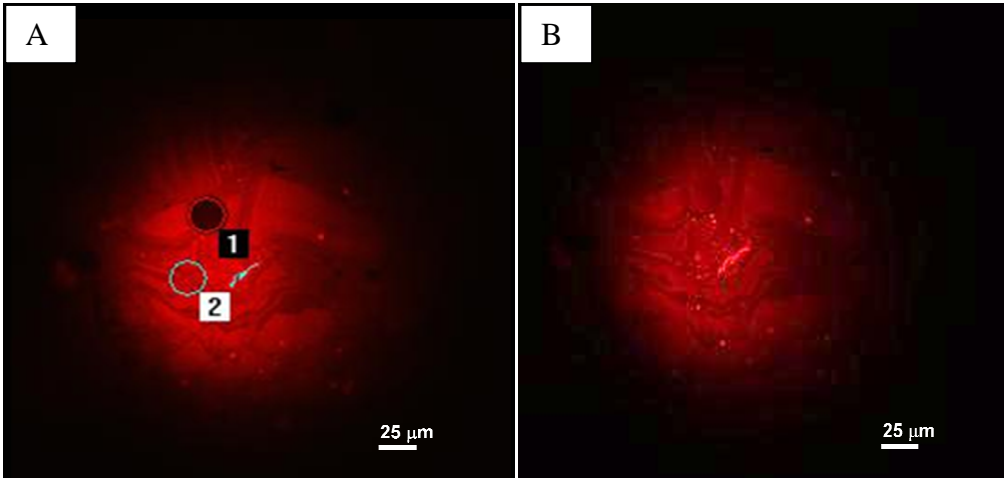


Figure 3-5 FRAP analysis on interface assembled ADH RS1  
 (A) Photo bleached circular area at the interface, spots 1 and 2 represent the bleached and the control area respectively. (B) Recovered area after 180 minutes

The recovery data was corrected for the photobleaching during recovery process due to exposure to the laser source (Figure 3-6). Fitting the corrected recovery curve with

equation 3-1 gave a characteristic time of 32.8 minutes. The bleach radius was 23  $\mu\text{m}$ , using the equation 3-2, the diffusion coefficient was calculated to be  $6.7 \times 10^{-10} \text{ cm}^2/\text{sec}$ . It is three orders of magnitude less than that of native protein in solution, which has a diffusion coefficient in the order of  $10^{-7} \text{ cm}^2/\text{sec}$ [155]. However, the diffusion coefficient obtained for interface-assembled enzyme is on the same magnitude as that for membrane binding proteins in natural systems[156]. The lower value of diffusion coefficient of interface-assembled enzyme than that of native enzymes is due to the limited mobility of the interface-assembled enzyme at the oil-water interface. This limited two dimensional mobility will affect the activity of the interface-assembled enzyme. The issue of limited mobility is addressed in subsequent chapters.

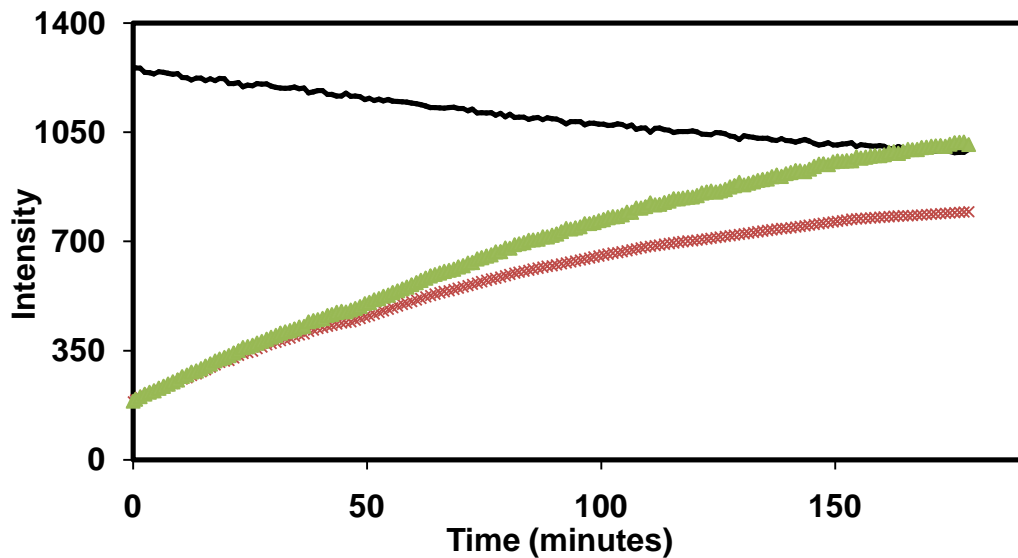


Figure 3-6 Quantitative FRAP data for evaluating diffusion coefficient (-) Normal photobleaching of control area (x) Recovery of the bleached spot (▲) Normalized recovery corrected for photobleaching

### **3.4 Conclusion**

Attachment of hydrophobic polymer to a dehydrogenase enzyme, ADH RS1, yielded a stable interface-assembled enzyme. Surface pressure analysis of the interface-assembled enzymes indicated a monolayer formation with distinct transformation of phases at the interface. The surface pressure isotherms were repeatable indicating a monolayer formation of interface-assembled enzymes with little or no aggregates formation at the interface. The FRAP analysis gave the two dimensional diffusion coefficient of the interface-assembled enzyme at the oil-water interface. The diffusion coefficient is three orders of magnitude less than that of native enzyme, indicating the mobility of the enzyme at the interface may be a chief limiting factor in evaluating the activity of the interface-assembled enzyme.

## CHAPTER IV

# STABILIZATION OF INTERFACE-BINDING CHLOROPEROXIDASE FOR INTERFACIAL BIOTRANSFORMATION

### 4.1 Introduction

An enzyme molecule on adsorption at an interface starts to unfold and results in rearrangement of the macromolecular structure. This occurs because of the enzyme experiences a different thermodynamic environment at the interface from that previously experienced in bulk phase, which alters the relative contributions of the various forces that determined its three dimensional structure[12]. Therefore, the enzyme molecule unfolds to attain the lowest free energy conformation in accordance with the new environment. The major driving force for protein unfolding at the interface is the hydrophobic effect that rearranges the structure of enzymes by placing predominantly non-polar polypeptide segments in oil phase and polar segments in aqueous phase. On modification of enzymes with polymer to self-assemble at oil-water interface, the presence of polymer protects the enzyme from unfolding. Also, the localization of the modified enzyme at the interface shields the enzyme from higher concentration of bulk phase denaturants. Epoxidation of styrene by chloroperoxidase (CPO) was chosen as a model reaction system to investigate the factors affecting the stability of interface-assembled enzyme.

CPO catalyzes the enantioselective synthesis of a broad range of valuable compounds[157-161]. In particular, the preparation of optically active epoxides, which



are versatile chiral intermediates[162] has been much explored over the past two decades. However, the lifetime of CPO under normal reaction conditions using  $\text{H}_2\text{O}_2$  as oxidant lasts for only about 30 min[163]. Longer lifetime of CPO can be realized by controlling the concentration of  $\text{H}_2\text{O}_2$  at low levels. However, this usually does not significantly improve the overall turnover number of the enzyme.

One additional issue in using CPO for organic synthesis is the immiscibility of its hydrophobic and hydrophilic substrates. Traditionally, biphasic reaction systems with enzymes applied in the aqueous phase have been employed to carry out biotransformation that involve immiscible reactants [91, 92]. An obvious drawback of such a reaction configuration is that only enzyme molecules in the vicinity of interfaces are effectively involved in the reaction, while the majority of the catalysts in the bulk aqueous phase are not used[101, 164]. Wang and coworkers [112, 165] recently reported that interfacial biocatalysis with interface-binding enzymes could significantly improve the overall catalytic efficiency of enzymes for biphasic reactions. Interface-binding enzymes were prepared by conjugating enzyme molecules with hydrophobic polymers such as polystyrene (PS). In the case of CPO, the PS-conjugated enzyme could improve the overall productivity of CPO by up to 25 times[165]. That was a combined result of the improved catalytic kinetics and reduced enzyme exposure to the aqueous phase-based  $\text{H}_2\text{O}_2$ . Still, deactivation by  $\text{H}_2\text{O}_2$  is the limiting factor.

One approach to improve the stability of CPO is to control the exposure of the enzyme to  $\text{H}_2\text{O}_2$ . There are different ways to achieve that. Slow addition of  $\text{H}_2\text{O}_2$  [166] and *in situ* generation of  $\text{H}_2\text{O}_2$  by using GOx[167], as attempts to avoid contacting the

enzyme with concentrated H<sub>2</sub>O<sub>2</sub>, have been reported effective in extending the duration of the enzyme activity. Compared to the addition of H<sub>2</sub>O<sub>2</sub>, *in situ* generation could avoid enzyme deactivation at the entry point of H<sub>2</sub>O<sub>2</sub> inlet where high local concentration of peroxide is expected[167]. Encapsulation is another way to control the exposure of CPO to H<sub>2</sub>O<sub>2</sub>. It was reported recently that encapsulation of CPO in porous silica glass also improved the enzyme stability[161, 168]. Even though various factors may contribute to this stabilization effect, it seems to us it is mostly due to the reduced direct exposure of the enzyme, or reduced local concentration of peroxide in the vicinity of the enzyme. Similar mechanisms resulted in enhanced stability of interface-binding CPO, which is also only partially exposed to the peroxide solution[165].

Another approach to stabilize CPO is the use of stabilizers. Andersson *et al.* [169] reported that the addition of polyethyleneimine (PEI) improved the storage stability of native CPO. In this work, as an attempt to further extend the operational life time of the interface-bound CPO, The effectiveness of both the stabilizers and *in situ* generation of H<sub>2</sub>O<sub>2</sub> in biphasic reaction systems was evaluated.

## **4.2 Materials and Methods**

### **4.2.1 Chemicals**

Chloroperoxidase (CPO) from *Caldariomyces fumago* (EC 1.11.1.10, 26 IU/mg, R<sub>Z</sub>-1.12) was provided as a gift from Bio-Research Products, Inc. (North Liberty, IA). Glucose oxidase (EC 1.1.3.4, 245.9 IU/mg) was obtained from Sigma. Styrene (99%) and citric acid were purchased from EM Science (Gibbstown, NJ). Potassium sodium tartrate,

polyethylene glycol (PEG, Mw 550), glucose, and ethylene glycol were purchased from Sigma (St. Louis, MO). (S)-(-)-styrene oxide (98%), (R)-(+)-styrene oxide (98%), polyethyleneimine (PEI, Mw 2000), polyvinyl alcohol (PVA, Mw 13000-23000), polyacrylonitrile (PAN) and bathocuproinedisulfonic acid disodium salt were purchased from Aldrich Chem. Co. (Milwaukee, WI). Glycerol was obtained from Fluka. sucrose monododecanoate (Ryoto sugar ester) was obtained from Mitsubishi-kugaku foods corporation (Japan). H<sub>2</sub>O<sub>2</sub> aqueous solution (30v/v) was purchased from Fisher Scientific (Fair Lawn, NJ). Sodium citrate (99%) was purchased from Alfa Aesar (Ward Hill, MA). Carboxyl chloride terminated polystyrene (PS-COCl, Mw 2020) was purchased from Polymer Source, Inc. (Canada). Toluene was purchased from J.T. Baker (Phillipsburg, NJ). Protein assay dye reagents and BSA standard were purchased from Bio-Rad laboratories (Hercules, CA). CuSO<sub>4</sub> (5H<sub>2</sub>O) and NaOH were purchased from VWR Sci. (PA). Ascorbic acid was purchased from Mallinckrodt, KY.

#### **4.2.2 Modification of enzymes**

The modification of chloroperoxidase with polystyrene in a biphasic system and subsequent characterization of the resulted interface-binding CPO was performed according to the method described by Zhu *et. al.*[112]. Typically, 5 mg of CPO was dissolved in 1 ml of 0.05M pH 4.5 citrate buffer and the solution subsequently added to 1 ml of toluene containing 5 mg of PS-COCl. The reaction was carried out at room temperature for 8 h under shaking at 240 rpm. The reaction mixture was then centrifuged at 12,000 rpm for phase separation. The interface-binding modified CPO, was recovered

by removing the bulk phase solutions. The product was further purified by washing with buffer and toluene, each for at least 5 times, to remove residual free enzyme and polymer modifier. The same procedure was followed for the modification of GOx.

Protein loadings of polymer-enzyme conjugates were determined by the reverse biuret method[147]. Two analytical reagent solutions were first prepared and stored at room temperature: reagent A was prepared by dissolving 15 mg  $\text{CuSO}_4 \cdot 5\text{H}_2\text{O}$ , 45 mg of potassium sodium-tartrate and 2.4 g NaOH into 100 ml DI water, while reagent B was prepared by dissolving 25 mg ascorbic acid and 37 mg of bathocuproinedisulfonic acid disodium salt in 100 ml DI water. Typically 1 mg of interface-binding CPO and 10  $\mu\text{l}$  water were added to 200  $\mu\text{l}$  reagent A and the mixture was incubated at  $37^\circ\text{C}$  for 5 min. Then 1000  $\mu\text{l}$  of reagent B was added and incubation was continued for an additional 0.5 minute. The solution was filtrated through 0.2  $\mu\text{m}$  syringe filters and the absorbance at 485 nm was measured for the filtrate on a Shimadzu uv-1601 UV-Vis spectrophotometer. The protein content was calculated using BSA calibration determined through the same procedure except that the 10  $\mu\text{l}$  water was replaced with protein solutions of the same volume. Typical protein loading was  $\sim 0.2$  mg-protein/mg conjugate.

#### **4.2.3 Styrene epoxidation by chloroperoxidase**

Reactions were carried out in a biphasic system. Batch reactions were conducted in a 50-ml magnet stirred reactor, stirred at 600 rpm. Styrene (4 ml) and toluene (1ml) was used as the organic phase, while 10 ml of pH 4.5 citrate buffer (0.05 M) was applied for the aqueous phase. For reactions with both native and interface-binding CPO, the

enzyme concentration was controlled at  $0.04 \text{ mg ml}^{-1}$ , totally 0.4 mg of CPO, in aqueous phase. The concentration of all the chemical stabilizers was maintained at 5 mM in aqueous phase.  $\text{H}_2\text{O}_2$  was introduced by either *in situ* generation or direct addition through syringe pump. For *in situ* generation, GOx concentration was maintained at  $0.08 \text{ mg ml}^{-1}$  in the aqueous phase. Initial concentration of glucose was made to 100 mM in the aqueous phase that had  $7.8 \text{ mg ml}^{-1}$  of dissolved oxygen. For reactions with interface-binding GOx, 0.8 mg of PS-conjugated GOx was used for the same reaction size. For direct addition, 100 mM of  $\text{H}_2\text{O}_2$  was added to the reaction mixture by a syringe pump at the rate of  $8.2 \times 10^{-3} \text{ ml min}^{-1}$ .

#### **4.2.4 GC analysis of styrene epoxides**

The reaction was monitored by measuring the concentration of products in organic phase using Gas Chromatography (GC-17A, Shimadzu) equipped with a  $\beta$ -DEX<sup>TM</sup> 225 fused silica capillary column (30 m x 0.25 mm x 0.25  $\mu\text{m}$ , from supelco Bellefonte PA) Aliquots of 180  $\mu\text{l}$  for GC analysis were taken periodically from the organic phase during the reactions. The temperature of the column was kept at  $110^\circ\text{C}$  with injection temperature at  $220^\circ\text{C}$  and detector temperature of  $300^\circ\text{C}$ . The GC chromatograms showed separated peaks for R- and S-styrene epoxides. Commercially purchased R- and S-styrene epoxide standards were used for calibrations.

#### **4.2.5 Pretreatment for stabilizer addition**

All the stabilizers were readily miscible with citrate buffer except sucrose monododecanoate, which was dissolved in hot buffer at 50°C. The buffer was cooled to 22°C before the reaction initiated. The pH of the buffer was adjusted to 4.5 after addition of PEI since the polymer is slightly basic.

### **4.3 Results and Discussions**

#### **4.3.1 Effect of stabilizers on operation stabilities of native and PS-conjugated CPO**

It is generally believed the deactivation of CPO by H<sub>2</sub>O<sub>2</sub> is caused by the oxidation of porphyrin ring by species such as superoxide anions, hydroxyl radicals and singlet oxygen that are produced during the catalytic cycle[170]. The oxidized intermediate form of CPO, compound I, possessing a heme radical cation coordinating Fe<sup>IV</sup>=O functionality was believed to cause enzyme deactivation if compound I is not quickly reduced by the subsequent oxidation reaction of substrates. Slower oxidation of the substrate generates higher possibilities for enzyme deactivation. Under normal reaction conditions, native CPO's activity lasts only about 20 minutes. Desired stabilizers should ideally be able to interact with the species that causes the oxidation of porphyrin ring, thereby slow down the oxidation and at the same time do not hinder the oxidation reaction of substrates.

Andersson *et al.* [169] reported that the addition of polyethyleneimine (PEI) improved the storage stability of native CPO. While the result was greatly interesting, that was not a systematic evaluation of different types of stabilizers. In this section, the

stabilization effect for native CPO of several different types of stabilizers including polymers and small molecules was first evaluated. Table 4-1 shows the effect of stabilizers on the operational stability of native CPO.

Table 4-1 Effect of stabilizer on native CPO productivity

Stabilizer	Initial reaction rate <sup>a</sup>	TTN <sup>b</sup>	Lifetime (min)	ee (%)
without stabilizer	0.37	260	20	47
PEG	0.28	346	50	58
PEI	0.32	217	20	57
PAN	0.33	261	40	58
Glucose	0.29	252	50	59
Glycerol	0.29	244	35	59
Ethylene glycol	0.33	200	12	53
Sucrose monododecanoate	0.45	284	20	52

<sup>a</sup>Initial reaction rate in  $\mu\text{mol}$  product per mg chloroperoxidase per minute

<sup>b</sup>Total turnover number (mol product/mol chloroperoxidase)

Although the use of PEI to extend the storage stability of CPO against  $\text{H}_2\text{O}_2$  was found effective, the activity of CPO was found slightly decreased [169]. In the evaluation of operational stability, PEI did not show any effect on the duration of the activity of the enzyme (Table 4-1). The initial reaction rate in the presence of PEI was slightly lower than that of CPO without addition of any stabilizers. Interestingly, PEG, PAN and glucose all effectively extended the duration of the CPO activity -- the operational lifetime was extended by up to 2.5 times. Although CPO still shows the highest initial reaction rate without any of these additives, PEG increased the total turnover number (TTN) of the enzyme by 33%. Glycerol, a widely used protein stabilizer, also showed stabilizing effect for CPO, but the resulted TTN was lower than

pure CPO. Noticeably, ethylene glycol, the monomer of PEG, decreased the operational lifetime of CPO. The actual reason for that is not clear at this moment. Sucrose monododecanoate did not alter the lifetime of CPO, but increased initial reaction rate. The increased reaction rate may be attributed to the functionality of sugar ester as a surfactant, which may help the dispersion and improves the availability of styrene for reaction in the aqueous solution.

All the stabilizers examined changed the enantioselectivity of CPO. The epoxidation reaction of styrene, CPO usually shows an *ee* number that ranges from 46 to 49% in either monophasic aqueous or biphasic reactions [163, 165, 171]. The selectivity of CPO also seemed to be quite sensitive to reaction conditions. The addition of stabilizers increased the *ee* number as high as 20%. That implies that the stabilizers may interact with active intermediates of CPO, and subsequently influence enzyme-substrate interactions. The *in situ* generation of H<sub>2</sub>O<sub>2</sub> by using GOx as to be discussed separately, the *ee* number of CPO was found in the range of 59~62%.

The effect of stabilizers on activity of interface binding CPO is shown in Table 4-2. Overall, the stabilizers showed similar effects on the reactions with interface-binding CPO. For interface binding CPO, the highest TTN with a value of 423 was observed with the addition of PEG. That is about 57% higher than that of the interface-binding CPO without any additives. From the results as shown in Table 4-1 and Table 4-2, PEG appeared to decrease the reaction rate for native CPO, but increased the initial reaction rate for interface-binding CPO. It is believed that PEG may help the dispersion of the interface-binding CPO at the oil-water interface; along with forming a solvent layer



around enzyme that can protect the enzyme from local high concentration of H<sub>2</sub>O<sub>2</sub> facilitate the reaction kinetics. Except PEG, all the other additives resulted in similar reaction rate with both native and interface binding CPO. Their effects on the enantioselectivity of the enzyme remained about the same.

Table 4-2 Effect of stabilizer on Interface-binding CPO productivity

Stabilizer	Initial reaction rate <sup>a</sup>	TTN <sup>b</sup>	Lifetime (min)	ee (%)
without stabilizer	0.35	269	30	49
PEG	0.48	423	50	59
PEI	0.31	239	30	57
PAN	0.28	216	45	59
PVA	0.22	144	20	53
Glucose	0.34	296	55	58
Glycerol	0.33	290	50	58
Ethylene glycol	0.34	211	15	54
Sucrose monododecanoate	0.45	284	25	52

<sup>a</sup>Initial reaction rate in μmol product per mg chloroperoxidase per minute

<sup>b</sup>Total turnover number (mol product/mol chloroperoxidase)

#### 4.3.2 Effect of stabilizers on storage stabilities of native and PS-conjugated CPO

One question remained unanswered is that at what stage the stabilizers influence the lifetime of enzyme: during the reaction or via pre-reaction interactions with the enzyme. Toward that, Experiments were conducted to evaluate the stabilizers' effects on the storage stability of CPO. This was performed by conditioning the CPO, both native and PS-conjugated, in the presence of both stabilizers and H<sub>2</sub>O<sub>2</sub> before initiate the reactions.

The results are shown in Figure 4-1 and Figure 4-2 for native and PS-conjugated CPO, respectively. The storage stability of CPO without stabilizers was examined by incubating CPO with 1 mM H<sub>2</sub>O<sub>2</sub> and toluene (buffer: solvent = 1:1 ml). After certain amount of time of incubation, the reaction was started with addition of styrene. Native CPO was found completely deactivated in less than 10 minutes, whereas interface-binding CPO's activity lasted for 30 minutes of incubation. Again, this stabilization may be due to partial exposure of the interface-bound CPO to H<sub>2</sub>O<sub>2</sub>, which was held in the bulk aqueous phase.

Not all the stabilizers improved storage stability of CPO against H<sub>2</sub>O<sub>2</sub>. In the case of native CPO, only PEG and PEI showed evident stabilization. After 60 minutes of incubation with 1 mM H<sub>2</sub>O<sub>2</sub> in the presence of PEG or PEI, native CPO retained 45% (with PEG) to 30% (with PEI) of its original activity (also tested in the presence of the corresponding stabilizers in order to offset their effects on reaction rates). The enzyme activity loss appeared to happen in the early stage of incubation, since the enzyme maintained that level of activity throughout the subsequent one day incubation. On the other hand, PEG and PEI enhanced the storage stability of PS-conjugated CPO against H<sub>2</sub>O<sub>2</sub> much more significantly. After incubation for one day, the enzyme still maintained about 60% of its original activity (Figure 4-2). In addition, the activity loss took place gradually throughout the course of incubation. One hypothesis is that the addition of polymeric species may hinder the interaction between the interface-bound CPO with H<sub>2</sub>O<sub>2</sub> by forming solvent layer around the enzyme's aqueous side through hydrogen

bonds. The actual cause for such observations, along with the mechanisms of the stabilizer's function, may need further systematic studies before being fully understood. In addition to PEG and PEI, glucose and glycerol showed modest but detectable stabilizing effect (Figure 4-2).

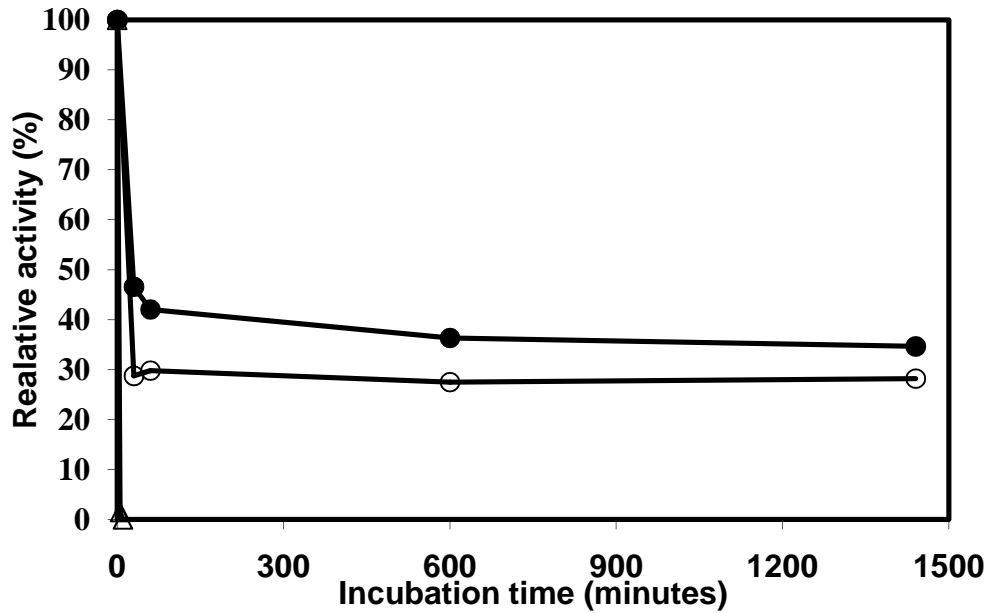


Figure 4-1 Storage stability of native CPO with 1 mM H<sub>2</sub>O<sub>2</sub> (Δ) without stabilizers; (●) with PEG; (○) with PEI.

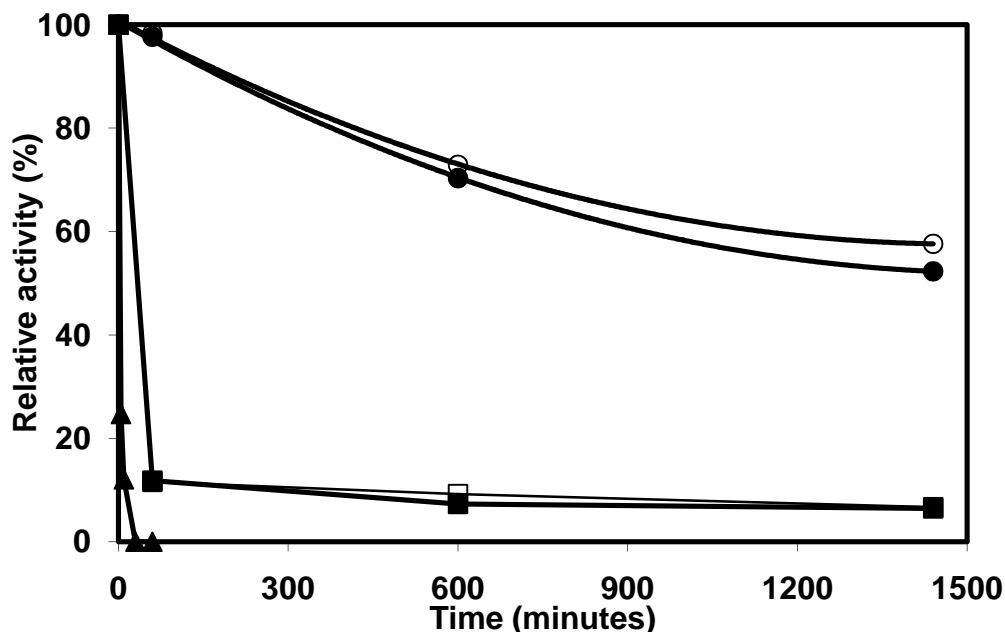


Figure 4-2 Storage stability of PS-CPO with 1 mM H<sub>2</sub>O<sub>2</sub> (▲) without stabilizers; (●) with PEG; (○) with PEI; (■) with Glucose; (□) with Glycerol.

#### 4.3.3 Enzyme stabilization via *in situ* generation of H<sub>2</sub>O<sub>2</sub>

As has been reported previously by others [167], It was also observed that the *in situ* generation of H<sub>2</sub>O<sub>2</sub> by using GOx improved the operational stability of CPO. Both native and PS-conjugated GOx were tested. With native CPO (Figure 4-3), the use PS-GOx resulted higher apparent reaction rate than the use of native GOx. PS-GOx, which has a structure as a surfactant, may help to reduce the size of oil droplet in the emulsion solution, and thus improve the overall reaction rate of CPO. At the same time, native CPO showed longer lifetime in the presence of PS-GOx. The reaction with PS-GOx continued even after one hour, while the reaction with native GOx stopped at 30 min (Figure 4-3). That may be a result of the fact that when PS-GOx is used, H<sub>2</sub>O<sub>2</sub> is mostly

generated and consumed in the interface region, while the majority of CPO is mostly exposed to glucose (which stabilizes CPO) in the aqueous solution. Whereas in the case of native GOx, even though CPO is also exposed to glucose, but since GOx is also dissolved in the same solution, H<sub>2</sub>O<sub>2</sub> is generated and exposed to CPO homogeneously. The lifetime is then a result that combines the stabilizing effect of glucose and the deactivation effect of H<sub>2</sub>O<sub>2</sub>. Different from what was observed for native CPO, PS-CPO exhibited lower reaction rate when PS-GOx instead of native GOx was used (Figure 4-4). It had been previously observed that when too much enzyme assembled at the interface, the reaction rate generally decreased since the thick assembly of proteins at the interface might present mass transfer resistance to the reaction[112]. That mechanism may explain the current observation with interface-bound GOx and CPO since the assembling of both may generate a thick film. However, the lifetime of PS-CPO was longer with PS-GOx than that with native GOx. Overall, comparison of the results presented in Figure 4-3 and Figure 4-4, it is obvious that the best productivity was achieved with the combination of native CPO and PS-GOx.

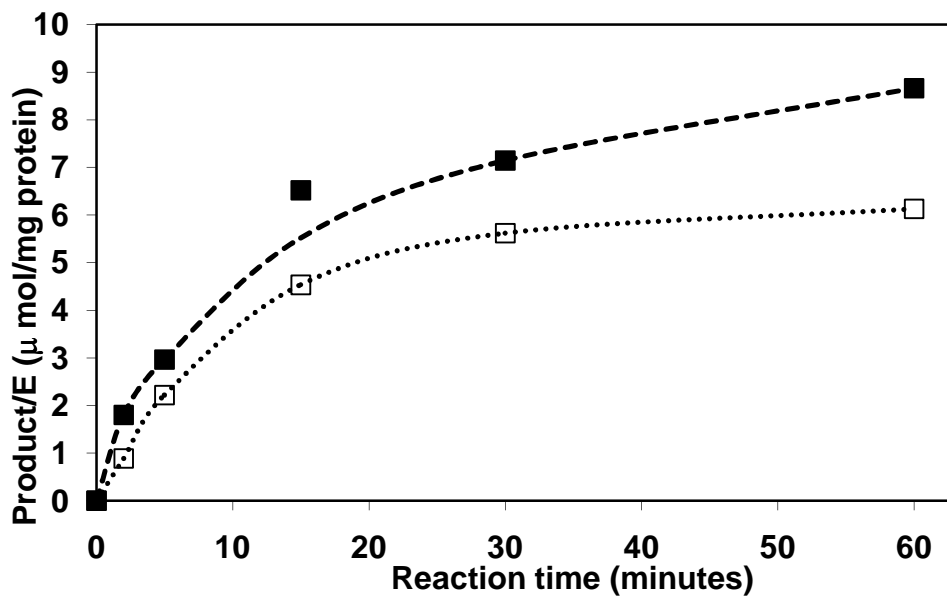


Figure 4-3 Time course of styrene epoxidation catalyzed by native CPO with *in situ* generation of H<sub>2</sub>O<sub>2</sub>  
 (■) interface-binding GOx and (□) native GOx

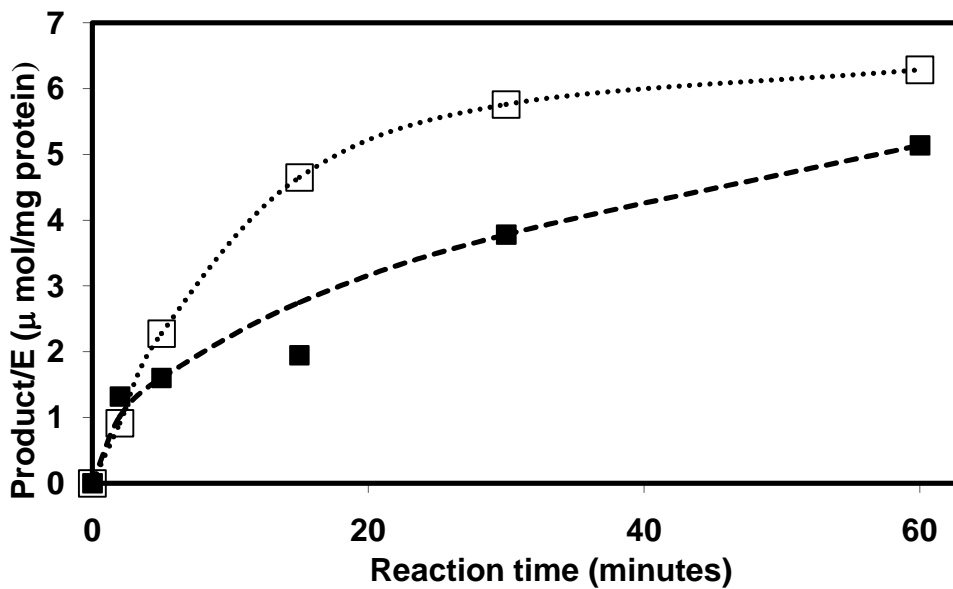


Figure 4-4 Time course of styrene epoxidation catalyzed by PS-CPO with *in situ* generation of H<sub>2</sub>O<sub>2</sub>  
 (■) interface-binding GOx and (□) native GOx

#### 4.4 Conclusion

In summary, the performance of CPO appeared to be sensitive to a number of factors; however the understanding of the effects of these factors remains preliminary at this stage. From the experimental observation, interface-assembled CPO was generally more stable against  $\text{H}_2\text{O}_2$  deactivation than native CPO under emulsion conditions. A number of additives including PEG, PEI and glucose were found effective in stabilizing the enzyme. Among the stabilizers examined, PEG appeared to be most effective by protecting the enzyme against hydrophobic and  $\text{H}_2\text{O}_2$  deactivation by forming a solvent layer around the aqueous side of enzyme. One interesting observation with PEI is that it enhanced the storage stability against  $\text{H}_2\text{O}_2$  deactivation, but did not affect the enzyme's operational stability. On the other hand, glucose enhanced the operational stability by 2 folds, but exhibited no significant effect on storage stability. *In situ* generation of  $\text{H}_2\text{O}_2$  using GOx improved the operational stability of CPO as a result of the stabilizing effect of glucose and the homogeneous generation of  $\text{H}_2\text{O}_2$ .

## CHAPTER V

# SYNTHESIS OF INTERFACE-BINDING COFACTORS FOR BIOTRANSFORMATIONS ACROSS OIL-WATER INTERFACES

### 5.1 Introduction

The application of interfacial enzyme catalysis can be broadened considerably by developing a method for interfacial biotransformations with multienzyme-cofactor systems. The advantage of using enzymes like dehydrogenases along with cofactor for biosynthesis is that they allow for a wide range of possible reactants, and provide a higher level of molecular recognition[172-174]. Cofactors are an important class of biochemicals essential to the activities of a dehydrogenase class of enzymes in biological systems. The role of cofactors has become increasingly important in biosynthesis and different applications that includes various analytical, biomedical and technological processes, wherein they take part in wide range of redox reaction in food and pharmaceutical industries[175-177]. Presently the main constraint in use of cofactors is economic, cofactors like NAD(P)H are unstable and expensive molecules[178, 179]. Unlike electron transfer centers such as heme, copper and flavin in other enzymes, cofactors for dehydrogenase exist free in solution and function by binding to enzymes transiently during enzymatic oxidation and reduction[180-182]. Stoichiometric cofactors that are consumed in dehydrogenase catalyzed reaction are required to be efficiently regenerated for process economy. Multienzyme coupled oxidation-reduction reactions



system has been used for cofactor regeneration[61, 183-185]. The hydrophilic nature of cofactors has limited their application to aqueous phase reactions, earlier efforts have attempted cofactor use and regeneration in organic phase[186, 187]. However, an important limitation had been the requirement of regeneration chemicals to be organic soluble, which are expensive and may not be available for many reaction systems. Alternatively, the cofactors can be modified to make them interface-binding, allowing organic phase synthesis with aqueous-based cofactor regeneration with relatively cheap and easily available chemicals. While modification of enzymes has been adopted widely for improvement of their efficiency in artificial reaction environments, little have been done with respect to chemical modification and engineering cofactors. Preparation of macromolecular derivatives and immobilization of cofactors have been reported previously[188-190]. However, this study represents the first attempt in modifying the cofactors for self-assembly at liquid-liquid interface.

It was previously shown that macromolecules like enzymes can be directed towards liquid-liquid interface by conjugation with polymers[112, 191] and interfacial multienzyme reactions can be realized with multiple turnover of cofactor[121]. In this study the activity and stability of interface-assembled cofactors with two separate multienzyme reaction systems with contrasting characteristics is evaluated. ADH LB and GluDH with free and interface assembled NADPH were used for reduction of acetophenone to S-(-)-1-phenylethanol in the organic phase with simultaneous oxidation of glucose to gluconic acid in aqueous phase. ADH RS1 and GDH with free and interface assembled NADH were used for reduction of acetophenone to R-(+)-1-phenylethanol in

the organic phase with simultaneous oxidation of glycerol to dihydroxyacetone in aqueous phase. This novel self-assembling multienzyme-cofactor system at liquid-liquid interfaces will open new avenues for interfacial science of proteins and promote advancement in bioprocessing technologies. The scaled up process of interfacial multienzyme reaction strategy is expected to enhance the potential of enzymes for various applications including organic synthesis, pollutant degradation, and fuel processing.

## **5.2 Materials and Methods**

### **5.2.1 Chemicals**

Glucose Dehydrogenase (GluDH) “Amano” NA ( EC 1.1.1.47, 286 IU/mg) was a gift from Amano Enzyme Inc. (Nagoya, Japan). Alcohol Dehydrogenase (ADH RS1) from *Rhodococcus* species (EC 1.1.1.1, 444 IU/ml) was obtained from Julich Chiral Solutions (Julich, Germany). Alcohol dehydrogenase (ADH LB) from *Lactobacillus Brevis* (EC 1.1.1.2, 0.44 IU/mg), Glycerol Dehydrogenase (GDH) from *cellulomonas* sp. (EC 1.1.1.6, 59 IU/mg), D-Glucose (CAS 50-99-7), Acetophenone (CAS 15753-50-1),  $\beta$ -nicotinamide adenine dinucleotide phosphate reduced tetrasodium salt (NADPH) and  $\beta$ -nicotinamide adenine dinucleotide phosphate (NADP<sup>+</sup>) and Bovine Serum Albumin (BSA) standard were purchased from Sigma-Aldrich (St. Louis, MO). Carboxyl chloride terminated polystyrene (PS-COCl, Mw 2020) was purchased from Polymer Source, Inc. (Canada). Toluene and Hexane was purchased from J.T.Baker (Philipsburg, NJ). Protein assay dye reagents were purchased from Bio-Rad laboratories (Hercules, CA). CuSO<sub>4</sub>

(5H<sub>2</sub>O) and NaOH were purchased from VWR Sci. (PA). Ascorbic acid was purchased from Mallinckrodt, KY.

### **5.2.2 Preparation of interface assembled Cofactor**

Interface assembled cofactor was achieved by conjugating cofactor with already interface assembled protein molecule in a one-pot synthesis. BSA was modified with PSCl to assemble at the interface according to the method described above. Typically 10 mg of native BSA in 1 ml of 0.05 M pH 7.8 phosphate buffer was contacted with 10 ml toluene containing 10 mg of PS-Cl. The mixture was shaken at 240 rpm in dark for 1 h at room temperature. The reaction mixture was then centrifuged at 10,000 G for 5 minutes for phase separation. The interface-binding BSA was recovered by removing the bulk phase solutions. The product was further purified by washing with buffer and toluene repeatedly for three times, to remove residual free BSA and polymer modifier. Protein loadings of polymer-BSA conjugates were determined by the reverse biuret method[147]. The modified BSA after purification was contacted with 10 ml of 0.05 M 7.8 pH phosphate buffer with cofactor (NADH, or NADPH), 25 mM N-Hydroxysuccinimide (CAS 6056-82-6) and 5 mM 1-(3-Dimethyl-aminopropyl)-3-ethylcarbodiimide hydrochloride (CAS 25952-53-8) for 1 hour in hexane-buffer biphasic system. The reaction mixture was then centrifuged at 10,000 G for 5 minutes for phase separation. The interface-binding modified cofactor was recovered by removing the bulk phase solutions. The product was further purified by washing with buffer and hexane repeatedly for three times, to remove residual free cofactor, EDC and NHS. The amount

of cofactor modified was determined by monitoring the change of absorbance of the aqueous solution at 340 nm both before and after modification.

### **5.2.3 Interfacial reactions**

Two separate reaction systems were used to evaluate the activity and stability of interface-assembled cofactor. Batch reactions were carried out in a reactor with an interfacial area of 19.6 cm<sup>2</sup> in a biphasic system. ADH LB and GluDH, both native and interface-assembled, with free and interface assembled NADPH were used for reduction of acetophenone to S-(-)-1-phenylethanol in the organic phase with simultaneous oxidation of glucose to gluconic acid in aqueous phase. ADH RS1 and GDH, both native and interface-assembled, with free and interface assembled NADH were used for reduction of acetophenone to R-(+)-1-phenylethanol in the organic phase with simultaneous oxidation of glycerol to dihydroxyacetone in aqueous phase. These reaction systems were carried out in a 50 ml reactor with 10 ml of 7.2 pH 100mM phosphate buffer as aqueous phase and the organic phase contained 5 ml Hexane, while the amounts of enzymes and cofactor, either interface-assembled or native, were adjusted as necessary. Mild stirring (120 rpm) of the interface was applied mechanically. The reaction was followed by analyzing the product, S-(-)-1-phenylethanol or R-(+)-1-phenylethanol, in organic phase using GC with aliquots of 0.15 mL withdrawn periodically from organic phase.

### **5.2.4 GC analysis**

Both reactions systems were monitored by measuring the concentration of products in organic phase using Gas Chromatography (GC-3100, Varian) equipped with

$\beta$ -DEX<sup>TM</sup> 225 fused silica capillary column (30m $\times$ 0.25mm $\times$ 0.25 $\mu$ m), from Supelco Bellefonte PA). Aliquots of 150  $\mu$ l of organic phase were used for GC analysis. The injection temperature was maintained 220  $^{\circ}$ C with detector temperature of 300  $^{\circ}$ C. The column temperature was maintained at 100  $^{\circ}$ C for 5 minutes and ramped to 210 C at 10  $^{\circ}$ C /min. Commercially purchased *R*-(+)-1-phenylethanol and *S*-(-)-1- phenylethanol standards were used for calibrations.

### 5.3 Results and Discussions

The structure of pyridine cofactors like NAD(P)H involves unique combination of functional groups that are required for different oxidoreductases enzymes to carry out biotransformations. The nicotinamide group is the oxidation, reduction center and the remaining portion of the molecule is needed for selective interactions with enzymes. The structure of NAD(P)H offers different functional groups for chemical modification (Figure 5-1). However, any changes to the nicotinamide moiety causes drastic reduction in enzyme's activity but radical changes to the adenosine-5-monophosphate moiety does not appreciably affect the cofactor's function. Crystallographic data for dehydrogenases indicate that the adenine ring exist in the hydrophobic pocket and is exposed to solvent[192]. Therefore, this part of the molecule is the most favored for chemical modification. Two positions of N<sup>6</sup> and C8 on the adenine ring have been the most studied for NAD(P)H modification. The high electron density at the C8 carbon on the adenine ring makes it the ideal position for electrophilic substitution[193]. However, N<sup>6</sup> modified NAD(P)H derivates exhibit a better activity by maintaining a more favorable access to

the adenine binding site in the enzyme[194]. The N<sup>6</sup> position in the adenine ring of NAD(P)H has been conventionally considered suitable site for synthesis of macromolecular derivatives of these cofactors, as deamino-NAD<sup>+</sup> exhibited appreciable activity with different dehydrogenases[195]. The attachment of a reactive functional group at this position has been used as a first step in many derivatizations of NAD(P). The modification of amino group in adenine ring of NAD(P)H is conventionally performed in multiple steps that includes alkylation of N<sup>1</sup> position, followed by a chemical reduction of the nicotinamide group, a subsequent Dimroth rearrangement from N<sup>1</sup> to N<sup>6</sup> position under alkaline conditions and finally an optional enzymatic oxidation of nicotinamide group. The N<sup>6</sup> position has been modified with various functional moieties like iodoacetic acid[196], 3-propiolactone[197] and 3-iodopropionic acid[198] for synthesis of N<sup>6</sup>-carboxymethyl NAD(P). N<sup>6</sup>-aminoethyl NAD(P) has been synthesized using ethyleneimine[194]. Epoxy functional groups at N<sup>6</sup> position were introduced using compounds like 1,2,7,8-diepoxycyclohexane[199] and alkylating agents like 3,4-epoxybutanoic acid has been used to synthesize N<sup>6</sup>-2-hydroxy-3-carboxypropyl NAD[200]. The main disadvantage of these preparations has been low yields due to losses during the purification step and long time for preparation.

### **5.3.1 Interfacial assembly of cofactors**

The present work reveals a quick, one-pot, high yield synthesis of macromolecule derivatized cofactor that can self-assemble at liquid-liquid interface. Modification of NAD(P)H for self-assembly at liquid-liquid interfaces has a tremendous potential in scaling up the interfacial biocatalysis process. The downstream processing of both

aqueous and organic phases will be greatly minimized by incorporating the cofactor at the interface. The method to synthesize the novel self assembling NAD(P)H is depicted in Figure 5-1. Both NADH and NADPH were assembled at the interface by similar modification procedure. BSA was first contacted with PSCl to form interface assembled protein. The carboxyl functional groups available on the surface of interface-assembled BSA were functionalized with EDC. EDC reacts with the carboxyl group on BSA surface to form an amine-reactive O-acylisourea intermediate. However, the intermediate is susceptible to hydrolysis, making it unstable and short-lived in aqueous solution. The presence of NHS stabilizes the amine-reactive intermediate by converting it to an amine-reactive NHS ester, thus increasing the efficiency of EDC-mediated coupling reactions. The amine-reactive NHS ester intermediate has sufficient stability to permit reaction with amine group in the adenine ring of NAD(P)H. This design for synthesis of modified NAD(P)H results in stable assembly of NAD(P)H at liquid-liquid interfaces, with a chemically well-defined linkage between NAD(P)H and interface-assembled BSA molecules. The method of synthesis also facilitates in easier purification of interface-assembled NAD(P)H. The modified cofactors were recovered by washing both aqueous and organic phases with fresh buffer and hexane respectively. The reaction for coupling NAD(P)H to macromolecules for interfacial assembly was complete in 60 minutes, compared to 24-48 hrs in conventional methods and does not require harsh conditions like high alkalinity. The amount of NAD(P)H assembled at the interface was quantified by observing the reduction of absorbance at 340 nm in aqueous phase. The stabilization

of amine reactive O-acylisourea intermediate by NHS improved the overall yield of modification procedure to 67%.

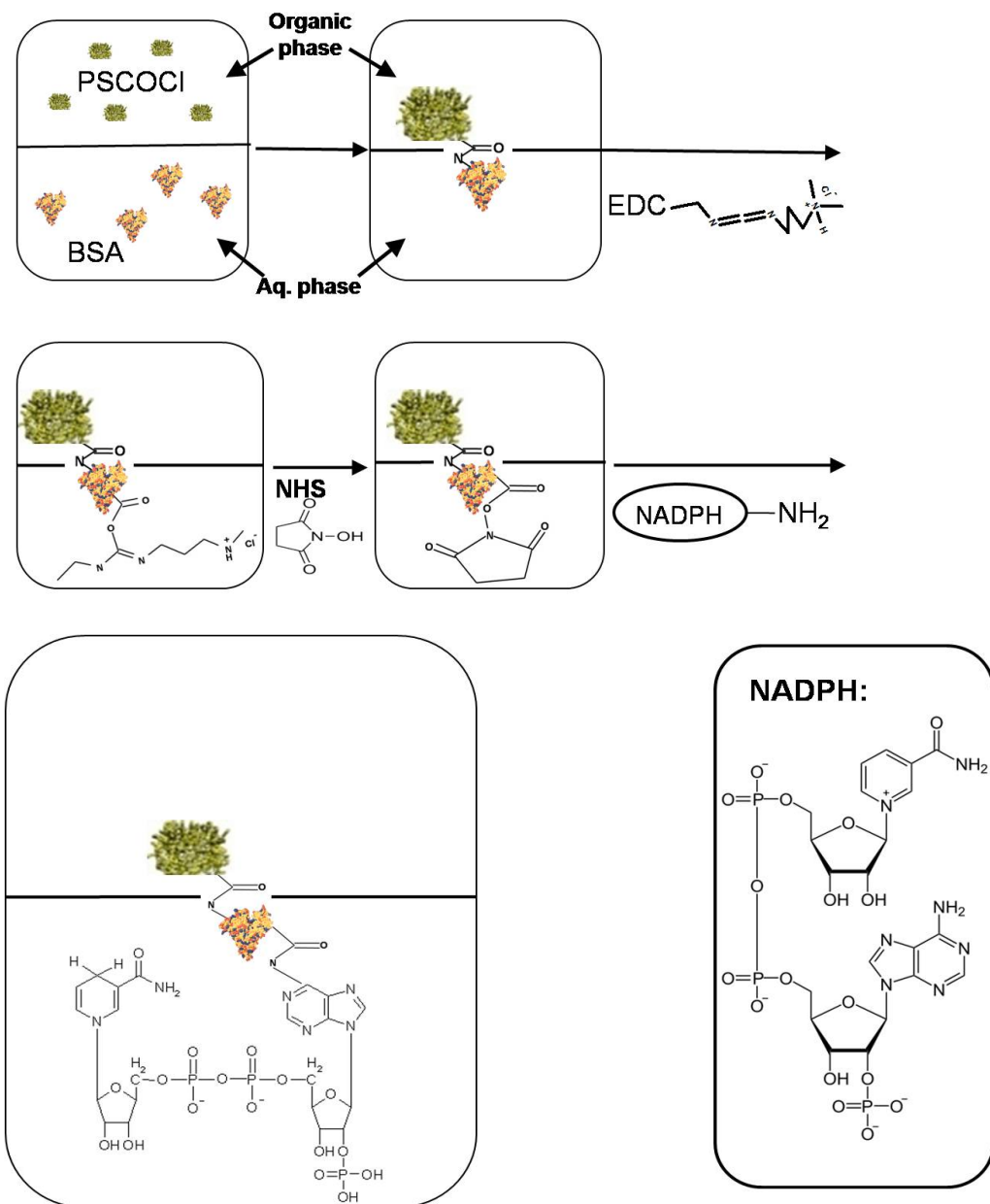


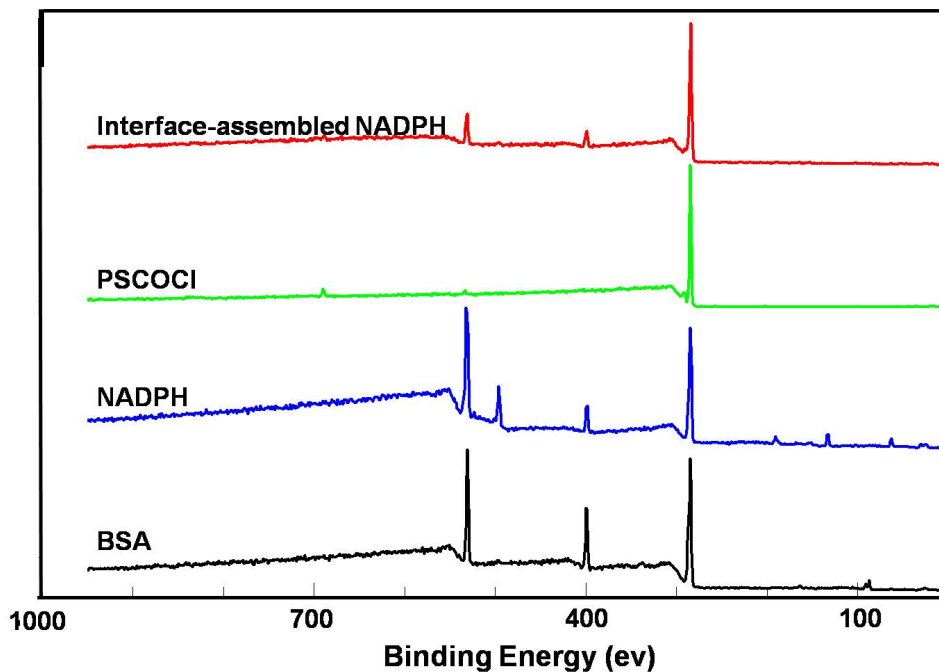
Figure 5-1 Synthesis of interface-assembled cofactor  
 BSA, bovine serum albumin; PSCOC1, carboxy chloride terminated polystyrene; EDC, 1-ethyl-3-(3-dimethylaminopropyl)carbodiimide; NHS, N-hydroxysuccinimide



### 5.3.2 Characterization of interface-assembled cofactors

The modification of NAD(P)H for interface assembly was characterized by X-ray photoelectron spectroscopy. Measurements were performed using Surface Science Instruments SSX100 with monochromatic Al K-alpha x-rays to excite spectra. Data were obtained at two pass energies: Survey 150 eV and High Resolution 50 eV. Before the XPS experiment, the interface-assembled cofactor was washed with high-purity deionized water and ultra pure toluene to remove all soluble materials from the interfacial material. The interface-assembled cofactor was then deposited over a gold plate and blow-dried in nitrogen gas.

(A)



(B)

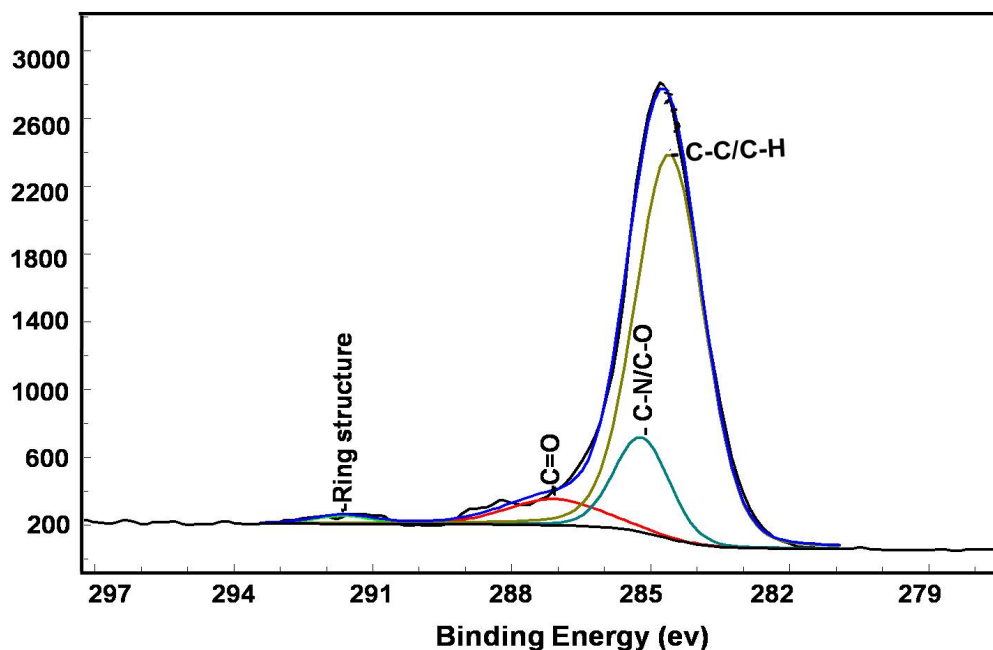


Figure 5-2 X-ray photoelectron spectroscopy spectral analysis  
(A) Comparison of spectral analysis of interface-assembled NADPH with that of its precursors (B) The peak fit of the C1s analysis of interface-assembled NADPH.

The XPS analysis provides only qualitative data as the functionalities from the XPS analysis is difficult to quantify since the surface is rough and the analysis is done only for the first few nm of the material. The presence of unique functionalities in interface-assembled cofactor that can come from only one of the precursors and can be taken as a confirmatory marker for the presence of that precursor in the final material of interface assembled cofactor. The spectral analysis of interface-assembled NADPH indicates presence of sulfur (Figure 5-2), which is from Cysteine or Methionine from BSA. The presence of sodium and phosphorous corresponds to that of NADPH from the spectral analysis, as all spectral analysis of other precursors does not contain sodium of

phosphorous. The presence of ring structure at 291 eV is unique to the benzene ring present in polystyrene and is not shown in the C1s analysis of rings from NADPH (Figure 5-2). The above observations clearly represent that the surface that self-assembled at liquid-liquid interface contains the modified cofactor. These results also confirm the purity and the feasibility of attempted reaction pathway for synthesis of stable, chemically well-defined linkage between NAD(P)H and interface-assembled BSA molecules for interfacial biotransformations involving interface-assembled cofactors.

The dehydrogenase-cofactor catalyzed biotransformations can become more economically viable on using coupled reaction systems for efficient use of expensive cofactors. The usefulness of a coupled reaction system is determined by the turnover number of the cofactor. The factors that influence the cofactor turnover include substrate solubility, stability of enzymes, product inhibition, rate of deactivation of cofactor and type of reactor [201-204]. The turnover number can be considerably increased if the cofactors can be retained in the reactor while the substrate is continuously added with simultaneous removal of product. A biphasic system with cofactor localized at the interface will offer access to reactants dissolved in either phase, allowing organic synthesis with regeneration half-cycle in the aqueous phase.

### **5.3.3 Activity and stability of interface-assembled cofactors**

The interface-assembled cofactor's efficiency to catalyze enzymatic reactions was studied by employing the interface-assembled cofactor in different reaction systems. Two distinct multienzymatic reaction systems that were cofactor dependent were used with

free and interface-assembled cofactor to evaluate the stability and efficiency of the prepared modified cofactor (Figure 5-3). One multienzymatic reaction system involved NADH/NAD<sup>+</sup> as cofactor with reduction of acetophenone to S-(-)-1-phenylethanol in the organic phase with simultaneous oxidation of glycerol to dihydroxyacetone in aqueous phase by enzymes ADH RS1 and GDH respectively (Figure 5-3a). Another multienzymatic reaction system involved ADH LB and GluDH with NADPH/NADP<sup>+</sup> as cofactor for reduction of acetophenone to R-(+)-1-phenylethanol and oxidation of glucose to gluconolactone in organic and aqueous phase respectively (Figure 5-3b).

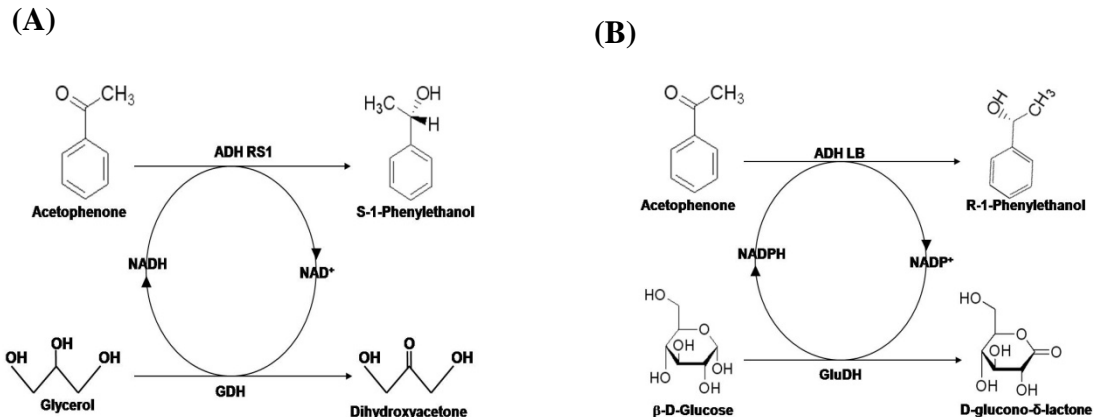


Figure 5-3 Multienzymatic reactions with potential importance for interface-assembled cofactors  
(A) NADH (B) NADPH

The multienzymatic reaction system involving ADH RS1 and GDH with NADH as cofactor is a very attractive reaction in producing two commercially important chemicals, S-1-phenylethanol is an important pharmaceutical intermediate and dihydroxyacetone is used in sunless tanning lotion apart from being an important

pharmaceutical chemical. However, this reaction system is a chemically a slow reaction that is thermodynamically limited around neutral pH range. The Gibbs free energy change for each reaction in the reaction system is a key component in determining the extent of overall regeneration of cofactor. As the reaction system involves two different phases, organic and aqueous, for a sustainable cofactor regeneration both reactions in either phase must be spontaneous or have a negative Gibbs free energy change separately.

To predict the extent of reaction in either phase the prediction model developed by Alberty[205] for biochemical reactions was used. This equation accounts for both ionic strength and pH of the solution. However, for the current reaction system,  $\Delta G$  for both acetophenone and phenylethanol was not adjusted to ionic strength and pH effects as these two compounds are in the organic phase and are not affected by the pH of aqueous solution. For all other compounds, the values of  $\Delta G$  after the pH adjustment as predicted by the equations were used.

$$\Delta G(I) = \Delta G(I=0) - 2.91482Z^2I^{1/2}/(1+BI^{1/2}) \quad 5-1$$

$$\Delta G^{app} = \Delta G(I) - N_i(H^+) [ \Delta G^0(H^+) + RT*\ln([H^+]) ] \quad 5-2$$

The prediction of extent of reaction by the above equations indicates that any pH above 10 will yield in a sustainable NADH regeneration cycle (Figure 5-4). This prediction does not account for the presence of interface assembled NADH or the presence of enzymes at the interface that may alter the local phase behavior of both reactions in either phase. However, the predictions give a general trend of the behavior of

the whole system involving two phases and two separate reactions. Based on these predictions, a pH above 10 will lead to multiple NADH regeneration.

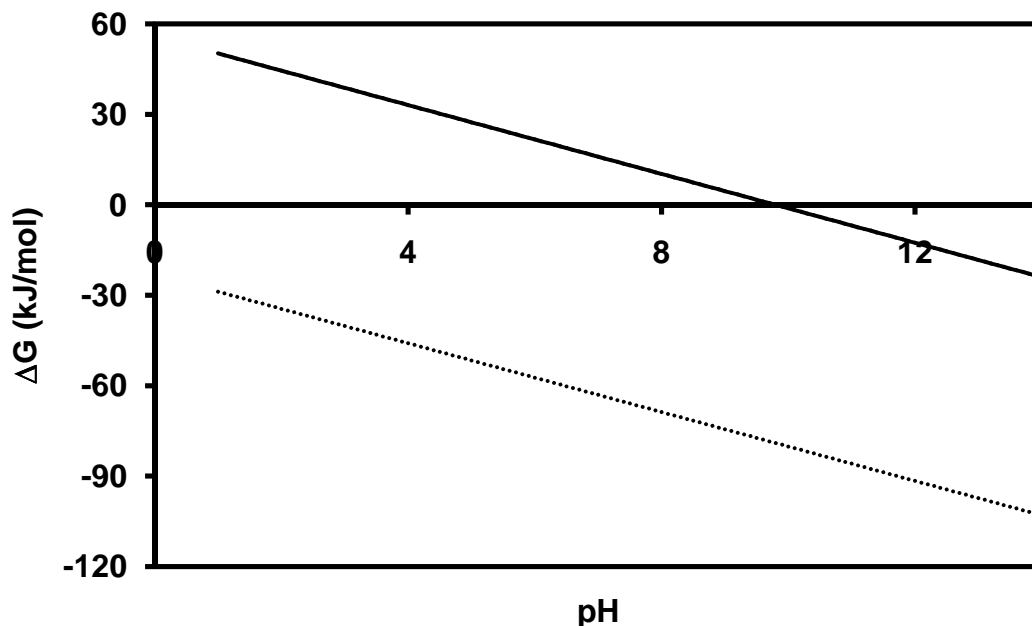


Figure 5-4 Theoretical predicted Gibbs free energy (solid) oxidation of glycerol (dotted) reduction of acetophenone

The predicted value may not be the optimum pH for this biotransformations reaction involving multienzymes. As seen from Figure 5-5 the enzyme ADH RS1 loses its activity rapidly above pH 7. This biochemical limitation forces the use of a pH below 7.5 for this particular reaction system. However, based on the Gibbs free energy calculation and the activity of GDH in aqueous phase at lower pH, the overall regeneration efficiency of NADH is limited. This combination of pH dependent behavior of both  $\Delta G$  and enzyme's activity greatly reduces the chances of multiple turnover of NADH on combining the reduction of acetophenone and oxidation of glycerol together.

Based on these observations a pH of 7.2 was used to carry out the multienzyme reaction system.

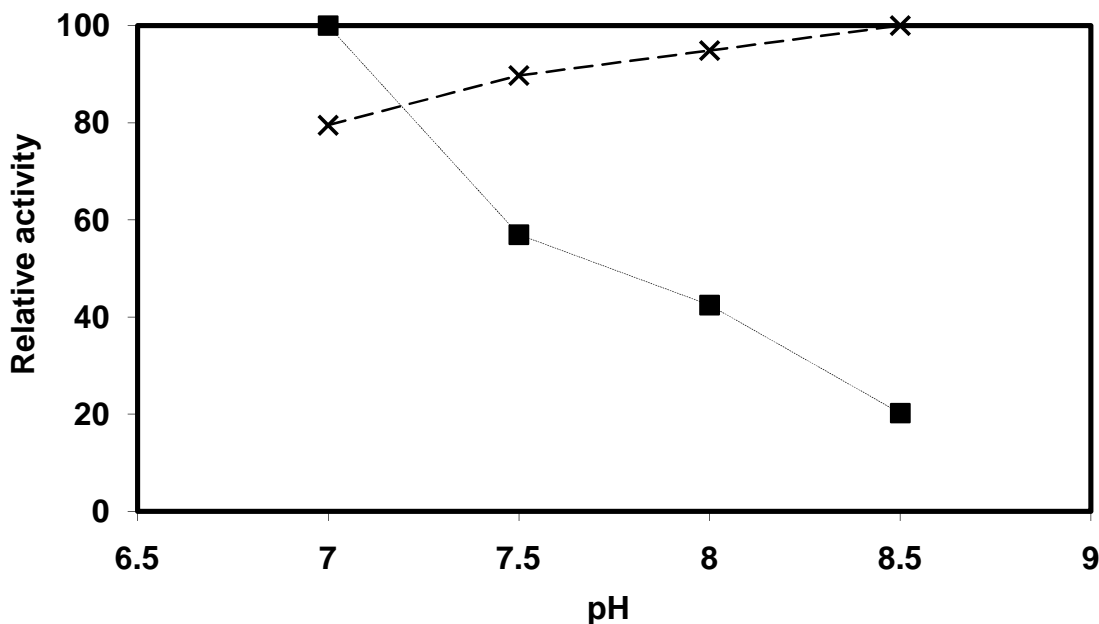


Figure 5-5 pH dependency of enzyme's activity in reaction system 1 with NADH/NAD<sup>+</sup> as cofactor  
(■) ADH RS1 (×) GDH

Figure 5-6 compares the initial reaction rate of reduction of acetophenone by native ADH RS1 with simultaneous oxidation of glycerol by native GDH with free NADH and with Interface-assembled NADH. The results clearly indicate an active modified NADH at the interface and establishes efficient effectiveness of modified NADH is taking part in enzymatic catalysis even after being covalently attached to a macromolecule. However, the interface-assembled NADH has a reduced activity when compared to free NADH. The activity is reduced by about 50% but this reduction on immobilization or modification of NADH was expected due to various factors like

limited interaction with native enzymes in aqueous solution as compared to free cofactors.

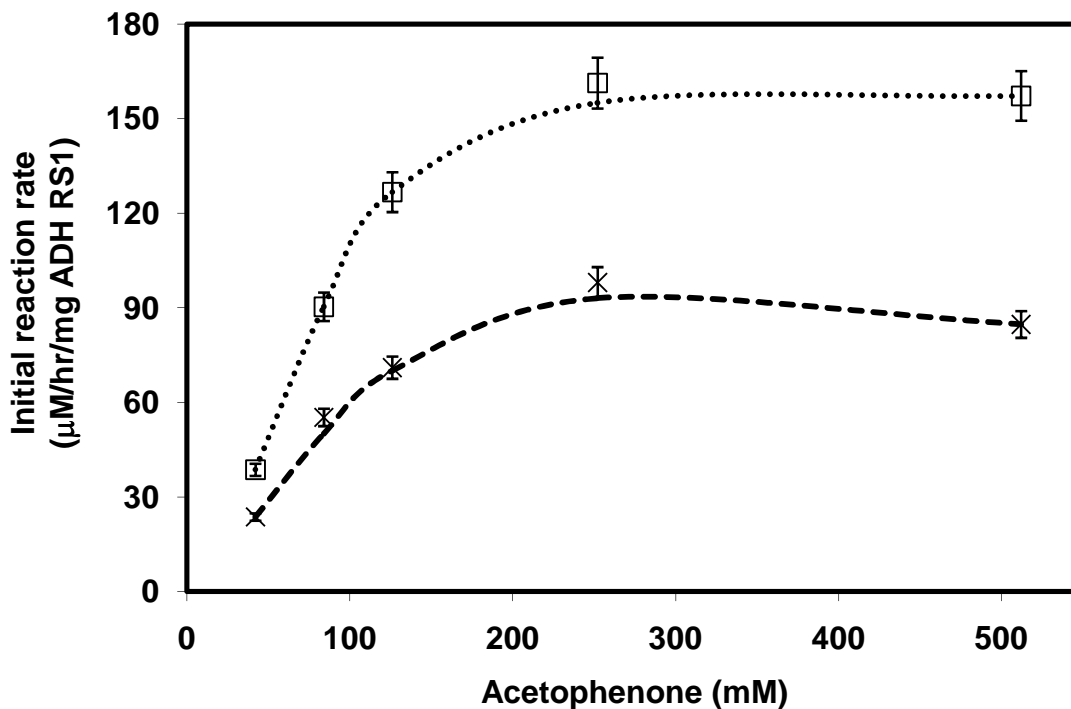


Figure 5-6 Initial reaction rate of reduction of acetophenone by ADH RS1 with simultaneous oxidation of glycerol by GDH  
(□) Free NADH (×) Interface-assembled NADH

As predicted by both theoretical calculations and pH dependency studies, the number of reuse or turnover number of NADH for multienzyme reaction system involving reduction of acetophenone by ADH RS1 with simultaneous oxidation of glycerol by GDH is drastically reduced as seen from Figure 5-7. The interface-assembled cofactor exhibited similar turnover number as that of free NADH with native enzymes, though the free NADH exhibited higher initial reaction rate. This is primarily due to



inherent nature of reaction system that is too slow to make any difference in turnover to be apparent. Moreover, the substrate in the aqueous phase glycerol can also hydrolyze free NADH in aqueous phase reducing its overall turnover. However, with modified NADH at the interface, the degree of hydrolysis may be reduced that increases the life of interface-assembled NADH leading to similar turnover number as that free NADH. Though the reaction system is thermodynamically limited, more than one turnover of NADH at the interface successfully establishes the effectiveness of modification procedure that was developed to synthesize the novel interface-assembling cofactor.

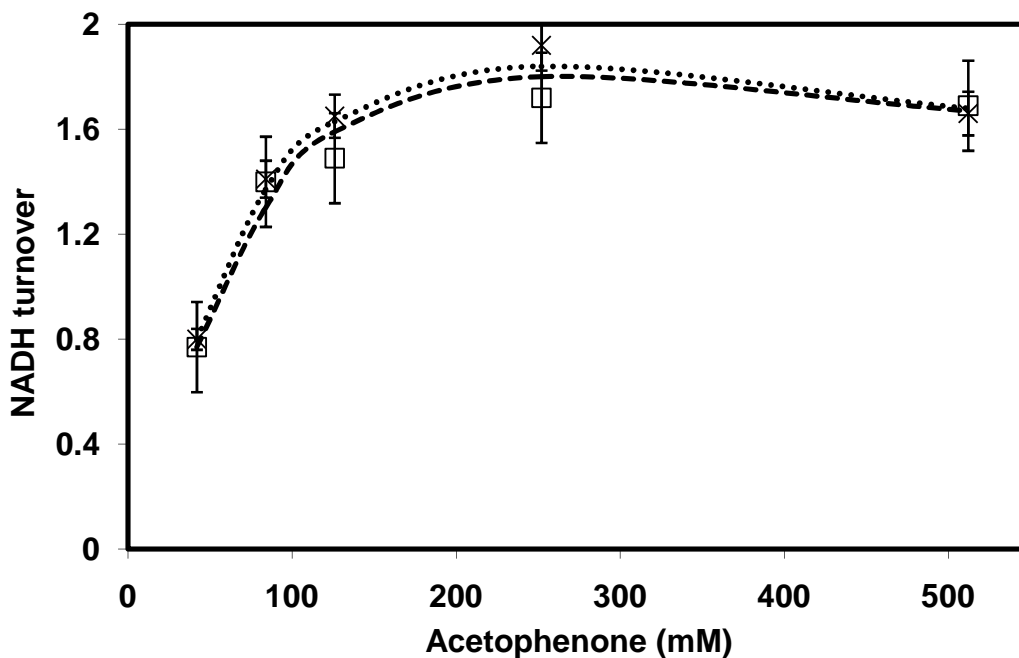


Figure 5-7 Cofactor turnover for the multienzyme reaction system involving reduction of acetophenone by ADH RS1 with simultaneous oxidation of glycerol by GDH  
(□) Free NADH (×) Interface-assembled NADH

Another multienzyme reaction system involved the cofactor NADPH and enzyme ADH LB and GluDH with reduction of acetophenone to R-(+)-1-phenylethanol in organic phase and oxidation of glucose in aqueous phase. This multienzymatic reaction system though similar in the organic phase reaction, the changing of aqueous phase enzyme and aqueous phase reaction drastically improves the chances achieving a sustainable regeneration of cofactor even after modification to self-assemble at the interface. The enzyme GluDH exhibits high specific activities even around neutral pH (Figure 5-8).

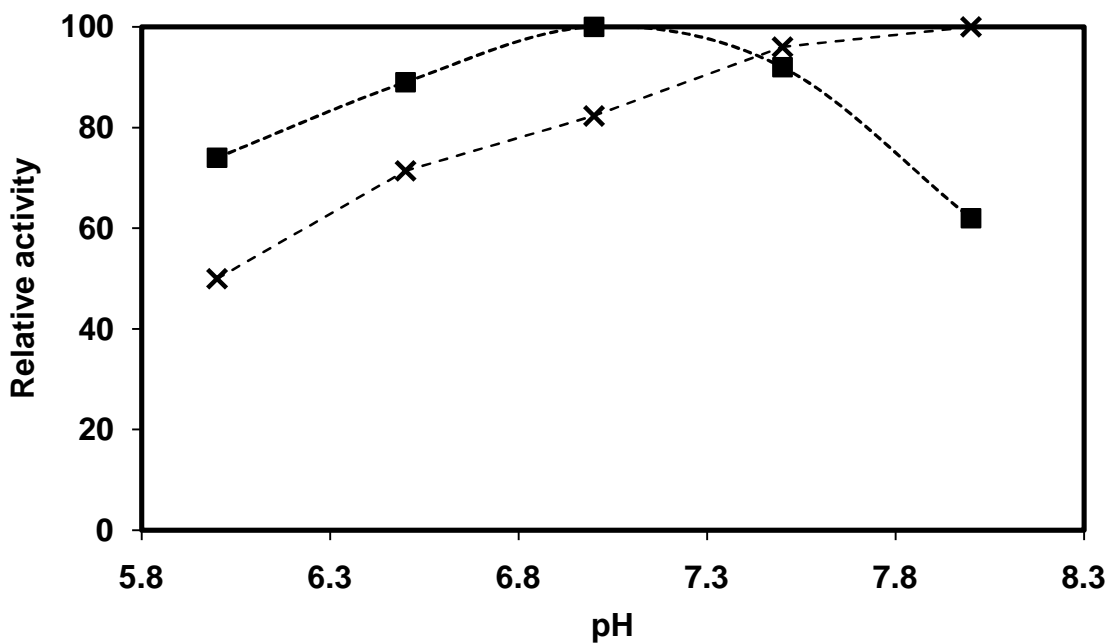


Figure 5-8 pH dependency of enzyme's activity in reaction system 2 with NADPH/NADP+ as cofactor  
 (■) ADH LB (×) GluDH

Its substrate, glucose, is strong reducing agent and does not catalyze the hydration of the reduced cofactor. In addition, the product, D-glucono- $\delta$ -lactone is spontaneously

hydrolyzed to gluconate, which makes the reaction irreversible. This reaction system involving NADPH as cofactor is more favorable because NADPH is less dependent on the buffer concentration than NADH. A pH of 7.5 was used to conduct the multienzyme reaction system involving ADH LB, GluDH with NADPH as cofactor. The coenzymatic activity of the interface-assembled NADPH was determined with the recycling reaction system with enzyme ADH LB and GluDH with reduction of acetophenone to R-(+)-1-phenylethanol in organic phase and oxidation of glucose in aqueous phase (Figure 5-9).

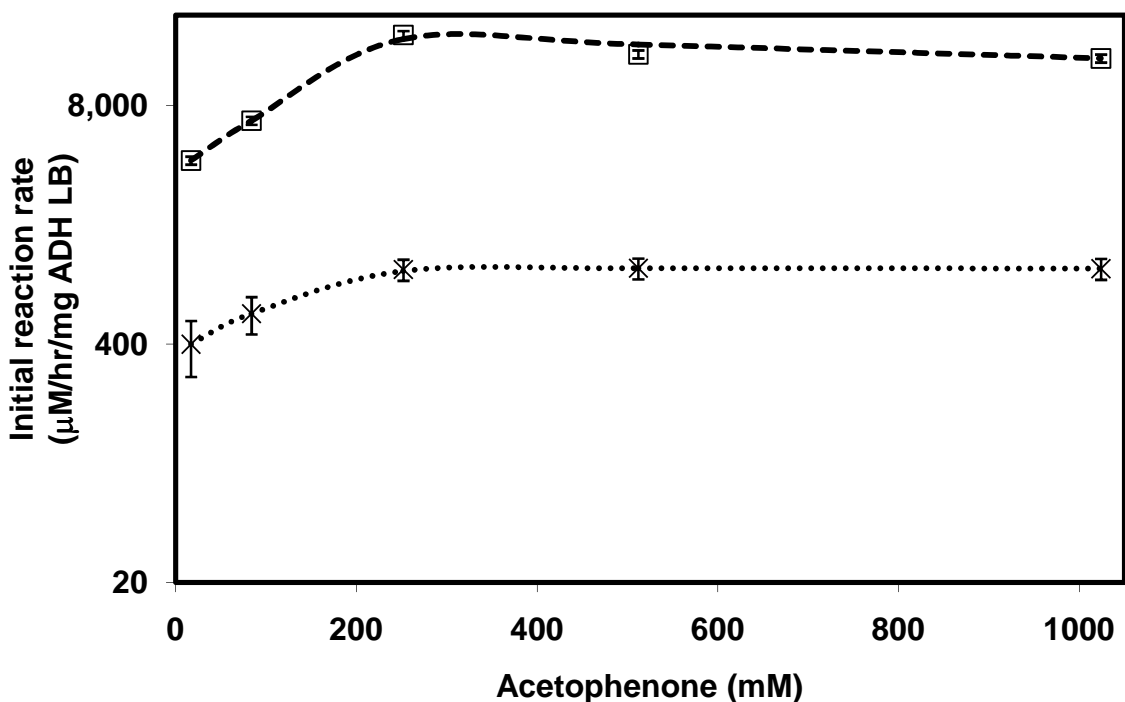


Figure 5-9 Initial reaction rate of reduction of acetophenone by ADH LB with simultaneous oxidation of glucose by GluDH  
 (□) Free NADPH (×) Interface-assembled NADPH

The multiple turnover of the cofactor indicated an active cofactor regeneration cycle at the interface. Interface-assembled cofactor showed improved stability as compared to native cofactor exposed to the interface. The native cofactor-enzyme system denatured after 48 hours of operation, whereas the interface-assembled cofactor did not lose the activity even after 28 reactions cycle with each cycle involving more than 80 turnovers of cofactor (Figure 5-10). This continuous operation of cofactor for more than 2150 hours in room temperature without losing its activity that is unprecedented and expected to have a positive impact on use of dehydrogenase-cofactor systems for industrial biotransformations.

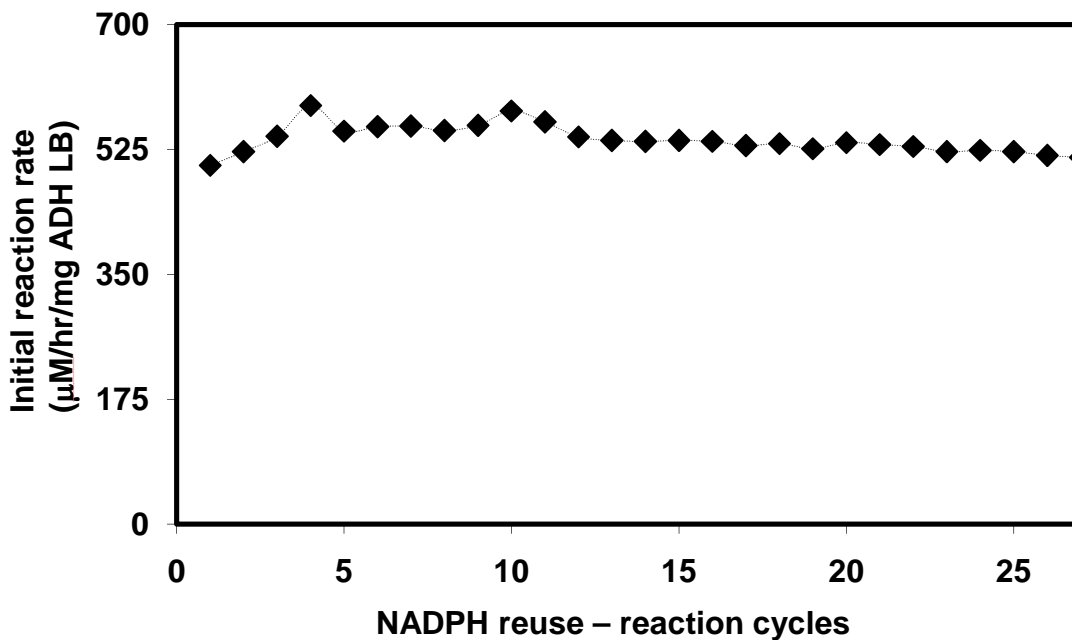


Figure 5-10 Sustainable reuse of interface assembled NADPH

The interface-assembled cofactor exhibited a remarkable stability with over 2150 hours of operation and a total turnover number of 2617 (Figure 5-11). These studies

reveal that the novel procedure for modification and further interface-assembly of cofactor is sustainable and can yield high turnover numbers on selection of a proper coupling reaction for cofactor regeneration with multienzyme system. Furthermore, in control experiments, where the reactions were the interface assembled BSA was not attached to any cofactor, no reaction was detected. Also, no reaction was detected in the presence of only polymer without any cofactor. These results clearly indicate that the successful production of products in both the phases is due to sustainable regeneration of interface-assembled cofactor.

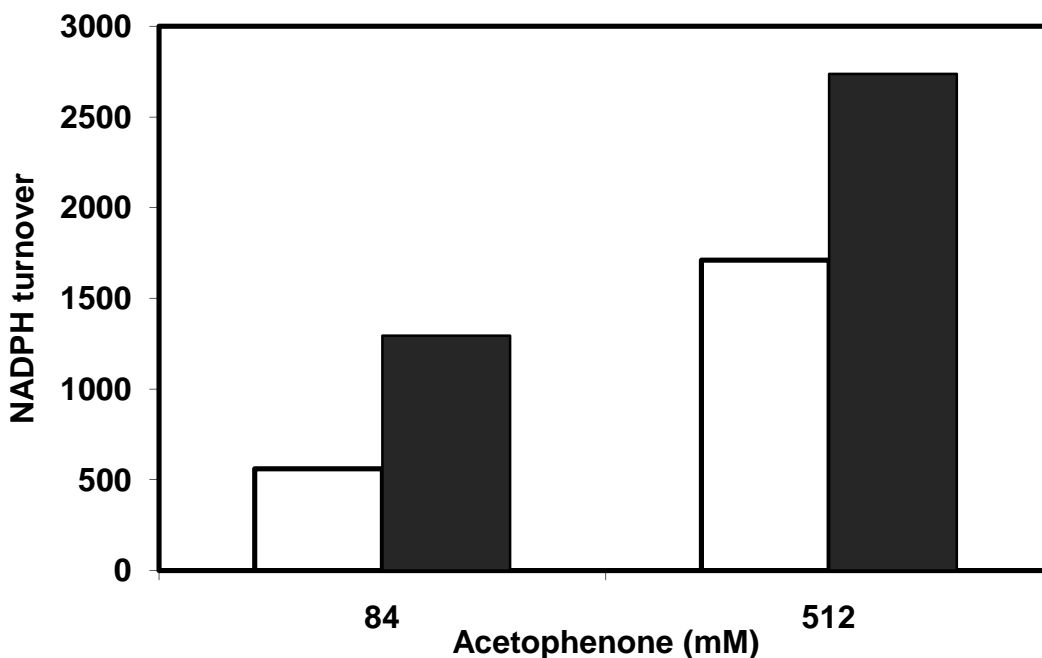


Figure 5-11 Cofactor turnover or number of regeneration for the multienzyme reaction system involving reduction of acetophenone by ADH LB with simultaneous oxidation of glucose by GluDH  
(□) Free NADPH (■) Interface-assembled NADPH

### 5.3.4 Kinetic study of cofactor turnover at the interface

The general scheme of interfacial reaction system is shown in Figure 5-12.

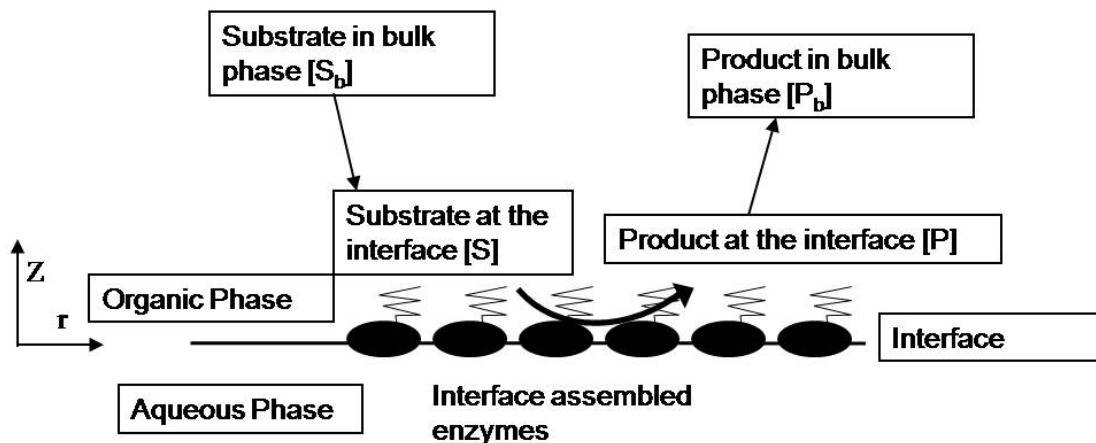


Figure 5-12 General scheme of interfacial reaction

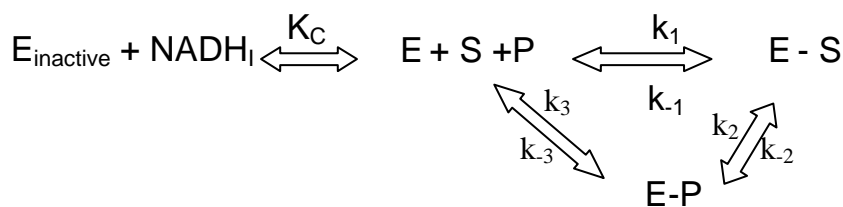


Figure 5-13 Relations of a complete set of equilibriums that define the primary parameters of the catalytic turnover cycle at the interface.

The binding of cofactor to the enzyme and subsequent reaction follows a series of equilibrium steps (Figure 5-13). The first step, that is, the binding of cofactor is an essential for binding of substrate to the catalytic site of the enzyme. The cofactor is also modified to assemble at the interface. The kinetic study is based on the factors that the cofactor is regenerated at the interface. Therefore, the cofactor concentration  $[C]$  remains

constant, the kinetic study involves only one enzyme with only one reactant and one product and both of them are in the same phase, the mole fraction of enzyme and the cofactor is negligible compared to the mole fraction of substrate and product at the interface. i.e,  $X_s + X_p \sim 1$ , all the concentrations are based on bulk solution volume, all bulk phase entities are given with subscript b, no subscripts are given to any interfacial concentration.

The Enzyme is active only when it is bound with cofactor. Then there will be a cofactor free enzyme at the interface,  $E_{inactive}$ , which will be present at the concentration

$$[E_{inactive}]/[E] = K_c/[C]$$

Here  $[C]$  denotes the concentration of cofactor in moles per bulk solution volume,  $[E]$  denotes the cofactor bound active enzyme at the interface and  $K_c$  is the dissociation constant for binding of C to E.

Now the three equilibrium steps of the turnover cycle by the enzyme bound to the interface are considered reversible. The evaluation of the parameters will give an insight about the actual reversibility of these reactions. The rate of substrate binding to the enzyme is directly proportional to the rate constant  $k_1$ , to the concentration of substrate available at the interface and to the probability that the enzyme is in cofactor bound active state. The concentration of the substrate at the interface is designated,  $X_s$ , which is more convenient variable.

At steady state, the flux across each step in the reaction is the same

$$j = k_1 X_s P_a - k_{-1} P_{bs} = k_2 P_{bs} - k_{-2} P_{bp} = k_3 P_{bp} - k_{-3} P_a = k_c [C] P_i - k_{-c} P_a \quad 5-3$$

Where,  $P_i$ ,  $P_a$ ,  $P_{bs}$  and  $P_{bp}$  correspond to the probabilities that the enzyme is in state  $E_{inactive}$ ,  $E$ ,  $E-S$  and  $E-P$  respectively.

These probabilities should sum to one

$$P_a + P_i + P_{bs} + P_{bp} = 1 \quad 5-4$$

This gives five equations and five unknowns. The probabilities estimated by these relations are:

$$P_a = \frac{1}{1 + \frac{X_s}{\left( \frac{k_{-1}k_3 + k_{-1}k_{-2} + k_2k_3}{k_1(k_2 + k_{-2} + k_3)} \right)} + \frac{X_p}{\left( \frac{k_{-1}k_3 + k_{-1}k_{-2} + k_2k_3}{k_{-3}(k_2 + k_{-1} + k_{-2})} \right)} + \frac{K_c}{[C]}} \quad 5-5$$

$$P_{bs} = \frac{X_s}{\left( \frac{k_{-1}k_3 + k_{-1}k_{-2} + k_2k_3}{k_1(k_2 + k_{-2} + k_3)} \right)} P_a \quad 5-6$$

$$P_{bp} = \frac{X_p}{\left( \frac{k_{-1}k_3 + k_{-1}k_{-2} + k_2k_3}{k_{-3}(k_2 + k_{-1} + k_{-2})} \right)} P_a \quad 5-7$$

$$P_i = \frac{K_c}{[C]} P_a \quad 5-8$$



Let,

$$k_{catS} = \frac{k_2 k_3}{k_2 + k_{-2} + k_3} \quad 5-9$$

$$k_{catP} = \frac{k_{-1} k_{-2}}{k_2 + k_{-2} + k_{-1}} \quad 5-10$$

$$K_{MS} = \left( \frac{k_{-1} k_3 + k_{-1} k_{-2} + k_2 k_3}{k_1 (k_2 + k_{-2} + k_3)} \right) \quad 5-11$$

$$K_{MP} = \left( \frac{k_{-1} k_3 + k_{-1} k_{-2} + k_2 k_3}{k_{-3} (k_2 + k_{-1} + k_{-2})} \right) \quad 5-12$$

Then the steady state flux,  $j$ , is

$$j = \frac{\frac{k_{catS}}{K_{MS}} X_S - \frac{k_{catP}}{K_{MP}} X_P}{1 + \frac{X_S}{K_{MS}} + \frac{X_P}{K_{MP}} + \frac{K_C}{[C]}} \quad 5-13$$

It had been shown in the literature [206, 207] that the reverse reaction for the chemical step is immeasurably slow. i.e,  $k_{-2} \sim 0$ . The chemical step is usually the rate-limiting step [208]. i.e,  $k_2 < k_3$ , which implies

$$j = \frac{k_{catS}}{1 + \frac{K_{MS}}{[S]} + \frac{K_C K_{MS}}{[C][S]}} \quad 5-14$$

Multiplying by total enzyme concentration  $[E]$  on either side

$$V = \frac{V_{\max}}{1 + \frac{K_{MS}}{[S]} + \frac{K_C K_{MS}}{[C][S]}}$$

5-15

Evaluation of damkohler number, Da for interfacial catalysis with different configurations like native enzymes and free cofactor, native enzymes and interface-assembled cofactor, interface-assembled enzyme and free cofactor provides the efficiency of each configuration on scale-up. To evaluate the Da the coefficient for mass transfer limited reaction is necessary.

In the diffusion limited regime (Figure 5-14), the concentration of substrate, far from the interface is  $[S_{b0}]$ . The reaction is comparatively rapid and the concentration of the substrate at the interface can be taken as zero. i.e.,  $[S_b] = 0$ .

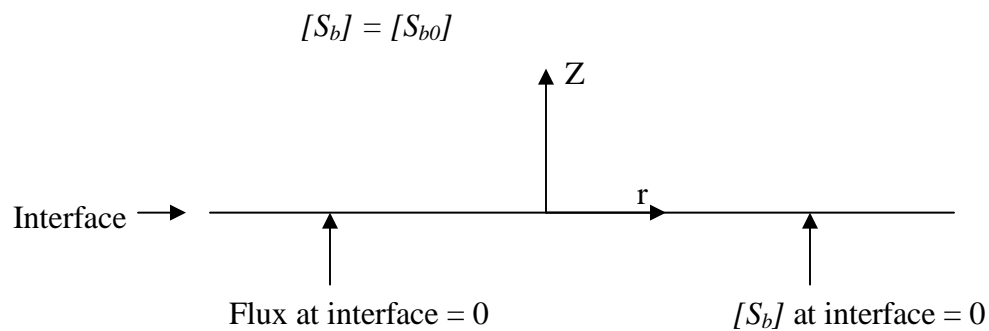


Figure 5-14 Schematic of diffusion limited interfacial reaction

The problem can be defined as, with an interface of radius R

$$\frac{1}{r} \frac{\partial}{\partial r} \left( r \frac{\partial [S_b]}{\partial r} \right) + \frac{\partial^2 [S_b]}{\partial Z^2} = 0 \quad 5-16$$

The boundary conditions are:

$$Z \rightarrow \infty \quad [S_b] = [S_{b0}]$$

$$Z = 0; 0 \leq r \leq R \quad [S_b] = 0$$

$$Z = 0; r > R \quad \frac{\partial [S_b]}{\partial r} = 0$$

Solving,

$$[S_b] = [S_{b0}] - \frac{2[S_{b0}]}{\pi} \int_0^\infty \frac{\sin(mR)}{m} J_0(mr) e^{-mZ} dm \quad 5-17$$

$$[S_b] = [S_{b0}] - \frac{2[S_{b0}]}{\pi} \tan^{-1} \left( \frac{R}{\sqrt{\left(0.5\left((r^2 + Z^2 - R^2) + \sqrt{\left((r^2 + Z^2 - R^2) + 4Z^2 R^2\right)}\right)\right)}} \right) \quad 5-18$$

The flux at the interface is given by,

$$D_L \left( \frac{\partial [S_b]}{\partial Z} \right)_{Z=0} = - \frac{2D_L [S_{b0}]}{\pi} \int_0^\infty \sin(mR) J_0(mr) dm \quad 5-19$$

$$D_L \left( \frac{\partial [S_b]}{\partial Z} \right)_{Z=0} = \frac{2D_L [S_{b0}]}{\pi} \frac{1}{\sqrt{(R^2 - r^2)}} \quad 5-20$$

In the diffusion limited reaction, the zero order term in Michaelis Menten kinetics will not be visible and the system behaves as first order rate based on the substrate in the solution.

This diffusion limited rate constant  $k_D$  can be estimated by equating the observed reaction rate and the rate of diffusion to the interface.

$$-\int_0^R D_L \left( \frac{\partial [S_b]}{\partial Z} \right)_{Z=0} 2\pi r \cdot dr = k_D [S_{b0}] \quad 5-21$$

$$-4D_L [S_{b0}] \left[ \sqrt{R^2 - r^2} \right]_0^R = k_D [S_{b0}] \quad 5-22$$

To evaluate the mass transfer limited reaction constant. The interfacial reaction system involving interface assembled ADH LB and interface-assembled GluDH with free NADPH for reduction of acetophenone to R-(+)-1-phenylethanol in organic phase and oxidation of glucose in aqueous phase was used. The whole reaction was carried out under mass transfer regime by using high amount of enzyme concentration, 25 Units of each interface assembled ADH LB and interface assembled GluDH maintained at the interface. The change in acetophenone concentration with such high enzyme concentration resulted in evaluation of mass transfer limited reaction constant,  $K_d$ , as  $0.0287 \text{ hr}^{-1}$  (Figure 5-15).

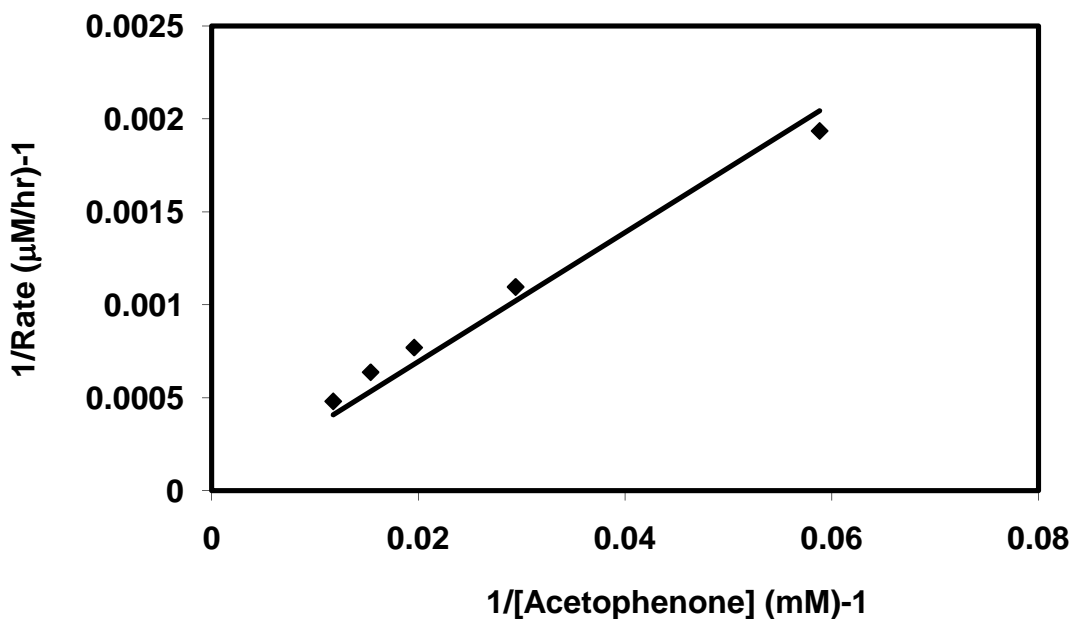


Figure 5-15 Concentration of substrate dependent reaction rate in mass transfer controlled regime

The kinetic parameters of all the configurations of multienzyme-cofactor system, Native enzyme-free cofactor (Figure 5-16), Interface-assembled enzyme and free cofactor (Figure 5-17), Native enzyme and interface-assembled cofactor (Figure 5-18) was evaluated by initial velocity analysis. This involved varying the NADPH concentration at five fixed levels of Acetophenone. The reaction velocity was defined as the amount of Phenylethanol formed after one hour from the start of multienzyme reaction with cofactor regeneration. The kinetic study in an interfacial system with two phases is subjected to influence of different parameters like pH, ionic strength, nature of head groups and nature of localization of enzyme [209, 210].

A linear relationship is obtained between the reciprocal initial velocity and the reciprocal concentration of the substrate for all the configuration of the multienzyme-cofactor system. However, the actual concentration of substrate chosen was different for different configuration because the apparent michealis constant  $K_{MS}$  is different based on the localization of enzymes and the cofactor.

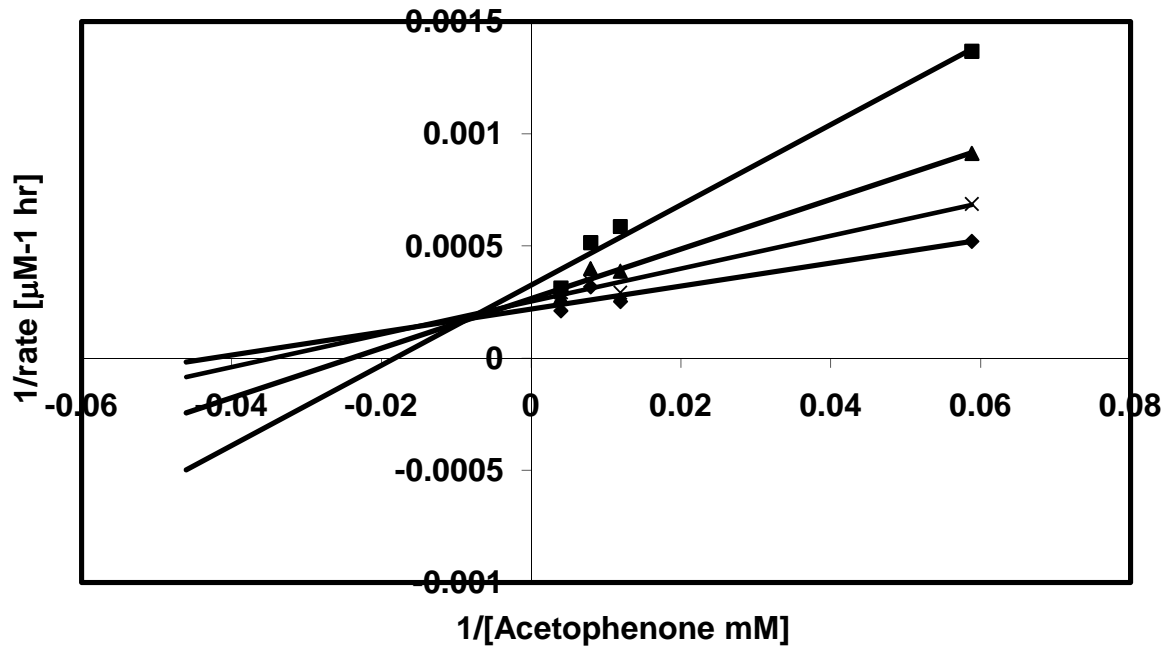


Figure 5-16 Double reciprocal plot of reaction system involving native ADH LB and native GluDH with free NADPH at four fixed levels  
 (■) 0.25 mg NADPH (▲) 0.5 mg NADPH (X) 1 mg NADPH (◇) 2 mg NADPH.

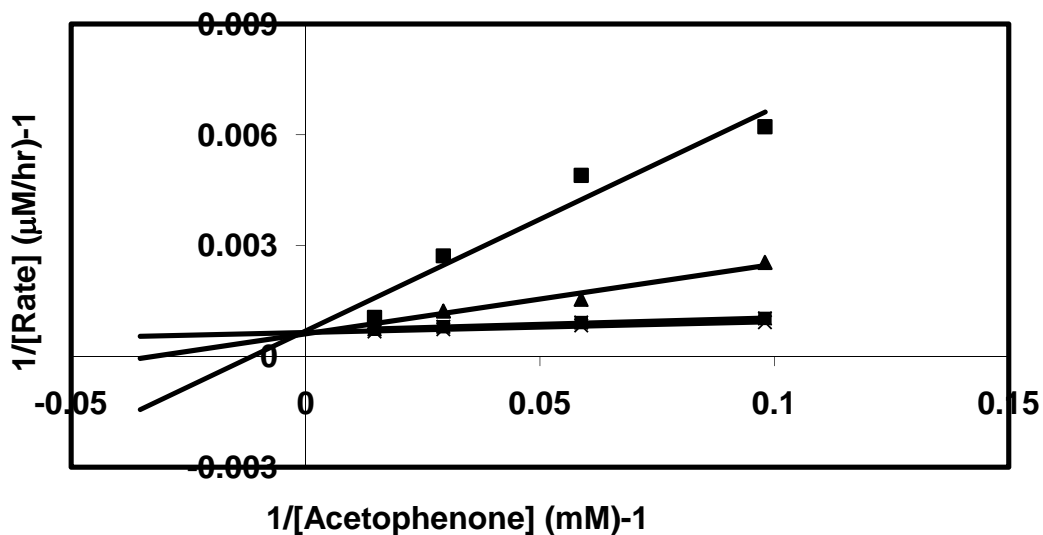


Figure 5-17 Double reciprocal plot of reaction system involving interface-assembled ADH LB and interface-assembled GluDH with free NADPH at four fixed levels  
 (■) 0.25 mg NADPH (▲) 0.5 mg NADPH (X) 1 mg NADPH (◇) 2 mg NADPH.

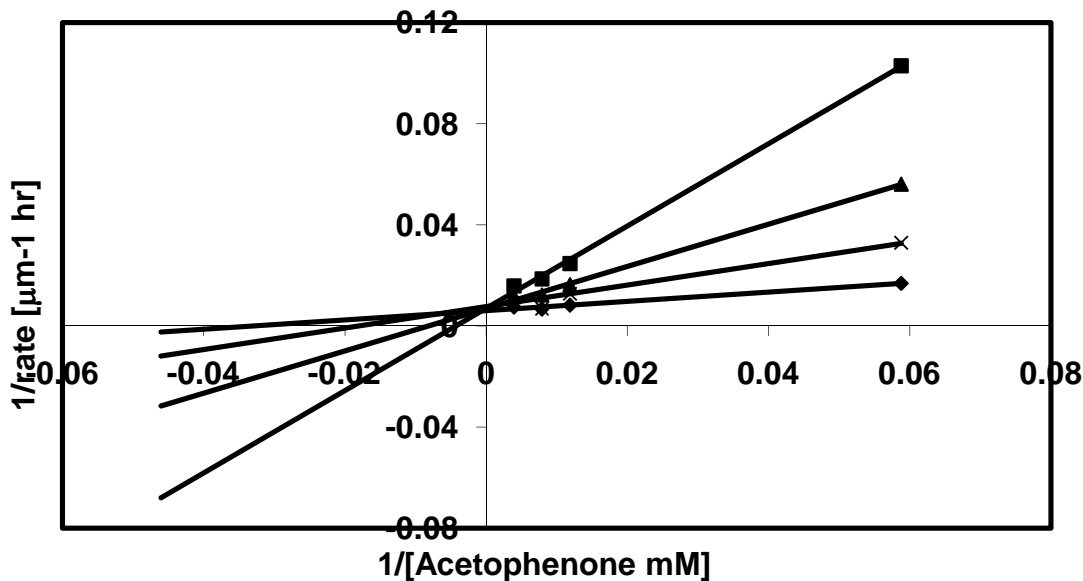


Figure 5-18 Double reciprocal plot of reaction system involving native ADH LB and native GluDH with interface-assembled NADPH at four fixed levels  
 (■) 0.25 mg NADPH (▲) 0.5 mg NADPH (X) 1 mg NADPH (◇) 2 mg NADPH.

The substitution of the present reaction with the general reaction rate expression developed results in:

$$V = V_{\max}[\text{Acetophenone}][\text{NADPH}] / (K_c * K_{MS} + K_{MS}[\text{NADPH}] + [\text{Acetophenone}][\text{NADPH}])$$

Table 5-1 Kinetic parameters of reaction system involving ADH LB and GluDH with NADPH as cofactor.

	<b>Native enzyme - Free NADPH</b>	<b>Interface assembled enzyme - Free NADPH</b>	<b>Native enzyme - Interface assembled NADPH</b>
$V_{\max} (uM hr^{-1})$	3846.15	1538.46	142.86
$K_{MS}(mM)$	1.53	5.23	39.59
$K_C (mM)$	0.03	0.09	0.18
<b>The damkohler number, Da, gives the ratio between reaction rate to diffusion rate</b>			
<b>Da</b>	87.49	10.24	0.13

The Damkohler number clearly indicates that the intrinsic reaction rate at the interface is lot slower, when cofactor is modified (Table 5-1). A physical explanation for this phenomena is that the modified cofactor contributes significantly to the reduction in reaction rate than the modified enzyme, due to the small molecule (NADPH) surrounded by the protein (BSA) at the interface contributing to difficult enzyme-cofactor complex formation with modified cofactor. The explanation is also supported quantitatively by the value  $K_C$ , which indicates the binding resistance of enzyme to cofactor at the interface. The higher value of  $K_C$  for modified cofactor ( $K_C = 0.18$ ) shows a huge resistance for



even with native enzyme to bind with modified cofactor. This explains the no reaction, when both cofactor and enzyme are modified.

## **5.4 Conclusion**

The present study has demonstrated a one-pot modification of cofactors for self-assembly at liquid-liquid interfaces. The interface-assembled cofactor exhibited multiple turnovers at the interface and it should be noted that the interface-assembled cofactor showed impressive stability and did not exhibit any degradation in performance upon continuous operation for 2150 hours at room temperature. The importance of sustainable regeneration of modified cofactor was demonstrated for reactions involving products that are pharmaceutical intermediates. At this point, the system suffers from the limitation of relatively slower reaction rate with interface-assembled cofactor. The understanding of the fundamental barriers and interaction of enzymes and cofactor at the interface suggests that with appropriate synthesis of molecular connectors between cofactor and protein molecule at the interface, the reaction rate can be improved.

## CHAPTER VI

# NANOSTIRRING OF MAGNETIC INTERFACIAL ENZYME FOR ENHANCEMENT OF INTERFACIAL BIOTRANSFORMATIONS

### 6.1 Introduction

The kinetic analysis combined with previous results has indicated that the reduced mobility of enzymes at the interface causes slow reactions for interfacial biotransformations. To improve the mobility of the interface assembled enzyme, concepts from biological world were applied to interfacial enzyme catalysis. In nature, molecular nanomotor proteins perform physical work by actively transporting other molecules or proteins within cellular systems[211]. Membrane bound enzymes in natural systems like ATP synthase have developed a rotary nanomotor action of its subunits by transferring protons across the inner mitochondrial membrane[212-215]. The mechanical force and the mobility of the subunit rotation is used for catalysis of ADP to ATP[216]. It is proposed to mimic such natural systems and develop a novel mechanism of nanostirring in vitro to improve the enzyme's catalytic efficiency for interfacial reactions. The mechanism of nanostirring is demonstrated by developing a self-assembling magnetic nanoparticles carrying enzymatic liquid membrane (MLM) at liquid-liquid interface, and employing an external alternating magnetic field to improve MLM's mobility at the interface. Interfacial biotransformations involve water-soluble substances and organic compounds that are incompatible to each other[91, 92, 217]. Enzymes

assembled at an organic-aqueous interface could provide the maximum accessibility to chemicals dissolved in both phases across the interface. Conjugation of enzymes with polymers to form amphiphilic structures for interfacial assembly of enzymes have been previously reported [112, 191]. The interfacial biocatalysis with interface-binding enzymes could significantly improve the overall catalytic efficiency of enzymes for biphasic reactions[165, 218]. However, enzymes have poor mobility when localized to a liquid-liquid interface. The low dispersion and limited 2-D mobility of enzymes at the interface limits the efficacy of the interface-assembled enzymes.

It is proposed to overcome these limitations of nanoscale dispersion and mobility at interfaces by development of magnetic nanoparticles carrying interface assembled enzymes. Biological molecules such as proteins, antibodies, antigens and DNA exhibit comparable dimensions to nanoparticles. Integrating biomolecules and magnetic nanoparticles results in new entities that combine the unique electronic, magnetic, and structural properties of nanoparticles with the unique recognition and catalytic properties of biomolecules [219]. Magnetite nanoparticles are key components to the development of many novel bio- and nanotechnological applications[220, 221]. Research in biosciences and nanotechnology has aimed at using magnetic nanoparticles as nanomotors, nanogenerators, nanopumps, and other similar nanometer-scale devices[222]. Indeed, substantial progress has been accomplished in recent years in the use of nanoparticles, nanorods, nanofibers and carbon nanotubes attached biomolecule systems as functional units for nanobiotechnology like drug delivery[223, 224], targeted cell entry[225], biosensors[226], nanobioelectronics[227-230] and biocatalysis[132].

Most of the enzyme conjugated magnetic nanoparticles reported so far have been to facilitate easy removal of immobilized enzymes. However, few cases of using the magnetic character of paramagnetic nanoparticles for spatial control of biomolecule-nanoparticles movement in tissue interstitial space have been reported[231-233].

Despite the growing interest in controlling the mobility of biomolecules in vitro using magnetic nanoparticles and magnetic field, relatively little is known about effect of the surface interaction, frequency of magnetic field and field strength on enzymatic activity. Apart from interfacial mobility, the efficiency of magnetic enzymes at liquid-liquid interface for a biphasic reaction system also depends on surface interaction of enzymes with magnetic nanoparticles. Therefore, it is important to protect the enzyme from inactivation due to surface spreading on the surface of hydrophobic magnetic nanoparticles. For this reason, a comprehensive study of nanoscale dispersion of enzymes at interface, effect of magnetic field on enzyme mobility and correlation of actual interfacial enzyme mobility with observed reaction rate, along with development of a novel mechanism of nanostirring that mimic the natural molecular nanomotors and is used for enhancing the productivity of industrial interfacial biotransformations is reported in this study.

## **6.2 Materials and methods**

### **6.2.1 Chemicals**

Glucose Dehydrogenase (GluDH) “Amano” NA ( EC 1.1.1.47, 286 IU/mg) was a gift from Amano Enzyme Inc. (Nagoya, Japan). Alcohol dehydrogenase (ADH LB) from

Lactobacillus Brevis (EC 1.1.1.2, 0.44 IU/mg), D-Glucose (CAS 50-99-7), Acetophenone (CAS 15753-50-1),  $\beta$ -nicotinamide adenine dinucleotide phosphate reduced tetrasodium salt (NADPH) and BSA standard were purchased from Sigma-Aldrich (St. Louis, MO). Chloroperoxidase (CPO) from Caldariomyces fumago (EC 1.11.1.10, 26 IU/mg, R<sub>Z</sub>-1.12) was provided as a gift from Bio-Research Products, Inc. (North Liberty, IA). Styrene (99%) and citric acid were purchased from EM Science (Gibbstown, NJ). H<sub>2</sub>O<sub>2</sub> aqueous solution (30v/v) was purchased from Fisher Scientific (Fair Lawn, NJ). Carboxyl chloride terminated polystyrene (PS-COCl, Mw 2020) was purchased from Polymer Source, Inc. (Canada). Toluene was purchased from J.T. Baker (Phillipsburg, NJ). Protein assay dye reagents and BSA standard were purchased from Bio-Rad laboratories (Hercules, CA). CuSO<sub>4</sub> (5H<sub>2</sub>O) and NaOH were purchased from VWR Sci. (PA). Ascorbic acid was purchased from Mallinckrodt, KY.

### **6.2.2 Synthesis of magnetic nanoparticles**

The magnetic nanoparticles were prepared by co-precipitation of ferrous and ferric salts. In a typical procedure, 0.39 g of FeCl<sub>3</sub> and 0.24 g FeCl<sub>2</sub> were added to 30 ml DI water that was purged with N<sub>2</sub> for 1h. 6 ml of 28% NH<sub>4</sub>OH was added slowly into the mixture at 80<sup>0</sup>C in N<sub>2</sub> atmosphere. The magnetic nanoparticles were separated from the solution using a permanent magnet and washed with DI water.

### **6.2.3 Interface assembly of magnetic nanoparticles**

The magnetic nanoparticles were assembled at the interface by physical adsorption with polymer-modified enzyme. For the multienzymatic system, interface assembly was carried out in a biphasic system consisting of a buffer solution and a

toluene phase. Enzyme (ADH or GluDH) was dissolved in 1ml of 0.05 M pH 7.8 phosphate buffer. The enzyme solution was then contacted with 10 ml toluene containing 10 mg of PS-COCl (Mw 2020). Magnetic nanoparticles were added to this mixture. The mixture was shaken at 240 rpm in dark for 1 h at room temperature. The reaction mixture was then centrifuged at 13,000 G for phase separation. The MLM was recovered by removing the bulk phase solutions. The product was further purified by washing with buffer and toluene, each for at least three times, to remove residual free enzyme, magnetic nanoparticles and polymer modifier. For reactions with both native and interface-binding multienzyme system, the each enzyme concentration was controlled at 0.5 Units ml<sup>-1</sup>, totally 5 Units of each enzyme (ADH and GluDH) in aqueous phase. A similar procedure was followed for interface assembly of magnetic nanoparticles with CPO, except the enzyme modification was carried out with shaking for 8 h at 240 rpm.

#### **6.2.4 Epoxidation of styrene**

Reactions were carried out in a biphasic system. Batch reactions were conducted in a 50-ml mechanically stirred reactor, stirred at 800 rpm. Styrene (5 ml) was used as the organic phase, while 10 ml of pH 4.5 citrate buffer (0.05 M) with 8 mM PEG was applied for the aqueous phase. For reactions with both native and interface-binding CPO, the enzyme concentration was controlled at 0.014 mg ml<sup>-1</sup>, totally 0.14 mg of CPO, in aqueous phase. 33.3 mM of H<sub>2</sub>O<sub>2</sub> was added to the reaction mixture by a syringe pump at the rate of 8.2×10<sup>-3</sup> ml min<sup>-1</sup>. For native enzyme reaction system, the magnetic nanoparticles were added separately to the reaction mixture. Samples of 0.4 ml from the

reaction mixture were taken periodically and centrifuged. The organic phase from the centrifuged sample was analyzed using GC for the product R- & S- Styrene Oxide.

### **6.2.5 Multienzyme reaction system with cofactor regeneration**

ADH and GluDH, both native and interface-assembled, with free NADPH were used for reduction of acetophenone in the organic phase with simultaneous oxidation of glucose in aqueous phase. Multienzymatic reactions were carried out in a 50 ml reactor with 10 ml of aqueous phase with 11.3 mM NADPH and 20 mM glucose. The organic phase contained 5 ml toluene with 84 mM acetophenone for interface assembled multienzymes and 17 mM for native enzymes. Mild stirring (120 rpm) of the interface was applied mechanically. The reaction was followed by analyzing the product, R-(+)-1-phenylethanol, in organic phase using GC with aliquots of 0.15 mL withdrawn periodically from organic phase.

### **6.2.6 GC analysis**

Both reactions was monitored by measuring the concentration of products in organic phase using Gas Chromatography (GC-3100, Varian) equipped with  $\beta$ -DEX<sup>TM</sup> 225 fused silica capillary column (30m $\times$ 0.25mm $\times$ 0.25 $\mu$ m), from Supelco Bellefonte PA). Aliquots of 150  $\mu$ l of organic phase were used for GC analysis. The injection temperature was maintained 220  $^{\circ}$ C with detector temperature of 300  $^{\circ}$ C. For Styrene epoxide analysis, the temperature of the column was kept at 110  $^{\circ}$ C for 10 minutes and a ramp of 10  $^{\circ}$ C /min till the temperature reached 220. The GC chromatograms showed separated peaks for R- and S-styrene epoxides. For R-(+)-1- phenylethanol analysis, the column temperature was maintained at 100  $^{\circ}$ C for 5 minutes and ramped to 210 C at 10  $^{\circ}$ C /min.

Commercially purchased *R*- and *S*-styrene epoxide and *S*-(-)-1- phenylethanol standards were used for calibrations.

### **6.2.7 External magnetic field production**

The alternating electromagnetic field was produced by equipment designed and built in collaboration with electronics shop, Department of Physics, University of Minnesota. The alternating magnetic system supplies the magnetic field with variable frequency (25, 50, 100, 200 and 500 Hz) and variable field strength to a solenoid (500 turns with #19 wire size) inside which the reactor was placed. There was not any significant increase in temperature of reaction mixture due to magnetic field during the normal operation.

### **6.2.8 Optical microscopy for enzyme mobility visualization**

The mobility of interface-assembled enzymes was measured with optical bright field microscope (Olympus X170) and analyzed with image analysis software (Image J). The enzymes were dyed with Oregon Green and subsequently assembled at interface along with magnetic nanoparticles to form dyed MLM. The dyed MLM was placed at the interface of a water-hexane system in a glass well of 50 mm diameter and cover slip as bottom. The glass well was placed above the objective and inside the solenoid that was connected to the alternating electromagnetic field generator. Preparations were viewed using a Olympus IX-70 inverted photomicroscope (Leeds Precision Instruments, Inc., Edina, MN 55439) equipped with brightfield, phase and fluorescence optics including a 100 W mercury lamp epi-fluorescence illumination with standard UV (excitation filter 330-380, barrier 420 nm), FITC (excitation filter 470-490 nm, barrier 520-580 nm) and



Rhodamine (excitation filter 510- 560 nm, barrier 570- 620 nm) filter sets. The samples were viewed using 10X, 0.30 plan fluor objectives. Digital images were collected using a Roper Cascade 512B camera and captured to a personal computer using Image Pro Plus version 6.1 software ( Media Cybernetics, Silver Springs, MD 20910) in streaming mode using a reduced area.

### **6.2.9 Characterization of MLM**

Magnetization measurements were obtained at room temperature in magnetic fields up to 3 kOe using a vibrating sample magnetometer (Princeton Measurements Micro VSM) at Institute for Rock Magnetism at University of Minnesota. The MLM was investigated with a PHILIPS CM120 transmission electron microscopy (TEM) with an accelerated voltage of 80 kV. The samples for TEM measurements were prepared by placing 100  $\mu$ l of suspension containing MLM onto a carbon stabilized copper grid (200 mesh).

## **6.3 Results and Discussion**

### **6.3.1 Interfacial assembly of bioactive magnetic nanoparticles**

Self-assembling of nanoparticles at fluid interfaces (liquid-vapor and liquid-liquid) have enabled fabrication of many functional materials[234]. However, the stability of nanoparticles at the interface is greatly influenced by factors like thermal fluctuations and interfacial forces like surface shear[235]. It was previously shown that stable macromolecular assemblies can be self-assembled at liquid interfaces by conjugation of enzymes with polymers to form amphiphilic structures[112, 191]. The

same procedure was introduced to fabricate stable interfacial assembly of magnetic nanoparticles along with enzymes forming a magnetic liquid membrane (MLM) at liquid-liquid interface. The magnetic nanoparticles were synthesized by co-precipitation method of ferrous and ferric salts. The nanoparticles prepared possess a mean size of 11 nm in diameter, and were added into a biphasic system consisting of an aqueous phase (pH 4.5, citrate buffer of 50 mM) and an organic phase of toluene. At the same time, chloroperoxidase (CPO), was added to the aqueous phase while the polystyrene (PS) of Mw as 2,020 Da functionalized with carboxyl chloride ending groups was applied to the organic phase. This procedure will then generate a complex in form of particle-PS-CPO (Figure 6-1) that can readily assemble at the interface.

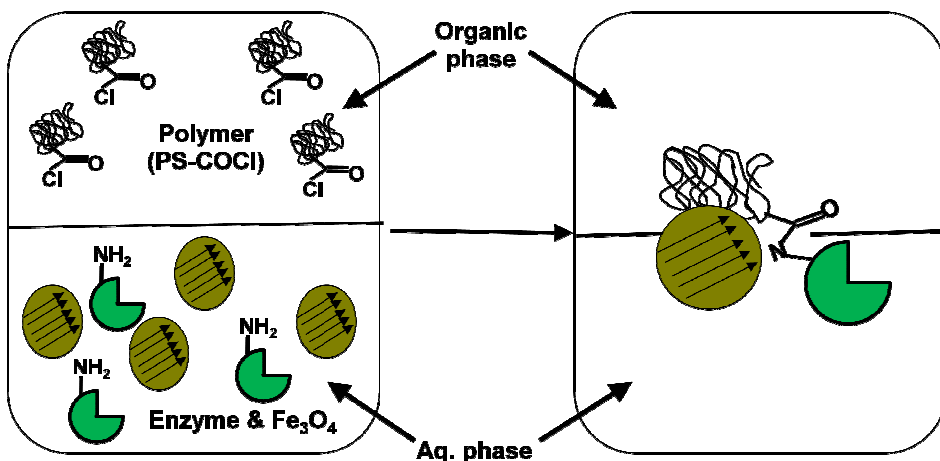


Figure 6-1 Fabrication of MLM to form thin film phase at oil-water interface.

### 6.3.2 Characterization of MLM

The amount of particles assembled at the interface was quantified by monitoring the remaining concentration of the particles in the aqueous solution and comparing to its initial amount. The assembling of the complex followed a Langmuir-adsorption curve

with a maximum adsorption occurring at 114.97 mg-nanoparticles/m<sup>2</sup> at the interface (Figure 6-2). The interface assembled MLM was repeatedly washed with buffer and toluene to remove excess nanoparticles, enzymes and polymer. The MLM showed a stable interfacial assembly (Figure 6-3) and the membrane was also catalytically active. The free nanoparticles in water were applied onto the TEM grid and dried before taking the images. The image for the MLM was taken with the dried sample of MLM extracted from oil-water interface onto the TEM copper grid (300 mesh formvar coated). A negative stain of ammonium molybdate to the sample was added to visualize the presence polymer and enzyme layer around the nanoparticles in a TEM (CM12, FEI, Hillsboro, OR). The stain cannot penetrate the thin layer of polymer and enzyme around the nanoparticles, which results in observance of the thin white layer around the nanoparticles in Figure 6-3B. However, on drying the MLM forms multiple layers on the grid as opposed to free nanoparticles, this causes the distortion of the size of the particles in MLM.

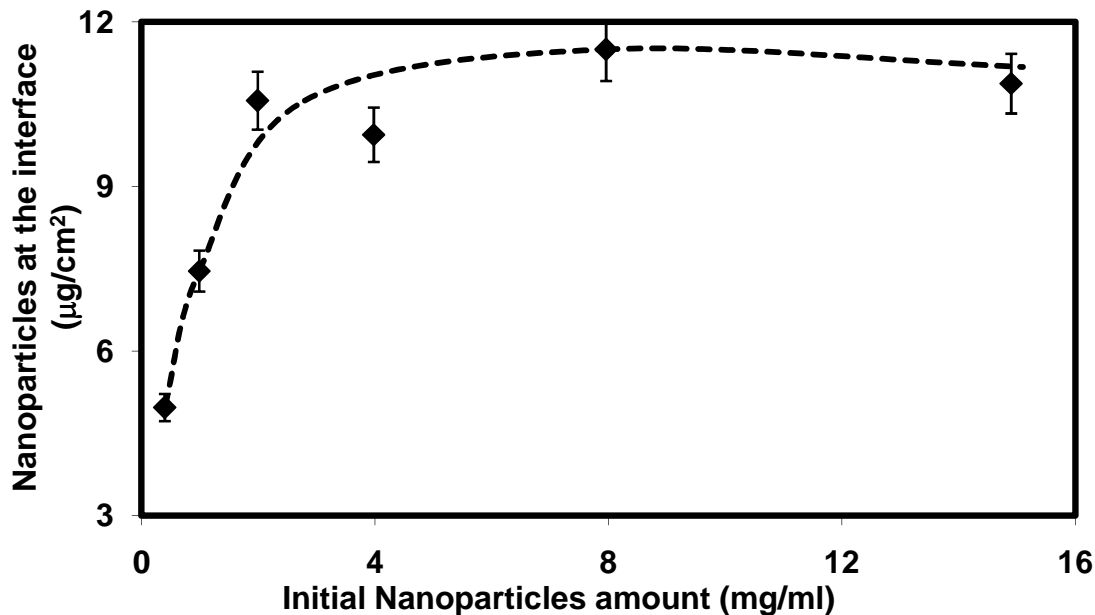


Figure 6-2 Amount of nanoparticles assembled at the interface

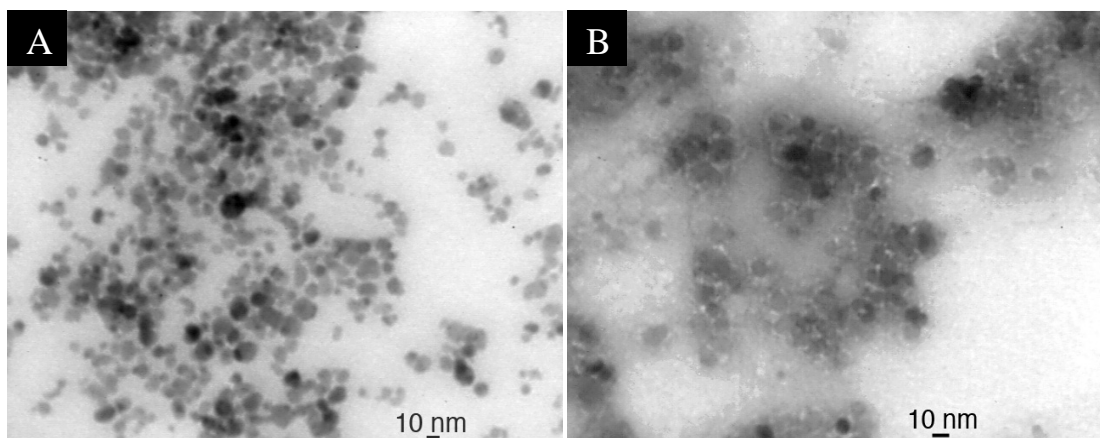


Figure 6-3 TEM images of MLM  
 (A) Free magnetic nanoparticles in aqueous solution. (B) MLM recovered from the interface, the thin white layer surrounding the nanoparticles are the polymer-enzyme conjugate at the interface.

The magnetic characteristic of MLM was confirmed by performing a magnetization analysis with a Magnetic Property Measurement System (Quantum designs, MPMS2 cryogenic susceptometer) at room temperature (Figure 6-4). The MLM

was deposited in a gelatin capsule and subjected to varying magnetic field strength with change in magnetization of MLM recorded. The MLM exhibited a combination of diamagnetic and superparamagnetic behavior. The presence of enzyme and polymer contributes to the diamagnetic behavior of negative slope at high fields on the MLM and magnetic nanoparticles contribute towards the superparamagnetic behavior that was observed as shown in Figure 6-4 near zero field. The analysis of magnetization curve of free nanoparticles gives a magnetic moment of  $3.22 \times 10^{-16}$  emu and an average particle size of 11 nm in diameter. However, the analysis of MLM magnetization yields a magnetic moment of  $3.52 \times 10^{-16}$  emu and magnetic particles of 6 nm. It is believed that this observed change in magnetic particle size is due better dispersion of magnetic nanoparticles at the interface covered with interface-assembled enzyme. At the interface the nanoparticles are uniformly covered with interface-assembled enzyme. Whereas, in solution, the magnetic nanoparticles can form aggregates and result higher value of observed magnetic particle size. This indicates a better and uniform dispersion of the particles at the interface, which facilitates a better dispersion of enzymes at the interface.

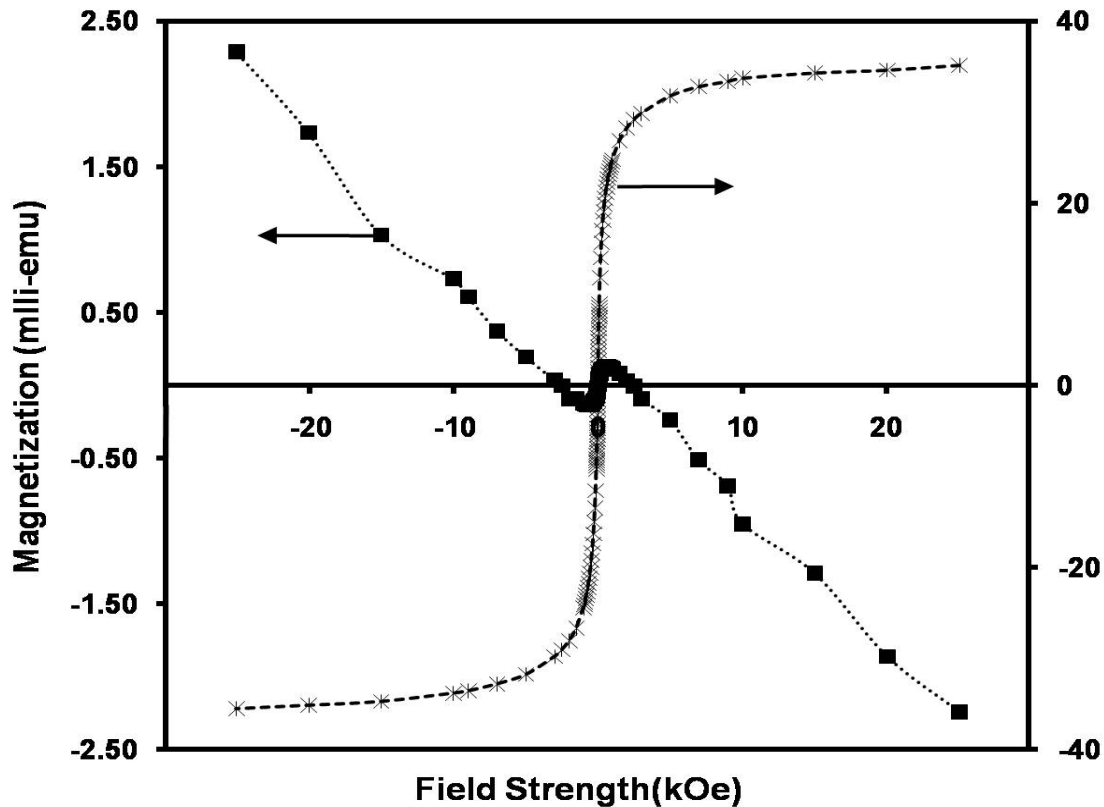


Figure 6-4 Magnetization curves  
 (■) MLM (×) free magnetic nanoparticles

### 6.3.3 Fabrication of alternating electromagnetic field generator

Integrating biomolecules and magnetic nanoparticles results in new entities that combine the unique electronic, magnetic, and structural properties of nanoparticles with the unique recognition and catalytic properties of biomolecules [236]. Despite the growing interest in controlling the mobility of biomolecules at interface using magnetic nanoparticles and magnetic field, relatively little is known about effect of the surface interaction, frequency of magnetic field and field strength on enzymatic activity. Enzymes have poor mobility when localized to a liquid-liquid interface. The low

dispersion and limited 2-D mobility of enzymes at the interface limits the efficacy of the interface-assembled enzymes. Apart from interfacial mobility, the efficiency of magnetic enzymes at liquid-liquid interface for a biphasic reaction system also depends on surface interaction of enzymes with nanostructure materials[237]. Therefore, it was important to protect the enzyme from inactivation due to surface spreading by conjugation with polymers. Epoxidation of styrene by chloroperoxidase was chosen as token reaction system to demonstrate the novel phenomenon of nanostirring. This enzyme requires two substrates, a hydrophobic styrene and the hydrophilic  $H_2O_2$ .

To improve the mobility of enzymes at the interface a novel mechanism of nanostirring was employed. An alternating electromagnetic field generator was built that can change the magnetic field strength (Gauss) and the frequency (Hz) for nanostirring the MLM at the interface (Figure 6-5). The reactions were conducted with changing the field strength from 2 G to 121 G and a frequency range of 25 Hz to 500 Hz. In the presence of external magnetic field the magnetic moments of MLM changes its alignment in the direction of field. The MLM experiences force in the direction corresponding to this change in alignment of magnetic moments, which results in novel nanostirring mechanism of MLM. This nanostirring of MLM causes the enzyme to behave more like fluid at the interface by increasing its mobility, which in turn increases its access to the substrate, thereby increasing the overall reaction rate. The effect of nanostirring is further enhanced by the unique structural characteristics of MLM. The uniform distribution of magnetic nanoparticles and the better dispersion of enzymes at the interface facilitates in a more uniform experience of magnetic force during nanostirring.

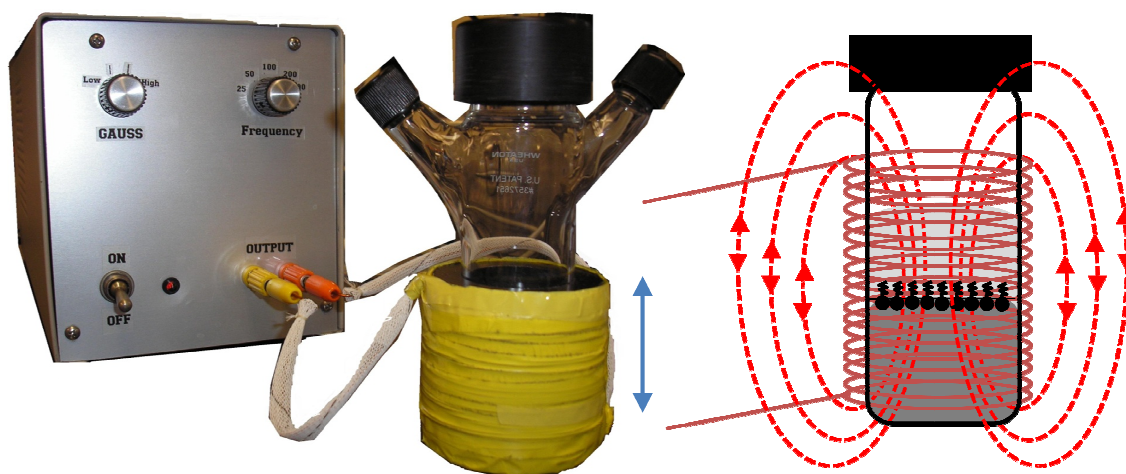


Figure 6-5 Alternating magnetic field generator for nanostirring.

It was seen that the frequency has greater influence on interfacial biotransformations than the magnetic field strength (Figure 6-6). The mobility of enzymes at the interface is directly governed by the change in direction of magnetic moment of the nanoparticles. On application of an external magnetic field, the magnetic moment of the MLM tries to align with the external magnetic field. The mobility of MLM is governed by this alignment of magnetic moment with field direction. As soon as the magnetic moment aligns with the field direction, the mobility of MLM is stopped. At lower frequencies the time available for magnetic moment to align with the field is sufficient enough to cease the vibration of modified enzyme. At higher frequency the field direction changes before the magnetic moment can align with the field direction. This rapid change keeps the magnetic moment of the nanoparticles from aligning with field direction, which in turn increases the mobility of MLM at the interface for the given frequency. However, the field strength increase does not affect the rate of alignment of magnetic moment to the external field direction. The frequency determines the number of



times the enzymes move at the interface. Hence, the mobility of MLM is predominantly governed by the frequency and for all the subsequent experiments the nanostirring was conducted at 500 Hz and 17 Gauss.

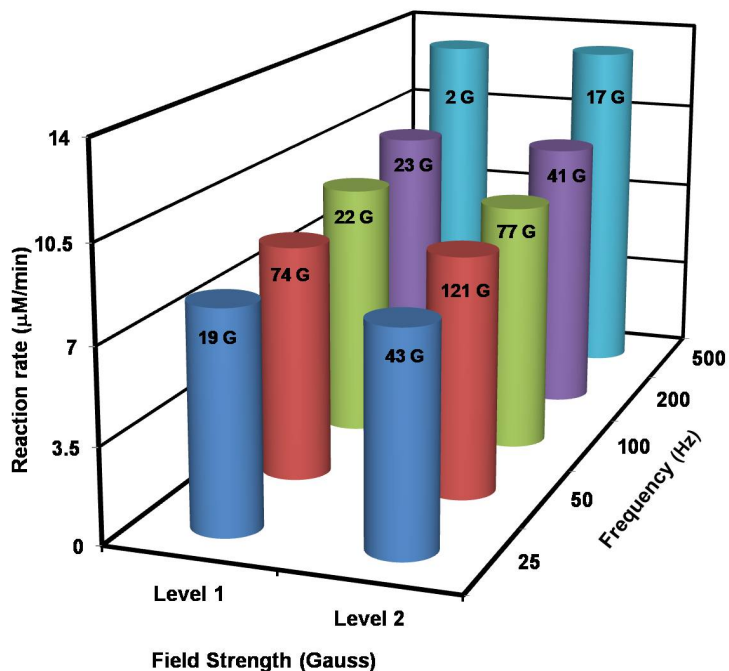


Figure 6-6 Effect on frequency and field strength of nanostirring on interface-assembled chloroperoxidase activity.

### 6.3.4 Visualization of mobility of MLM at interface

The actual mobility of MLM was visualized using bright field microscope with fluorescent dye attached enzyme at the interface. To capture the mobility in the presence of alternating magnetic field with frequency as high as 500 Hz, a high resolution camera with a high frame rate 1 millisecond was used. The water – hexane system with fluorescent dyed MLM was placed in glass well with cover slip bottom. The MLM assembled at the meniscus formed between water as the bottom phase and hexane as

upper phase. This meniscus was observed through the fluorescence microscope (Figure 6-7). The glass well was placed inside the solenoid that was connected to alternating electromagnetic field generator. The external magnetic field forced the dyed enzymes to move at the interface. This movement will result in observation of change in intensity of particular pixel at interface over time. This intensity change corresponding to the mobility can be visually observed in the fluorescence microscopy. The mobility of enzymes at the interface can be quantified by analyzing the intensity change of the surface plot for the corresponding image of dyed MLM at the interface.

The dyed MLM at the interface observed in bright field microscopy was subjected to external magnetic field with frequency ranging from 25 to 500 Hz and the corresponding change in intensity over time was calculated at different points on the interface. The intensity change in a pixel data over 1.25 seconds for each frequency was corrected with that of change in intensity of 0 Hertz or in the absence of external magnetic field. A differential analysis of this corrected change in intensity over time gave the relative mobility of MLM with frequency change (Figure 6-8). The correlation clearly indicates the increase in reaction rate with frequency is direct effect of mobility improvement enzymes at the interface. The change in intensity results from the movement of the dyed enzyme at the interface due to nanostirring. The distance travelled by the enzyme at the interface is given by the parameter  $\Delta\text{intensity}/\Delta t$ . The longer distance travelled by the enzyme at higher frequency is due to non-alignment of magnetic moment with field direction and this increased mobility improves the reaction rate with increase in frequency. Hence, the mobility of MLM is predominantly governed by the

frequency and for all the subsequent experiments the nanostirring was conducted at 500 Hz and 17 Gauss.

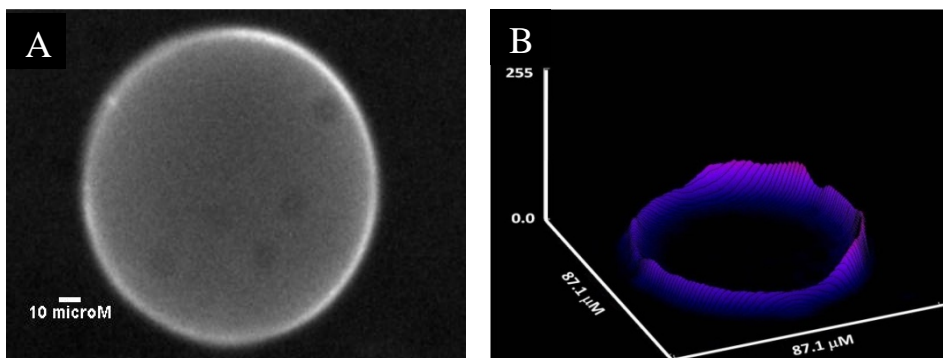


Figure 6-7 Visualization of mobility of MLM at interface  
 (A) Interface of a meniscus between hexane and water. (B) The surface intensity plot of corresponding interface after background subtraction.

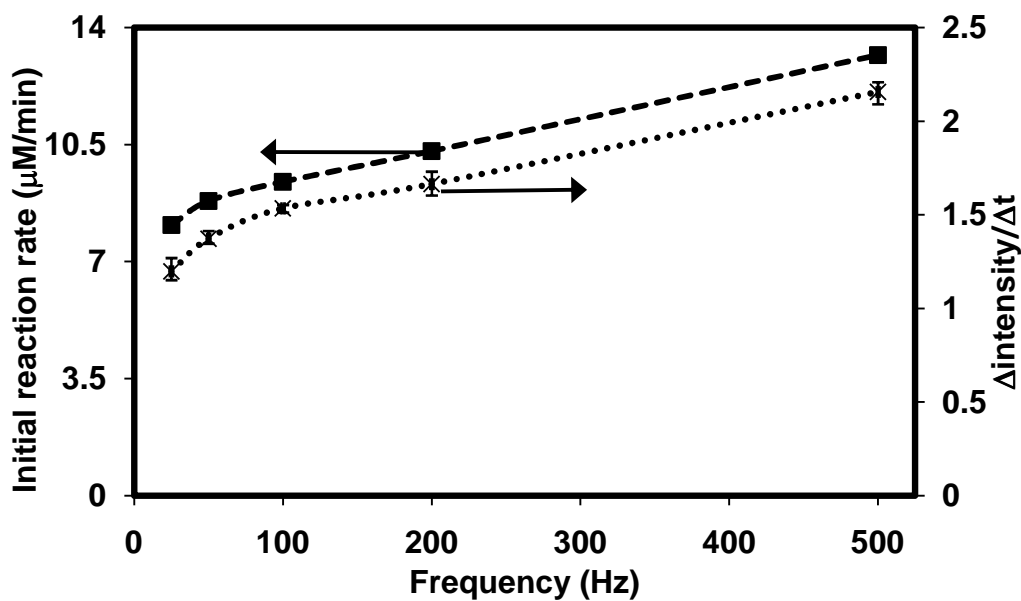


Figure 6-8 Correlation of actual mobility of MLM with the improvement in reaction rate on increasing the frequency.

### **6.3.5 Nanostirring effect on interface-assembled enzyme's activity**

It was previously shown that conjugating water-soluble enzymes with hydrophobic polymers facilitated the assembling of enzymes at oil/water interfaces[112]. Though the reaction efficiency in with the interface assembled enzyme is improved to a certain extent, slow reaction rate due to limited mobility of enzymes at the interface still remains as a considerable limitation. To improve the mobility of enzymes at the interface, superparamagnetic nanoparticles were conjugated with interface assembled enzymes and novel mechanism of nanostirring was employed. Application of force by external alternating electromagnetic field on interface assembled superparamagnetic nanoparticles vehicle resulted in nanostirring of entire MLM with improved mobility of enzymes at the interface.

Two distinct biphasic reaction systems that were transport limited were improved by nanostirring on MLM. One reaction system involved epoxidation of styrene by chloroperoxidase. This enzyme requires two substrates, a hydrophobic styrene and the hydrophilic  $H_2O_2$ . Another reaction system involved multiple enzymes with in situ cofactor regeneration. Alcohol dehydrogenase and glucose dehydrogenase were employed for reduction of acetophenone to S-1-phenylethanol and oxidation of glucose to gluconolactone in organic and aqueous phase respectively with NADPH/NADP<sup>+</sup> used as cofactor in the aqueous phase.

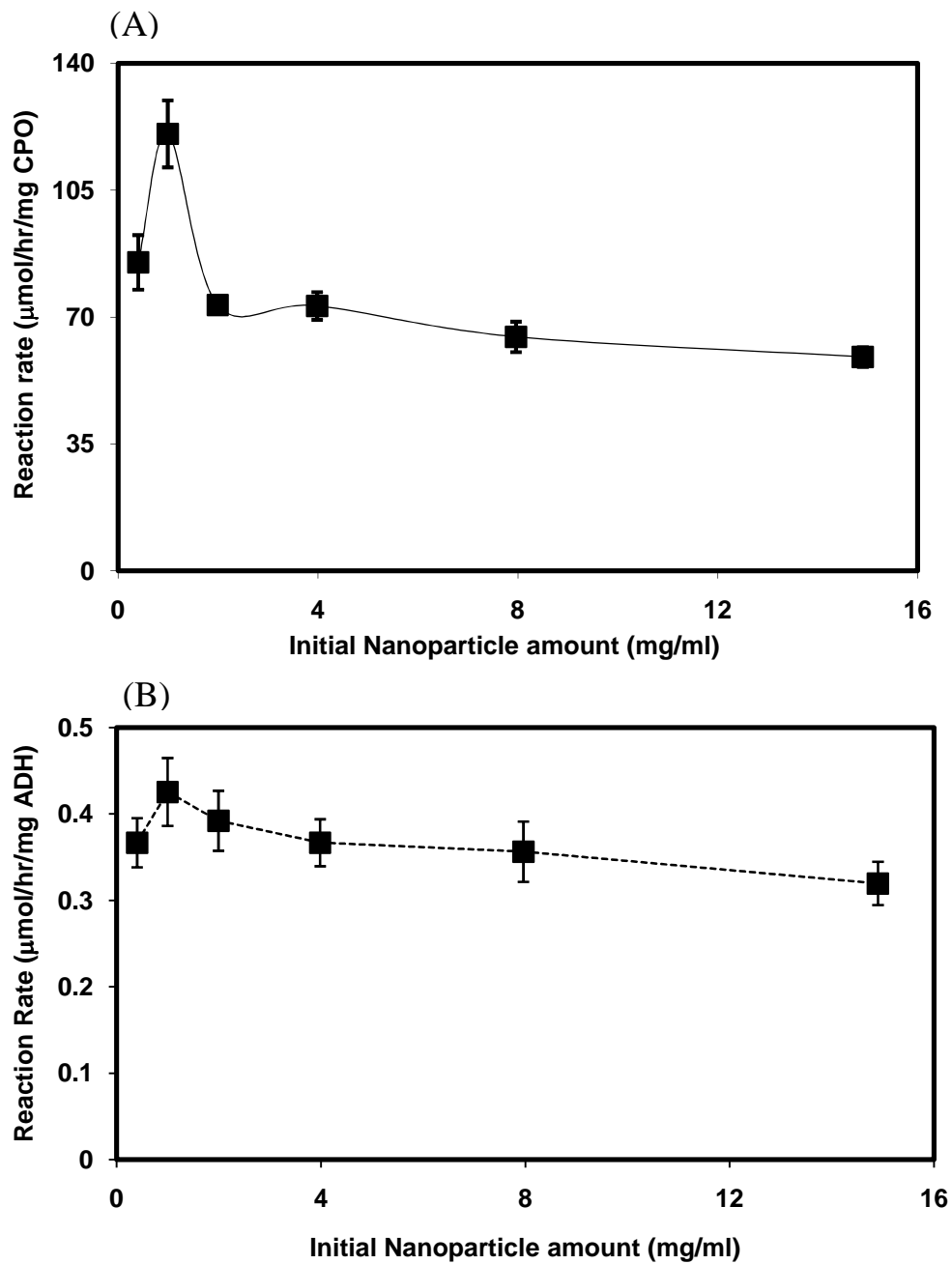


Figure 6-9 Effect of nanoparticles on reaction rate  
 (A) Epoxidation of styrene by chloroperoxidase (B) Reduction of acetophenone by Multienzymatic system.

The reaction was also influenced by the surface coverage of nanoparticles at the interface. As seen from Figure 6-9 the MLM showed optimum nanoparticles concentration that resulted in maximum reaction rate. It was seen that unlike CPO reaction system, the multienzyme reaction system was not influenced significantly with change in nanoparticles conc. This is due to multistep reaction at the interface, after a certain increase in rate by magnetic fields, the reaction is no longer dependent on nanoparticles concentration but is governed by intrinsic modified enzyme reaction parameters at the interface.

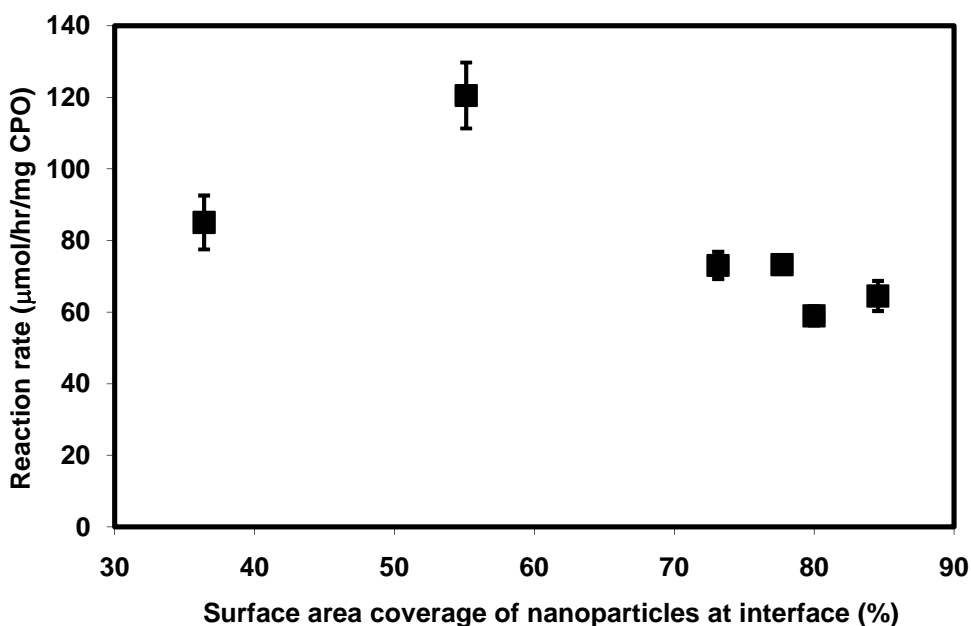


Figure 6-10 Enzymatic activity as function of surface coverage by nanoparticles at the interface.

The effect of nanostirring on the two transport limited reaction systems were performed at 500 Hz, 17 Gauss with 55.12% surface coverage of magnetic nanoparticles at the interface.

Another interesting observation was that the optimum nanoparticles concentration does not correspond to saturation concentration of nanoparticles at the interface. This phenomenon can be explained by the relative surface coverage of nanoparticles at the interface (Figure 6-10). At saturation nanoparticles concentration, the interface is predominantly occupied by the nanoparticles, which limits the interfacial area that is exposed to the enzyme for the reaction thus lowering the reaction rate per enzyme molecule. However, at the optimum nanoparticles concentration the amount of nanoparticles is just enough to disperse the enzymes throughout the interface and providing the MLM with sufficient strength for effective nanostirring.

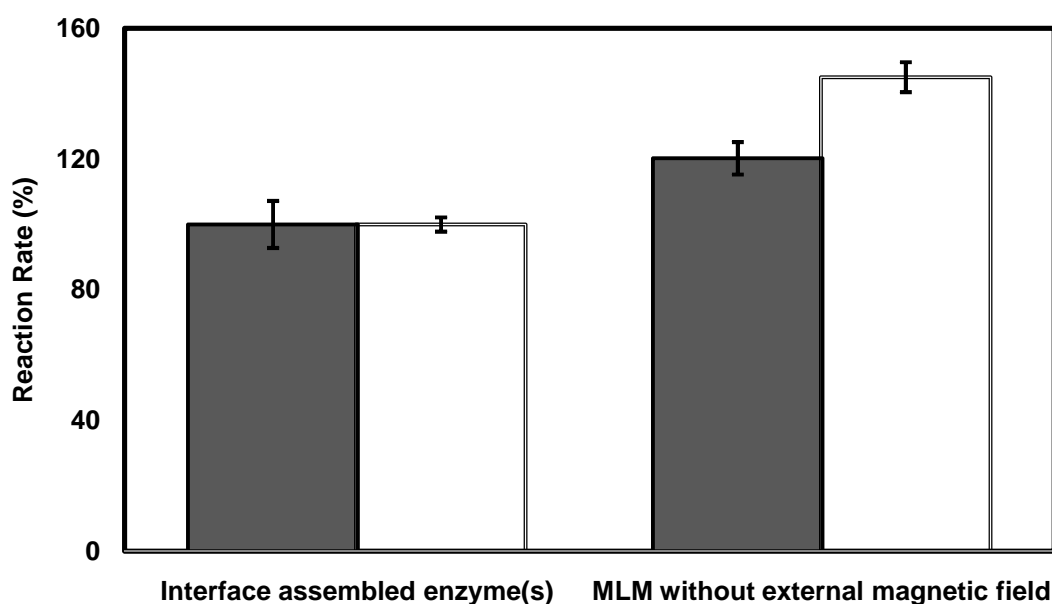


Figure 6-11 Effect of nanoparticles on interface-assembled enzyme's activity (■) Multienzyme reaction system (□) CPO reaction system.

Although both the reaction system was catalyzed by oxidoreductases, the observed effect of nanoparticles conjugation and subsequent nanostirring was significantly different. In Figure 6-11 the activity of interface-assembled enzyme without nanoparticles attachment to activity of MLM. 5 Units of total enzyme concentration was used for both the reaction system. It was seen that there is a significant increase in reaction rate for both the reaction system on attachment of nanoparticles to interface-assembled enzyme. This increase in reaction rate can be attributed to higher dispersion of enzymes at the interface due to presence of nanoparticles. The higher dispersion disrupts aggregation of enzymes at the interface and facilitates a more uniform assembly of enzymes throughout the interface.

In the presence of nanostirring the reaction rate of MLM is improved by over six times (Figure 6-12). The nanostirring improved the interfacial enzymatic reaction rate by two different processes: Enhancement of interfacial enzyme mobility and disruption of boundary layer for reactant/product mass transfer. The enhanced mobility of enzymes at the interface improves higher contact of enzymes with cofactor and reactants at the interface, improving the overall observed reaction rate. The boundary layer at the interface also contributes towards the mass transfer limitation for the reactants and slows down the entire reaction. The novel nanostirring mechanism disrupts the boundary layer and overcomes the mass transfer limitation resulting in higher reaction rate. The combination of these factors results in the observed increase of interfacial reaction rate with employment of nanostirring.



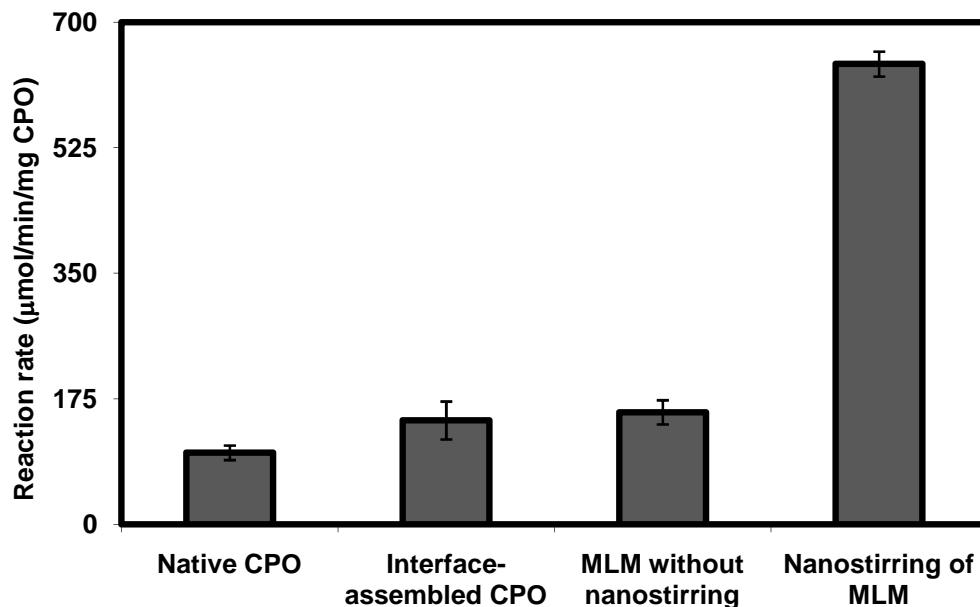


Figure 6-12 Effect of nanoparticles on interface-assembled CPO's activity.

The phenomenon of higher dispersion on attachment of nanoparticles to interface-assembled enzyme is further observed in Figure 6-13. The effect of dispersion of enzymes at the interface was evaluated by changing the total interface assembled enzyme concentration with and without attachment of magnetic nanoparticles. On attachment of nanoparticles and employing nanostirring, it was seen the rate gradually increases with enzyme concentration and then becomes flat in the mass transfer controlled regime around total enzyme concentration of 25.44 Units before decreasing due to aggregation of enzymes at the interface (Figure 6-13). This phenomenon is in sharp contrast to interfacial enzyme that was not adsorbed to nanoparticle. The results for interfacial enzymes without nanostirring indicate that initially the rate increases slowly with enzyme concentration then there is an exponential relationship and finally the rate becomes mass transfer controlled around total enzyme concentration of 12.72 Units.

It is seen that without nanoparticles, there is an initial lag in the enzyme concentration - rate relationship due to not fully saturated interface at low enzyme concentration, though there may be aggregates at the interface. At low enzyme concentration with limited mobility of interface-assembled enzyme and most of the interface is empty resulting in lower reaction rate. As the interface-assembled enzyme concentration is increased, it saturates the interface, giving rise to higher slope in the relationship.

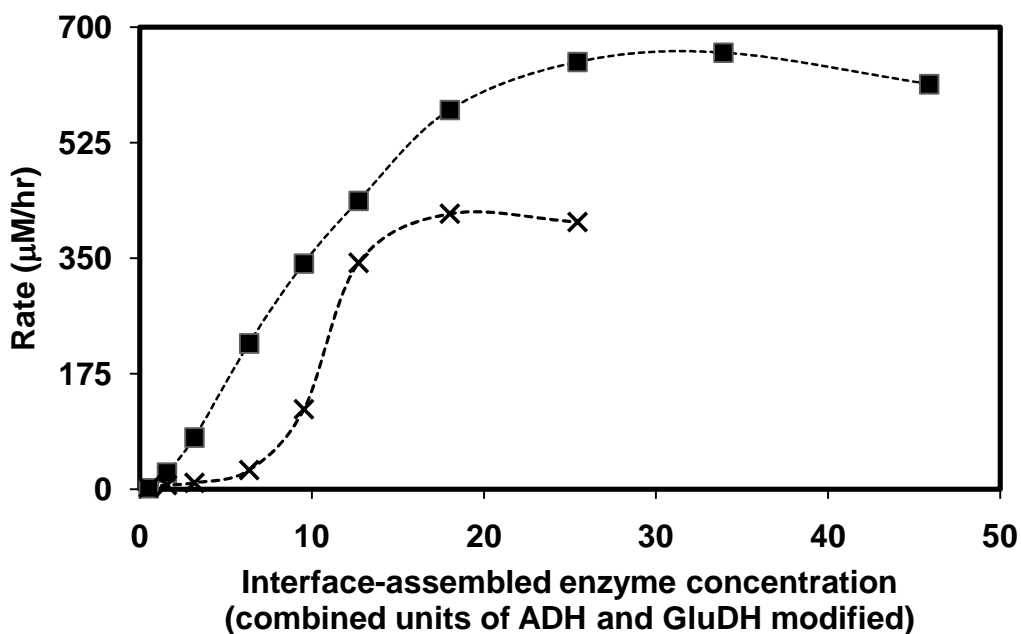


Figure 6-13 Effect of interface-assembled enzyme concentration.  
 (■) MLM in the presence of nanostirring (×) Interface-assembled enzyme in the absence of nanostirring.

Attachment of nanoparticles facilitates in the dispersion of enzymes at the interface. This is evident from the absence of sigmoidal curve shown by interfacial enzymes that were not properly dispersed. However, there are two competing factors that

govern the enzyme concentration-rate behavior with MLM on nanostirring. The nanoparticles attachment leads to higher dispersion of MLM at the interface resulting in increased rate initially but as the enzyme concentration is increased the surface occupied by the nanoparticles reduces the surface available for enzymes at the interface, this reduces the rate but at the same time the nanostirring effect offsets this short coming by improving the mobility of MLM at the interface. In Figure 6-13 the absence of sudden increase in reaction rate for any enzyme concentration with MLM is because of the above mentioned competing factors, the reduced actual surface area available for enzyme slows the rate but mobility improvement by nanostirring causes the rate to increase further. However, at very high enzyme concentration the effect of reduced surface area overcomes nanostirring and reduces the reaction rate on further increase in enzyme concentration. Therefore for MLM with nanostirring at lower enzyme concentration, higher dispersion of enzyme and nanostirring effect dominates and at higher concentration the low dispersion due to reduced available interfacial surface area dominates.

### **6.3.6 Effect of nanostirring on native enzyme's activity**

The adsorption of magnetic nanoparticles to native enzymes exhibited a contrasting behavior to that of interface assembled enzyme (Figure 6-14). 5 Units of total enzyme concentration was used for both the reaction system. The attachment of nanoparticles drastically reduced the activity of native enzymes. The reduction in activity though observed with both reaction system, it is far more significant with multienzymes

reaction system than chloroperoxidase. CPO retained significant specific activity of about 60% of native activity. However multienzyme reaction system with dehydrogenases exhibited only 18% activity retention on adsorption with nanoparticles. The enzymatic activity depends on the retention of enzyme's native structure on binding with another surface. The adsorption of enzymes on superparamagnetic nanoparticles is due to hydrophobic interactions. The surface spreading due to nanoscale and hydrophobic interactions with the nanoparticles resulted in this drop in activity of native enzymes. The difference of these interactions between two enzyme systems leads to the drastic disparity observed between the two reaction systems.

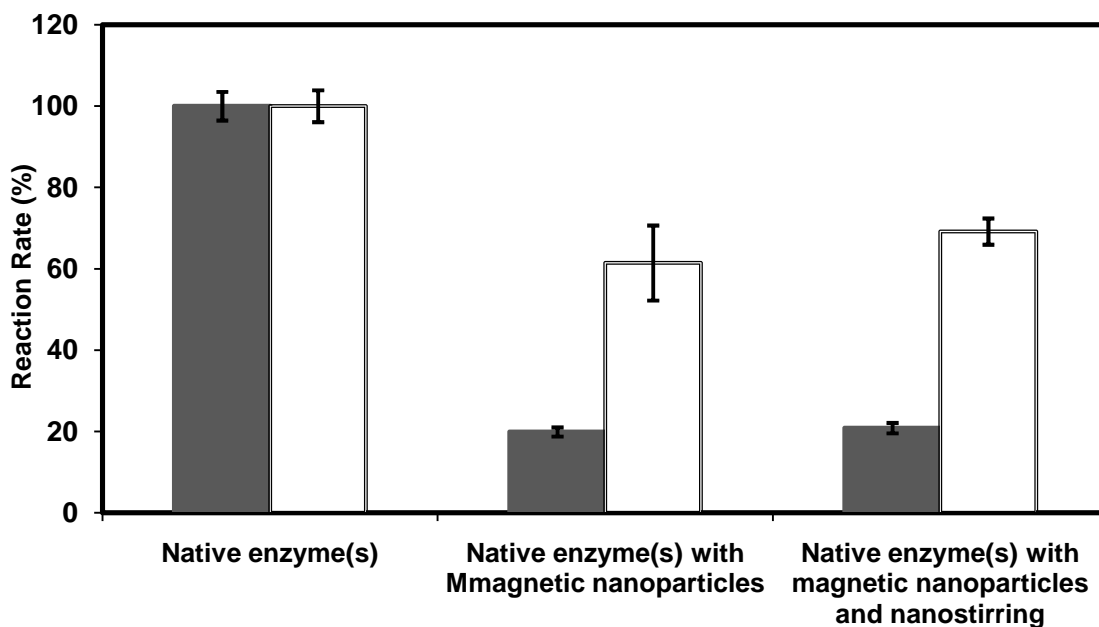


Figure 6-14 Effect of nanoparticles on native enzyme's activity.  
 (■) Multienzyme reaction system (□) CPO reaction system.

The interface assembled enzyme is protected from the hydrophobic interactions by the presence conjugated polymer. This reduces direct contact of enzyme surface with the

nanoscale and hydrophobic environment of nanoparticles, which decreases the inactivation due to surface spreading.

## **6.4 Conclusion**

In summary, it was demonstrated that interface-assembled magnetic nanoparticle bound enzyme can be prepared. The MLM showed stable interfacial assembly and magnetization curves indicated well dispersed superparamagnetic nanoparticles in MLM. The mechanism of nanostirring improved the mobility of enzyme at the liquid-liquid interface, which in turn was correlated with the observed increase in catalytic efficiency. Interface-assembled enzyme was effectively shielded from nanoscale hydrophobic interaction with nanoparticles by the presence of polymer in interface-assembled enzyme, thereby maintaining the enzyme's activity. This novel enzyme carrying magnetic nanoparticles at oil-water interfaces and mechanism of nanostirring will open new avenues for drug delivery, protein circuitry and nanobioelectronics.

# **CHAPTER VII**

## **MULTIENZYMATIC REACTIONS AT THE INTERFACE WITH BOTH ENZYME AND COFACTOR ASSEMBLED AT THE INTERFACE**

### **7.1 Introduction**

The high cost of both enzymes and cofactors is usually a great hurdle for their large scale applications[238, 239]. Efficient method to retain both enzymes and cofactors inside the reactor is necessary for process economy. Ultrafiltration membrane bioreactor has been used for enzyme-cofactor catalyzed reactions in homogenous solutions[194]. A continuous supply of substrate can be added with the concomitant removal of products. Most of the macromolecular derivatives have been retained with commercially available ultrafiltration membrane. Nanofiltration membranes have been used in the synthesis of xylitol and mannitol[240]. However, the flow characteristics of these membranes are very poor. The possibility of substrate or product retention is also a factor to be considered.

In the interfacial enzymatic reaction systems, an ideal configuration would be to have both enzymes and the cofactor assembled at the interface with products taken from either phase. This will reduce the downstream operations to a great extent and also elimination of membranes, increase the process flow conditions. High yields can be achieved in such reaction systems with efficient regeneration and reuse of enzymes and cofactors inside the reactor. However, a major constraint in employing such configuration is interfacial binding of cofactor and the enzyme. The limited two-dimensional mobility

of both enzyme and cofactor possesses a major hurdle in sustainable cofactor regeneration.

Another important constraint is the high sensitivity of dehydrogenases for stirring. Dehydrogenases are very susceptible and are easily denatured by shear caused by the conditions inside a process reactor. The process conditions like the interfacial area of contact, nature of stirring, stirring speed and reaction conditions like thermodynamics and kinetics should be carefully chosen to realize the difficult interaction of interface-assembled enzyme with interface-assembled cofactor for sustainable multienzymatic reactions at oil-water interface.

## **7.2 Materials and Methods**

### **7.2.1 Chemicals**

Glucose Dehydrogenase (GluDH) “Amano” NA ( EC 1.1.1.47, 286 IU/mg) was a gift from Amano Enzyme Inc. (Nagoya, Japan). Alcohol Dehydrogenase (ADH RS1) from *Rhodococcus* species (EC 1.1.1.1, 444 IU/ml) was obtained from Julich Chiral Solutions (Julich, Germany). D-Glucose (CAS 50-99-7), Acetophenone (CAS 15753-50-1),  $\beta$ -nicotinamide adenine dinucleotide phosphate reduced tetrasodium salt (NADPH) and Bovine Serum Albumin (BSA) standard were purchased from Sigma-Aldrich (St. Louis, MO). Carboxyl chloride terminated polystyrene (PS-COCl, Mw 2020) was purchased from Polymer Source, Inc. (Canada). Toluene and Hexane was purchased from J.T.Baker (Philipsburg, NJ). Protein assay dye reagents were purchased from Bio-

Rad laboratories (Hercules, CA). CuSO<sub>4</sub> (5H<sub>2</sub>O) and NaOH were purchased from VWR Sci. (PA). Ascorbic acid was purchased from Mallinckrodt, KY.

### **7.2.2 Enzyme modification for interfacial assembly**

Enzyme (ADH RS1 or GluDH) was dissolved in 1 ml of 0.05 M pH 7.8 phosphate buffer. The enzyme solution was then contacted with 10 ml toluene containing 10 mg of PS-COCl (M<sub>w</sub> 2020). The mixture was shaken at 240 rpm in dark for 1 h at room temperature. The reaction mixture was then centrifuged at 13,000 G for phase separation. The interface-assembled enzyme was recovered by removing the bulk phase solutions. The product was further purified by washing with buffer and toluene, each for at least three times, to remove residual free enzyme and polymer modifier.

### **7.2.3 Cofactor modification for interfacial assembly**

NADH was used as the cofactor. The cofactor modification was done in same way as outlined in chapter 5.

### **7.2.4 Interfacial reaction**

ADH RS1 and GluDH, both interface-assembled, with interface-assembled NADH were used for reduction of acetophenone in the organic phase with simultaneous oxidation of glucose in aqueous phase. Multienzymatic reactions were carried out in a 50 ml reactor with 10 ml of aqueous phase with 1.18 mmol NADH, with varying amount of glucose. The organic phase contained 5 ml toluene with varying amount of acetophenone



for interface assembled multienzymes. The enzyme ratios were varied for optimization. Mild magnetic stirring (75 rpm) of the interface was applied mechanically. The reaction was followed by analyzing the product, S-(-)-1-phenylethanol, in organic phase using GC with aliquots of 0.15 mL withdrawn periodically from organic phase.

### **7.2.5 GC analysis**

The reaction progress was monitored by measuring the concentration of S-(-)-1-phenylethanol in organic phase using Gas Chromatography (GC-3100, Varian) equipped with  $\beta$ -DEX<sup>TM</sup> 225 fused silica capillary column (30m $\times$ 0.25mm $\times$ 0.25 $\mu$ m), from Supelco Bellefonte PA). Aliquots of 150  $\mu$ l of organic phase were used for GC analysis. The injection temperature was maintained 220  $^{\circ}$ C with detector temperature of 300  $^{\circ}$ C, the column temperature was maintained at 100  $^{\circ}$ C for 5 minutes and ramped to 210 C at 10  $^{\circ}$ C/min. Commercially purchased S-(-)-1- phenylethanol standards were used for calibrations.

## **7.3 Results and Discussions**

### **7.3.1 Reaction system**

The multienzyme reaction system involving cofactors like that shown in Figure 5-3, could not be employed for the configuration with both enzymes and cofactor assembled at the interface. The reaction system 1 shown in Figure 5-3 was thermodynamically limited and carrying out that reaction with both enzymes and cofactor assembled at the interface will be too slow for any appreciable reaction in reasonable

time. The reaction system 2 shown in Figure 5-3 is fast but as seen from the kinetic analysis the dissociation constant  $K_C$  between enzyme and cofactor is very large, which makes the reaction slower. The enzyme ADH LB in this reaction system is very susceptible to the shear caused by the stirring employed to increase the reaction rate. Therefore, the bottlenecks of slow reaction coupled with quick denaturation of dehydrogenases due to stirring, possessed a challenging problem to carry out reaction with interface-assembled enzyme and interface-assembled cofactor.

The major criteria for a sustainable reaction at the interface with both enzymes and cofactor assembled at the interface is a reaction system that is thermodynamically favorable with enzymes that are not very susceptible to the shear caused by stirring to improve the interfacial reaction rate. Therefore, a combination of reactions from Figure 5-3 was chosen to study the interfacial interaction of interface-assembled enzyme and interface-assembled cofactor. The enzyme GluDH is known to be active with both cofactors NADH and NADPH, with a reduced activity with NADH. This enzyme when combined with ADH RS1 can result in a reaction system that satisfies both the criteria for all interfacial reaction. The enzyme GluDH also exhibits high specific activities even around neutral pH (Figure 5-8), which results in easy use with ADH RS1 that loses its activity rapidly above neutral pH. The substrate, glucose for GluDH, is strong reducing agent and does not catalyze the hydration of the reduced cofactor. In addition, the product, D-glucono- $\delta$ -lactone is spontaneously hydrolyzed to gluconate, which makes the reaction irreversible. Therefore, the reaction system as shown in Figure 7-1 was used for interfacial reactions with both enzyme and cofactor assembled at the oil-water interface.

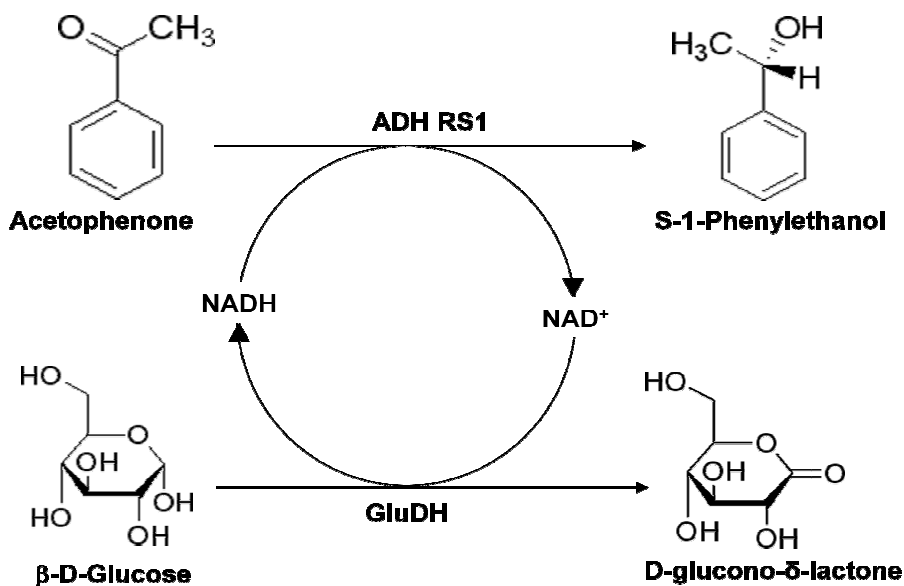


Figure 7-1 Reaction system used with multienzymes and cofactor modified at the interface

### 7.3.2 Effect of polymer modifier

The limited or no interaction between interface-assembled enzyme and interface-assembled cofactor was observed previously with many reaction systems. Based on surface characterization in chapter 3, it was thought that the polymer modifier added during the enzyme modification may entangle at the interface and have limit enzyme's mobility at the interface and prevent it from efficient interaction with interface-assembled cofactor. In Figure 3-3, the small kink in the transition phase (plateau region) of the isotherm may be due the entanglement of polymer head groups in interface-assembled enzyme. To verify this hypothesis, the polymer modifier concentration was varied during enzyme modification. It was previously observed that 3.67 mg of polymer modified is consumed for 130 μg of ADH modified. Based on this observation, the polymer

concentration was varied below and above this critical value for the given amount of ADH in aqueous solution during modification.

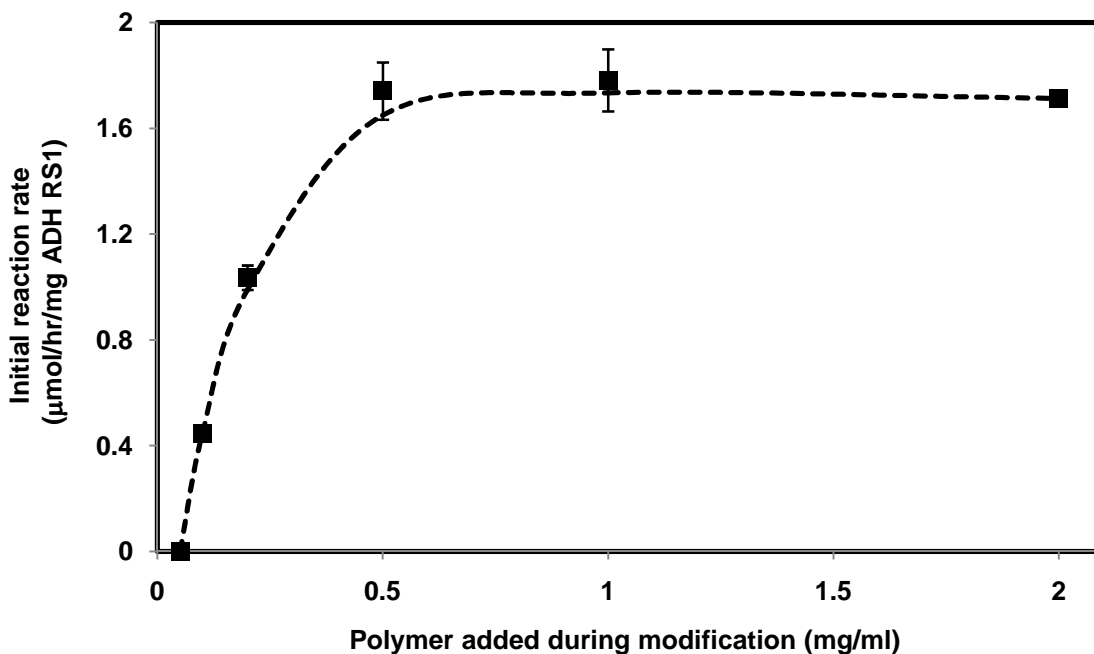


Figure 7-2 Effect of polymer added during enzyme modification on reaction rate with both enzymes and cofactor assembled at the interface

As seen from Figure 7-2, it was seen that the reaction rate increased with increase in polymer concentration but above the concentration of 0.5 mg/ml polymer, the reaction rate does not increase much. It was suspected that the presence of too much polymer may lead to entanglement of modified enzymes at the interface and affect the rate. However, the results indicate that initially the rate increases with increase in polymer concentration, it was previously found that 3.67 mg polymer is required for enzyme's modification, and above this polymer concentration the reaction rate is hardly affected by further increase of polymer. This indicates that the higher amount of polymer modifier is not critical for the reaction.

### 7.3.3 Effect of substrate concentrations

The concentration dependence of initial reaction rate showed a typical Michaelis-Menten pattern. The acetophenone concentration was varied with a fixed glucose concentration of 20 mM (Figure 7-3). At lower concentration of substrate acetophenone, the reaction rate is directly proportional to the substrate concentration behaving like a first order reaction. At higher concentration of the substrates the reaction behaves like zero order reaction.

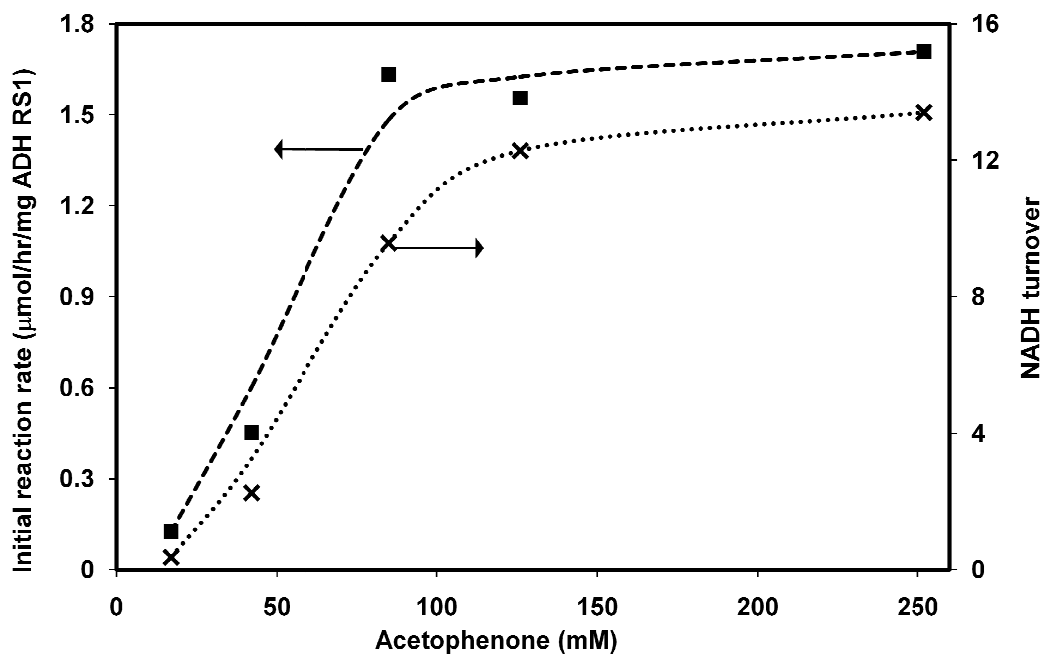


Figure 7-3 Effect of Acetophenone concentration on reaction rate with both enzymes and cofactor assembled at the interface.

An interesting observation was increase in NADH turnover with substrate concentration and becoming steady after a particular concentration of substrate. This observation can be explained by the total time for which the enzyme is active at the

interface. The operational time of the polymer conjugated enzyme at the interface is determined by several factors like, stirring speed, nature of stirring, interfacial interaction between enzyme, cofactor and substrate. A combination of all these factors determines the operational stability of the interface-assembled enzyme. In this particular configuration of both enzymes and cofactor assembled at the interface, it was noticed that the operational stability of interface-assembled enzyme was 44 hours. Therefore, at higher substrate concentration with the reaction rate remaining constant and also the operational not changing much, the NADH turnover remains constant. A similar trend was observed on changing glucose concentration at fixed acetophenone concentration of 84 mM (Figure 7-4)

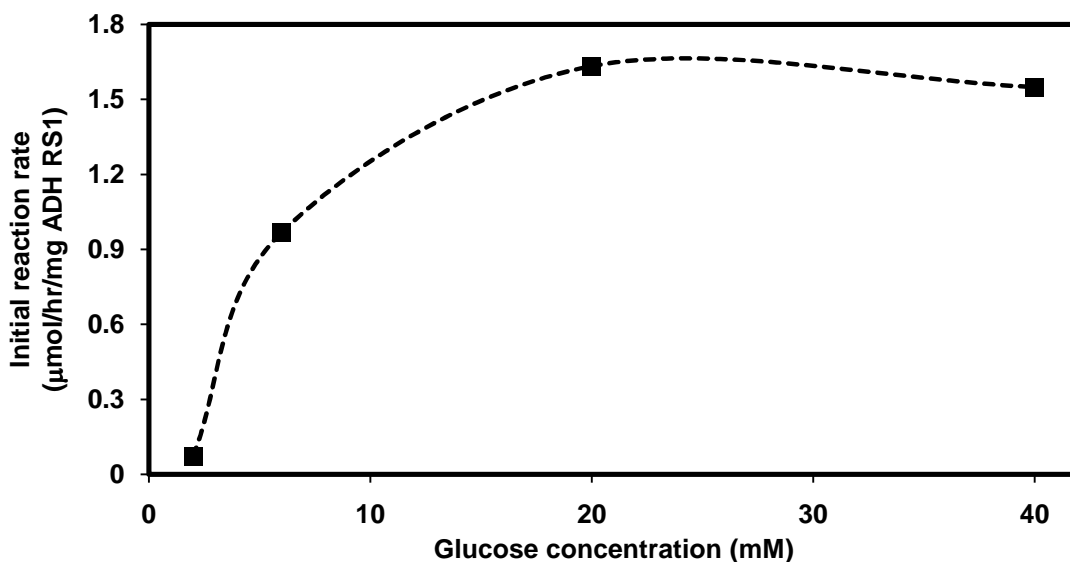


Figure 7-4 Effect of Glucose concentration on reaction rate with both enzymes and cofactor assembled at the interface.

### 7.3.4 Effect of enzyme ratio

The effect of enzyme ratio was studied with total protein content at the interface maintained constant at 183.2  $\mu\text{g}$  protein. The ratio was defined in terms of protein of ADH RS1 to protein of GluDH. The ratio was varied from 0.1 to 10. The reaction rate shows an interesting behavior with change in enzyme ratio. The results indicate an inverted bell curve with the minimum near the ratio of 1. Above an enzyme ratio of 1 the rate increases with more amount of ADH (Figure 7-5). At higher ratio the increase is not as steep as at lower ratio above 1. The curve will be reversed on defining the enzyme ratio in terms of GluDH protein to ADH RS1 protein.

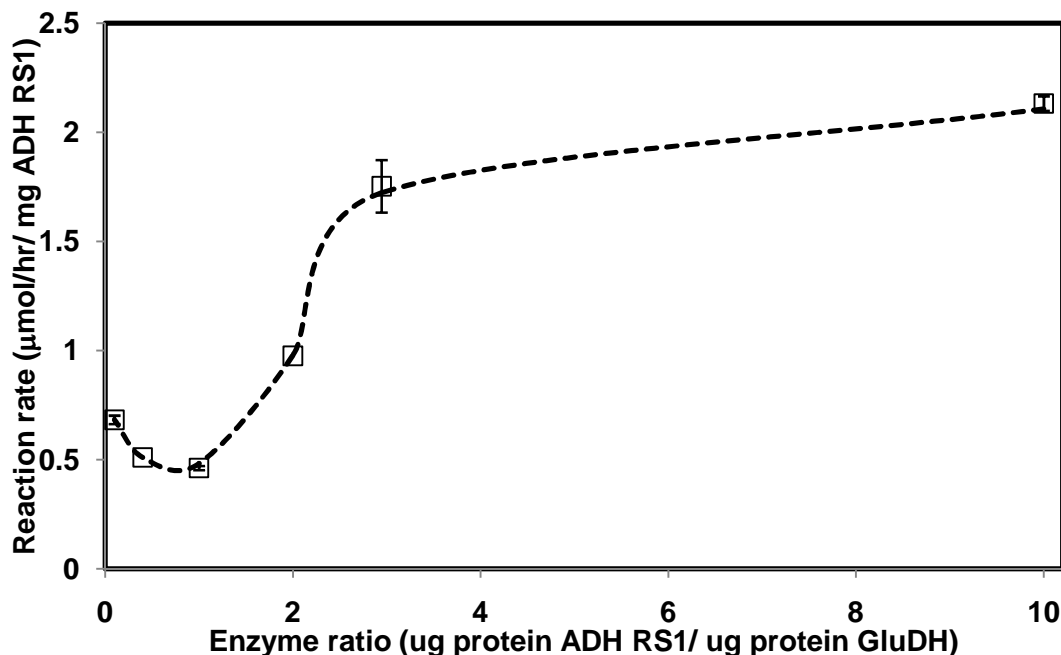


Figure 7-5 Effect of enzyme ratio on reaction rate with modified enzymes and modified cofactor

The curve indicates three distinct regions as the enzyme ratio is changed at the interface. Below a ratio of 1, ADH RS1 is present in very little amount with high amount of GluDH, this makes the reaction directly proportional to the amount of GluDH present. At a lower ratio the amount of GluDH is greatest hence the reaction rate is high but as the ratio increases below 1, the amount of GluDH decreases that makes the rate to decrease. At enzymes ratios higher than 1, initially the rate is directly proportional to ADH and increases with the enzyme ratio till the amount of GluDH required for efficient regeneration is high enough to maintain this increase in reaction rate. At higher ratios of above 3, the amount of GluDH is very low to have a fast regeneration, which makes a slower increase in reaction rate.

#### **7.4 Conclusion**

A main prerequisite for the development of interfacial biocatalysis with multienzyme systems is that it can be carried out efficiently and economically. Realization of reaction with enzymes and cofactor assembled at the interface is a critical step towards that goal. This work has demonstrated that an interfacial reaction with interface-assembled enzyme and interface-assembled cofactor can be possible. The reaction system exhibited multiple turnovers of interface assembled cofactor at the, which indicates an interfacial interaction between polymer conjugated enzyme and macromolecular derivative of cofactor. However, further systematic analysis of interfacial interaction between enzyme and cofactor is necessary for improving the efficiency of interfacial biocatalysis.



## CHAPTER VIII

# ENZYME-POLYMER COMPOSITE NANOFIBERS WITH HIGH ENZYME LOADINGS FOR USE AS BIOSENSORS

### 8.1 Introduction

The hydrophobic manipulation of microenvironment of enzyme can be further extended to obtain organic soluble enzyme that can be used in development of many functional materials. Nanostructures are ideal for functional materials whenever high specific surface area is desired. Electrospun nanofibers, a unique class of one-dimensional nanomaterials that are suited for low-cost large-scale production, have attracted extensive research interests and have been functionalized for applications including electronics[241], tissue engineering[242], reinforced composites[243] and filtration [244]. Among other forms of bioactive nanomaterials[15, 132, 245], enzyme-carrying nanofibers are particularly promising for biosensors[246] and biocatalysts[132, 137, 138] due to their excellent performance and great flexibility in both preparation and application [138, 247, 248]. Electrospinning is a widely adapted method for preparation of polymeric nanofibers [133, 134]. Electrospun nanofibers functionalized with enzymes for use as highly active biocatalysts have been demonstrated recently[132, 138].

Most of the enzyme-carrying nanofibers reported so far have been prepared through surface attachment of enzymes onto nanofibers, and in most cases only partial surface coverage have been achieved. Factors such as the availability of functional groups and the compatibility between the enzyme and the polymeric nanofibers may

determine the overall loading and distribution of the enzymes on the nanofibers. One alternative way is to entrap enzymes within the nanofibers. That can be achieved through spinning a solution that contains both the enzyme and polymer. A good compatibility between the enzyme and polymer is needed, and water-soluble polymers have been successfully spun in the presence of native enzymes [136, 137, 245]. It was also demonstrated that enzymes with enhanced hydrophobicity can also be co-spun with hydrophobic polymers [138], although only moderate enzyme loadings were achieved. Compare to surface attachment, entrapment should lead to higher loadings and uniform distribution of enzymes, thus generating high performance bioactive materials. The current study examines the upper limits in preparing hydrophobic nanofibers with enzymes embodied. Specifically the preparation and performance of glucose oxidase (GOx)-polyurethane composite nanofibers were examined. GOx was solubilized in organic solvents via ion-pairing with a surfactant and was then co-spun with polyurethane.

Enzyme entrapment with traditional methods usually generate materials with the majority of the enzyme not available for reactions[15, 249], while nanofibers have the potential to expose a great portion of the entrapped enzyme to reaction media and thus leading to high active materials. Such high active nanofibers were examined for biosensor applications in this study. Enzyme-based biosensors have been applied for detection of a wide range for chemicals ranging from toxic agents, environmental pollutants to biochemicals including blood sugars[250, 251]. The catalytic efficiency of the enzymes is critical in determining the performance of a sensor in terms of sensitivity,

selectivity, response time, reproducibility and lifetime. Nanofibrous enzymes appear to be greatly appealing for development of high performance biosensors.

## **8.2 Materials and materials**

### **8.2.1 Chemicals**

Glucose oxidase (GOx) from *aspergillus niger*, polyurethane (PU), didodecyl diammoniumbromide (DDAB), Docusate sodium salt (AOT), Cetyltrimethylammonium bromide (CTAB), pyridine, *N,N*-dimethylformamide (DMF), dimethyl sulfoxide (DMSO), methylene chloride (dichloromethane) were purchased from Sigma Chemical Co. (St. Louis, MO). Sucrose monododecanoate was a generous gift from Mitsubishi Chemical performance polymers, inc. (Greer, SC). HPLC grade toluene was purchased from J. T. Baker (Phillipsburg, NJ). Lithium chloride (LiCl) was purchased from Aldrich (Milwaukee, WI). Stainless mesh (type 304 woven wire cloths, 24×24, 0.014 in. wire diameter) was obtained from McMaster-Carr Supply Company (Aurora, OH).

### **8.2.2 Solubilization of Glucose Oxidase in organic solvent**

Unless specified, the extraction of GOx was performed with the following typical procedure: An aqueous phase consisted of 10 ml of 0.7 mg/mL glucose oxidase and 20 mM Acetate buffer of pH 5.5 was prepared. The solution was then contacted under stirring at 300 rpm and 25 °C for 2 min with 10 ml of toluene that contained 2 mM DDAB. Phase separation was achieved by centrifugation. The organic soluble enzyme was then dried by bubbling N<sub>2</sub> through the solution to give an enzyme-surfactant ion-paired complex that can be dissolved in different organic solvents. The concentration of

GOx in the organic phase was determined spectrophotometrically at 450 nm by monitoring the yellow color of FAD that is attached to the enzyme. The higher pH values that are outside the buffering range of this buffer was attained by preparing an acetate solution with acidic and basic components corresponding to the pH. A common hydrophobic solvent, toluene, which has a polarity index of 2.4 was selected as the solvent.

### **8.2.3 Electrospinning**

A polymer-enzyme mixture solution was prepared at room temperature by dissolving polyurethane (PU) in a mixture of tetrahydrofuran (THF) containing 0.2 wt % LiCl and toluene (3:1 v/v) containing ion-paired DDAB-GOx complex. The polymer-enzyme solution was electrospun as described in a previous work[132], with electric field strength of 1 kV/cm. A Teflon capillary tube with an orifice diameter of 0.5 mm was used as the jet. An electrospinning speed of 2  $\mu$ l/min was found to give good fibers without much chocking of the jet. Fibers were collected on carbon paper that was used as an electrode in biofuel cell. The weight of carbon paper was measured before and after the collection to monitor the net weight of accumulated fibers with enzymes. The amount of GOx in the fiber corresponds to the ratio of polymer to enzyme in the solution.

### **8.2.4 Enzyme Activity**

The activity of GOx in nanofibers was measured using glucose as substrate in pH 5.1, 100 mM acetate buffer. The reaction with nanofibrous GOx was conducted in 50-mL vials. Nanofibers with known weight were added to 30 mL of 1M glucose solution containing 0.2 mg horseradish peroxidase and 2 mg O-dianisidine. The time course of the

reaction catalyzed by the nanofibrous GOx was obtained spectrophotometrically by measuring the absorbance of 1 ml of aliquots from the reaction mixture taken at constant time interval.

### **8.2.5 Enzyme Stability in Organic Solvent**

GOx solubilized in toluene was dried by passing N<sub>2</sub> to remove toluene and re-dissolved into different solvents like THF, Pyridine, DMF and Dioxane. The solvents were chosen such that both PU and DDAB are soluble in it. The re-dissolved GOx in solvents was incubated at room temperature (22 °C) for 24 hours. The incubation was stopped by purging N<sub>2</sub> to remove the solvent. The activity was then measured using glucose as substrate in aqueous buffer, according to the procedure described above.

### **8.2.6 Electrochemical experiments**

A three-electrode electrochemical cell was used to evaluate the potential use of enzyme carrying nanofibers as biosensors. The cell consisted of an (Model CH111, CH Instruments, Austin, TX), a platinum-wire counter electrode, and a modified working electrode made with fiber-coated over a carbon paper. The cyclic voltammetry of the sensor was performed in a phosphate buffer solution (pH 7.0, 0.5M). The sensitivity of the biosensor was monitored at the potential of +0.69 V versus Ag/AgCl reference electrode. The cell was operated at room temperature, in an O<sub>2</sub> purged unstirred solution and it was calibrated with different concentration of glucose. The glucose solution of unknown concentration was then analyzed at this voltage. After applying the desired working potential, enough time was allowed for the cell to contact with oxygen.

## 8.3 Results and Discussions

### 8.3.1 Solubilization of GOx in organic solvent

Enzyme-polymer composite materials are generally difficult to prepare when hydrophobic polymers are used. To achieve that, hydrophobic modification of the enzymes is needed[83]. Several physical and chemical modifications have been found efficient to achieve molecular solubilization of proteins in hydrophobic solvents. It has been demonstrated that enzymes can be solubilized into organic solvents via chemical modification with hydrophobic moieties [252, 253], physical complexation with chemicals such as polymers [254]and lipids[255]or ion-pairing with surfactants [85, 256]. Conjugation of enzymes with polymers to form amphiphilic structures for interfacial assembly of enzymes have also been reported [112, 191]. Among others, ion-pairing is regarded as an effective process that involves simple operations and the use of cheap agents, surfactants. The solubilization of GOx in organic solvents by covalent attachment with alkyl chains[257] or by reverse micelle[258] has been reported previously. GOx is a dimeric glycoprotein of molecular weight 150–160 kDa containing up to 16% of mannose-type carbohydrate and one flavin adenine dinucleotide (FAD) group per monomer as the cofactor[259].

In the present study, GOx was solubilized into toluene via ion-pairing with a cationic surfactant DDAB. The formation of ion pairs requires oppositely charged enzyme and surfactant. The pI of GOx is 4.2 and the optimum pH for native GOx's activity is pH 5.5. That led us to select the cationic surfactant DDAB. The concentration of DDAB was maintained lower than its CMC value (15 mM) to avoid micelle formation

[260]. Maximum solubilization of GOx was observed with 2 mM DDAB. The pH appeared to be critical in determining the solubilization yield of the enzyme. As shown in Figure 8-1, the highest solubilization yield was observed at pH 5.5. According to the consideration of electrostatic interactions, higher pH values which promise stronger binding forces between the enzyme and surfactant should lead to better solubilization. However, the increased attraction may also lead to change in the structure of the enzyme and cause denaturation and precipitation, thereby decreasing the solubilization yield of GOx extracted[261]. Similar pH dependency has been reported previously for horseradish peroxidase[256] and  $\alpha$ -chymotrypsin[85].

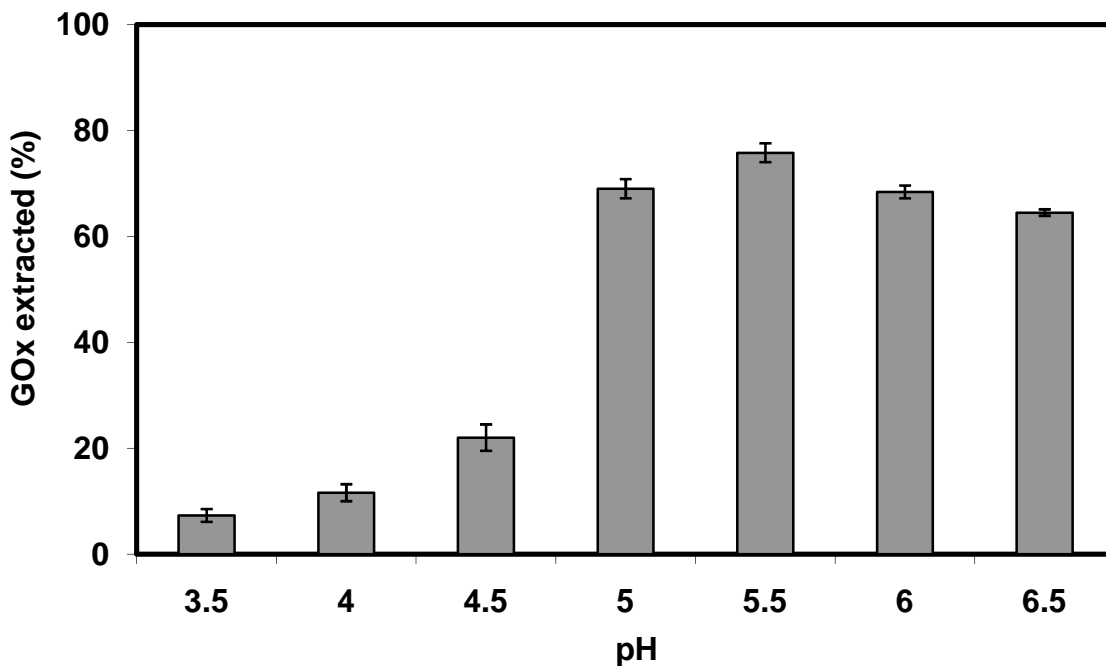


Figure 8-1 Effect of aqueous phase pH on extraction efficiency of GOx.

The effect of solvent on solubilization of GOx was evaluated by changing the solvent based on their log P value. The hydrophobicity of DDAB in GOx-DDAB ion pair makes it easily extractable into a solvent with a weaker solvent-solvent interaction than water. The free energy change for the extraction process will favor a solvent with least polarity. Among the solvents benzene, dichloromethane, chloroform and toluene in which DDAB is soluble, toluene with a polarity index of 2.3 is least polar. This makes toluene effective solvent for extraction. Lower concentration of DDAB is not sufficient to extract GOx from aqueous phase. A higher concentration leads to reverse micelle formation, which has to be avoided to form a uniform phase during electrospinning. The CMC of DDAB in water is 15 mM (Mehta et. al.) Therefore, the effect of DDAB concentration was studied under the CMC value. An optimum concentration of 2 mM DDAB was selected.

In other trials, different surfactants like AOT, CTAB and Sugar monododecanoate were tested. AOT being anionic surfactant did not extract any GOx above pH 4.2 and below that pH; the conditions are too acidic for the enzyme. CTAB though cationic, did not have groups that have enough hydrophobicity to extract enzyme in organic phase. Sugar monododecanoate being non-ionic and soluble in aqueous phase, did not result in any extraction of GOx in the organic phase.

### **8.3.2 Electrospinning of solubilized GOx**

The solubilized GOx was electrospun with PU for NEM fabrication. The process of electrospinning a mixture of polymer-enzyme solution is influenced by various factors.



The presence of compounds with high degree of difference in physical and electrochemical properties in polymer-enzyme solution requires a careful selection of electrospinning conditions that results in high loading of enzyme on PU nanofibers without compromising the integrity of the spun nanofiber. To start with, the solvent system for electrospinning should satisfy the primary criteria of dissolving PU while maintaining solubilized GOx stability and activity. Figure 8-2 summarizes the effect of potential solvents on solubilized GOx stability. The solubilized enzyme was incubated with a solvent for 24 hours in room temperature. The activity of solubilized enzyme decreases as the solvent polarity increases. The solvents with high polarity compete for the intrinsic water of hydration of enzyme, thereby, denaturing the enzyme. Toluene with relatively lower polarity index resulted in activity closer to that of enzyme that has not been incubated with any solvent.

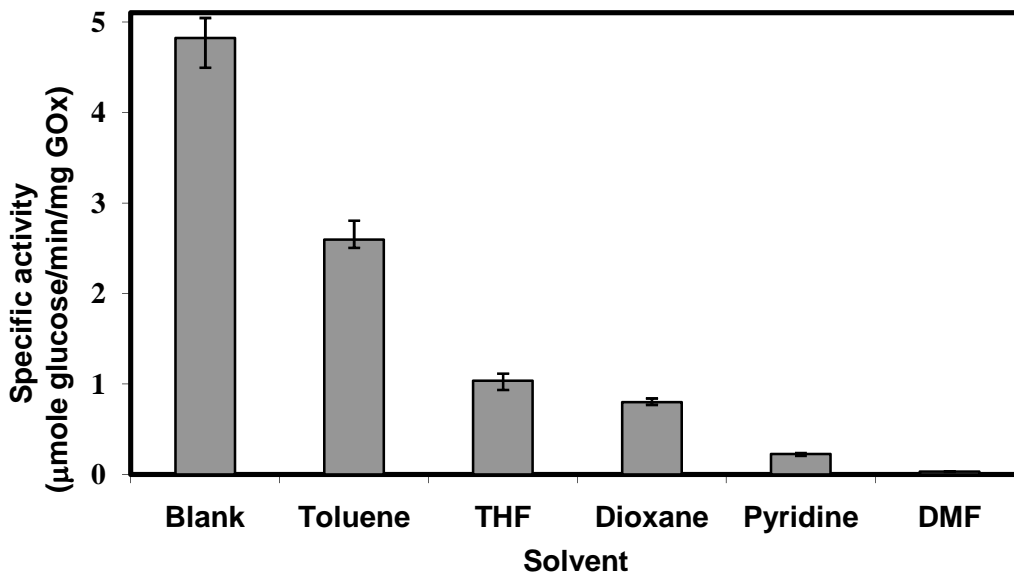


Figure 8-2 Effect of solvent on organic-soluble GOx stability

However, PU is not soluble in toluene. Therefore, for electrospinning solution toluene was used as a co solvent along with THF that dissolve PU. The selection toluene-THF solvent system for electrospinning also helps in maintaining the integrity of NEM (Figure 8-3). Addition of salt (LiCl) eliminated the problem of particle formation in NEM by increasing the charge in the solution and making it more homogenous. However, a higher concentration of LiCl (2 wt %) resulted in very thick fibers. Therefore, the polymer-enzyme solution was made with THF and toluene to increase the activity of GOx and salt was added in low concentration (0.2 wt %) to reduce the precipitation of enzyme during electrospinning. Other conditions like speed of electrospinning, electric field strength and humidity also affected the fiber.

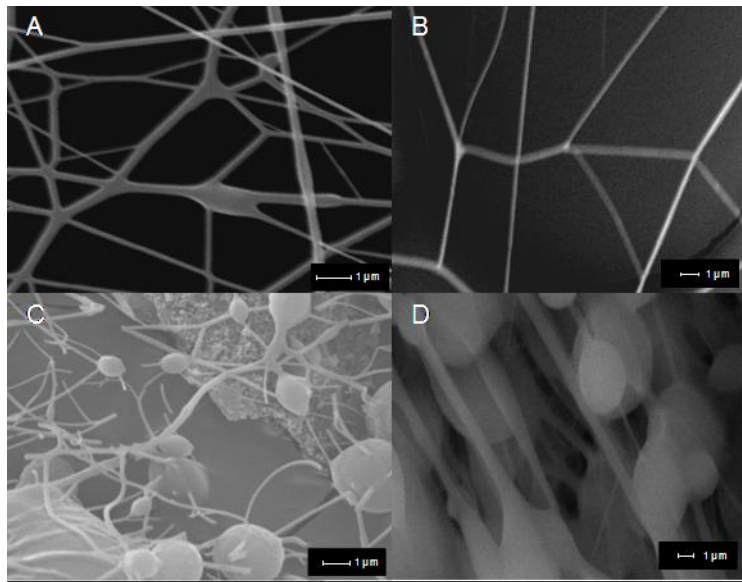


Figure 8-3 Effect of different parameters on nanofiber quality. (A) Nanofibers without beads. Conditions: 0.2% Salt, 1THF:3Toluene and 5% GOx. (B) Uniform nanofibers without beads. Conditions: 0.2% Salt, 3THF:1Toluene and 5% GOx. (C) Nanofibers with beads. Conditions: 0% Salt, 3THF:1Toluene and 5% GOx. (D) Predominantly beads. Conditions: 0% Salt, 1THF:3Toluene and 5% GOx.

NEM was fabricated with a maximum enzyme loading of 30 % (w/w) GOx in nanofiber. Above 30 % (w/w), GOx precipitated in the polymer enzyme solution, electrospinning such solution will lead to particle formation in NEM due to denatured enzymes. Therefore, the maximum achievable enzyme loading in NEM is determined by the phase behavior of polymer enzyme solution. In a previous work[132], a theoretical loading maximum of 11 % monolayer coverage was reported with chemical attachment of enzyme and polymer fiber. The higher enzyme loading reported here had been possible by utilizing the inner volume of nanofiber mat through encapsulation of enzymes in nanofibers and electrostatic interaction between the charged enzyme and PU fiber at molecular level, which is a unique characteristic of direct electrospinning of polymer-enzyme solution. The nanofibers were collected on carbon paper for use in electrochemical cell and on steel mesh for evaluating the aqueous activity of NEM (Figure 8-4). The effective encapsulation of enzymes inside NEM was assessed by incubating NEM in buffer at room temperature under stirring. At regular intervals, the sample from incubation mixture was centrifuged and the supernatant was analyzed for GOx. The supernatant did not exhibit any appreciable GOx activity, indicating efficient entrapment of GOx by the nanofibers.

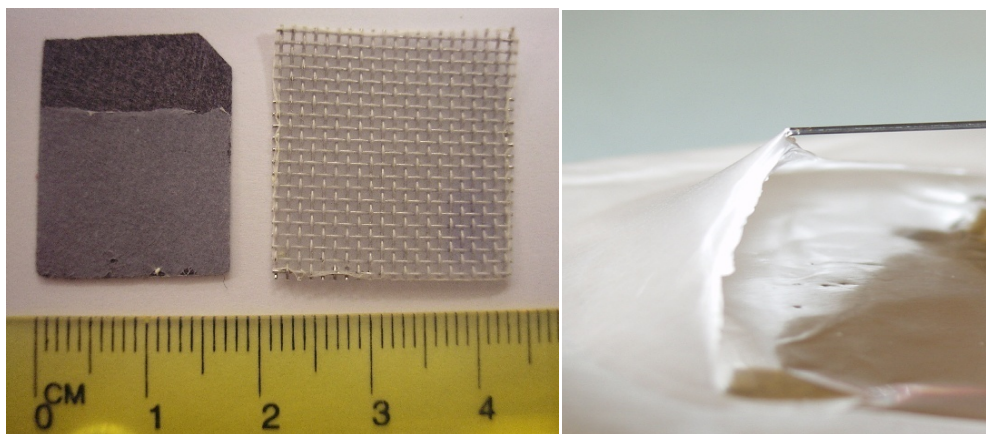


Figure 8-4 Nanofibrous enzyme material (NEM)

### 8.3.3 Use of NEM as biosensor

Apart from high enzyme loading and homogenous material distribution of NEM with effective encapsulation, the activity of enzymes in NEM is important for sensitive biosensor development. The specific activity of NEM was studied with respect to the enzyme loading and weight of the nanofiber sheet. The weight was increased by increasing the collection time of the nanofibers, which in turn increases the thickness of collected nanofiber sheet. Thicker NEM leads to more mass transfer limitations for reactants and products. The activity assays of NEM gave the effect of extreme electrospinning conditions on specific activity of GOx. The perspective of mass transfer limitations on catalytic efficiency of NEM will provide an insight on corresponding biosensor performance. The highest observed activity of NEM was 0.15 U/mg Table 8-1. The weight of NEM had a significant influence on the initial activity of nanofibrous enzyme. From Figure 8-1, the reduction in activity for 5 % and 20 % enzyme loading

were similar based on weight of the collected nanofibers. This indicates that the activity reduction is due to mass transfer limitation with more fibers.

Table 8-1 Effect of enzyme loading and weight (based on electrospinning time) of nanofibrous enzyme activity

<b>Enzyme loading</b> (wt % of PU)	<b>Weight of NEM</b> (mg)	<b>Activity of GOx in NEM based on amount of enzyme</b> ( $\mu\text{mole glucose min}^{-1}$ mg GOx <sup>-1</sup> )	<b>Activity of GOx in NEM based on weight of nanofibers</b> ( $\mu\text{mole glucose min}^{-1}$ mg NEM <sup>-1</sup> )
5	0.12	0.154	0.008
5	0.3	0.097	0.005
5	0.54	0.052	0.003
20	0.12	0.146	0.029
20	0.3	0.08	0.016
20	0.54	0.01	0.002
30	0.12	0.011	0.003
30	0.3	0.006	0.002
30	0.54	0.002	0.001

The specific activity did not change appreciably for change in enzyme loading from 5% to 20 % (Figure 8-5). This suggests that filling inner volume of nanofibers with GOx does not affect the intrinsic activity of nanofibrous enzymes. However, as the enzyme loading is increased to 30 %, the activity dropped sharply. The nanofiber with 30 % enzyme contains more enzymes that are not active. At such a high enzyme amount in electrospinning solution, the GOx is easily denatured by THF. The denatured enzyme fastens the denaturation of other active enzyme by forming aggregation; this causes precipitation of enzyme in the polymer enzyme solution during electrospinning. The

maximum amount of enzyme loading achievable is determined by the phase behavior of polymer-enzyme solution.

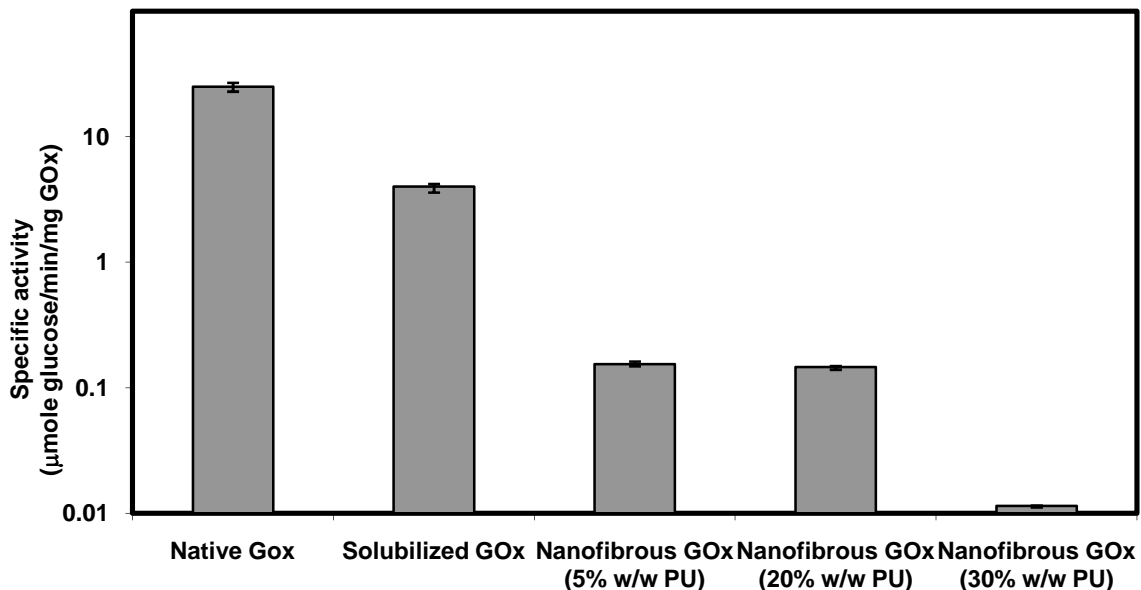


Figure 8-5 Specific activity of different forms of GOx

Traditional biosensors have involved immobilization of GOx over metallic or carbon transducers to monitor the current associated with the release of  $\text{H}_2\text{O}_2$ [262]. In the present study, the nanofibers were spun onto carbon electrode that was used to evaluate the electrochemical properties of the NEM. The surfactant-stabilized enzyme is water insoluble. It solves the problem of enzyme leaching during the biosensor application in aqueous environment. The particular property of water insoluble nature of solubilized enzymes will enable to get rid of multiple membranes that are used to protect the enzyme leaching in traditional biosensors. The combined effect of high enzyme loading and single membrane biosensor will lead to development of very sensitive biosensors. Apart

from the enzyme activity and loading, the electrochemical properties influence the NEM application as biosensor [263]. Therefore, the electrochemical signal transduction ability of the NEM was studied by employing cyclic voltammetry and sensitivity was evaluated amperometrically at a potential of 0.69 V.

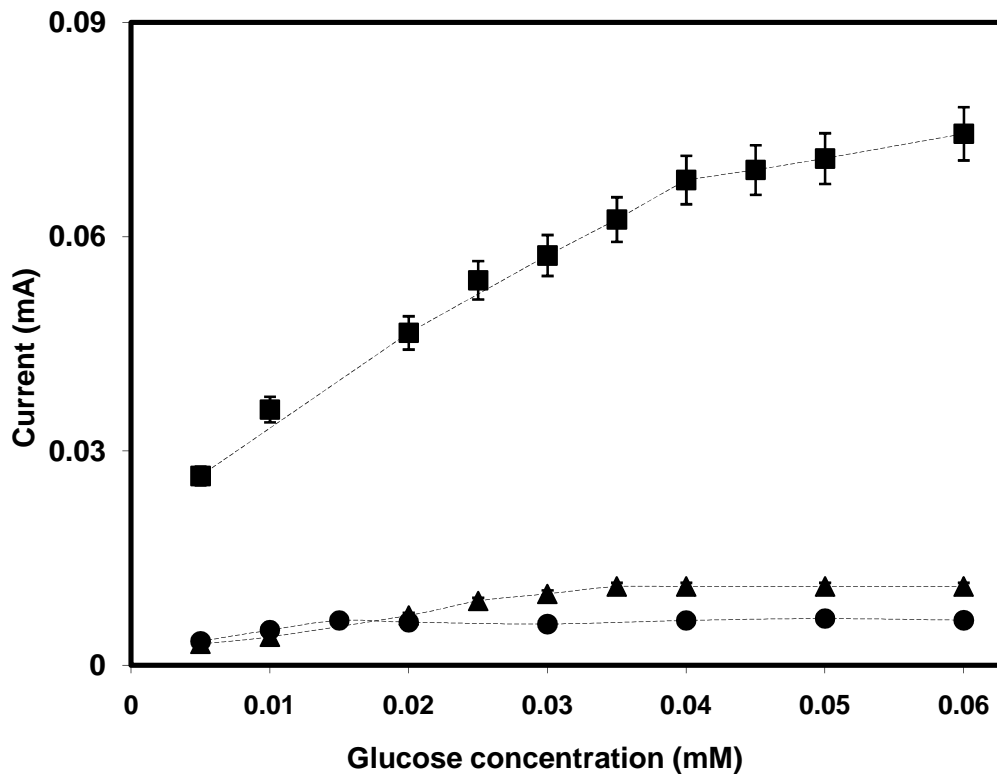


Figure 8-6 Current response of the NEM electrode containing different percentage of enzyme loading for 0.12 mg NEM. (●) NEM containing 5% (w/w PU) enzyme (■) NEM containing 20% (w/w PU) enzyme (▲)NEM containing 30% (w/w PU) enzyme.

Figure 8-6 shows the current response of NEM electrode. The current was measured at 0.69 V with respect to the reference electrode. At 0.69 V, the hydrogen peroxide produced by enzymatic oxidation of glucose is oxidized at the NEM electrode.

This electrons released from this reaction is detected amperometrically. As expected the current increases with increase in enzyme loading until 20%. However, at 30% enzyme loading the decrease in current is due to the bulk of denatured enzyme that is present in NEM. This is result is analogues to activity assay of NEM. At very high enzyme loading, precipitation of enzyme occurs in the electrospinning solution, which causes inactive enzymes in NEM.

The NEM showed very high sensitivity (Table 8-2), almost 100 times more based on enzyme weight and almost 10 times higher based on the surface area of the biosensor than reported previously[15, 264]. A sensitivity of  $0.39 \text{ AM}^{-1}\text{cm}^{-2}$  and  $66.6 \text{ AM}^{-1}\text{mg GOx}^{-1}$  was achieved in the linear range of operation. In general, the sensitivity for biosensors employing either nanostructured materials[15]or membranes[264] have been reported only to be in the range of  $10^{-5}$  to  $10^{-2} \text{ AM}^{-1}\text{cm}^{-2}$  based on biosensor weight and from 0.03 to  $0.5 \text{ AM}^{-1}\text{mg GOx}^{-1}$  based on amount of enzyme. This high sensitivity was observed in the linear range till  $40 \mu\text{M}$  glucose with the lower detection limit of  $5 \mu\text{M}$ . These values are similar to the glucose level that is available for non-invasive transdermal blood glucose level measurements.

Table 8-2 Performance of NEM with 20 % (w/w) enzyme as glucose biosensor.

<b>Enzyme loading</b> (wt % of PU)	<b>Weight of NEM</b> (mg)	<b>Detection limit</b> (mM)	<b>Dynamic range</b> (mM)	<b>Biosensor sensitivity</b> ( $\text{AM}^{-1}\text{cm}^{-2}$ )	<b>Biosensor sensitivity</b> ( $\text{AM}^{-1}\text{mg GOx}^{-1}$ )
20	0.12	0.005	0.04	0.39	66.6
20	0.3	0.005	0.06	0.26	14.3
20	0.54	0.005	0.1	0.04	2.3



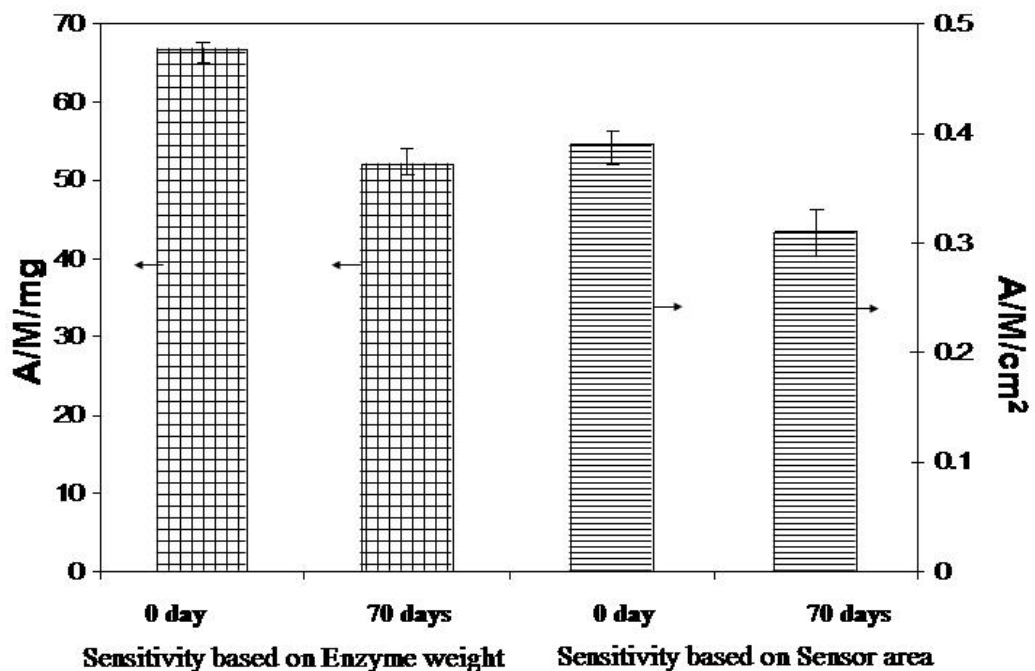


Figure 8-7 Effect of storage at 4<sup>0</sup>C on sensitivity of NEM

The sensitivity of biosensor achieved in this study is higher than that reported in literature for glucose biosensor employing different nanostructured materials [15, 245, 264]. The sensitivity is not appreciable with low enzyme loading. The electron transfer from the enzyme to the electrode is reduced by the polyurethane fiber at lower enzyme loading. However, at higher enzyme loading the enzyme is present all over the fiber, which reduces the problems associated with electron transfer. An important feature of the NEM is its reusability. The sensitivity was retained even after six continuous cycles. The storage stability of the biosensor was assayed by storing the biosensor at 4<sup>0</sup>C (Figure 8-7). The biosensor retained 80% of sensitivity even after 70 days.

## **8.4 Conclusion**

In this section, enzyme carrying nanofibers were fabricated for the development of biosensors. A comprehensive optimized procedure for maximum solubilization of GOx in organic solvent coupled with direct electrospinning resulted in very high loading of GOx in NEM. The aqueous insoluble nature of enzyme prevented it from leaching into aqueous solution during catalytic applications. The high enzyme loading and low mass transfer limitations of NEM, with effective entrapment of GOx resulted in high biocatalytic efficiency. The versatility of this technique is great leap forward in the development of highly sensitive, stable and reproducible biosensors.

## CHAPTER IX

### CONCLUSIONS AND PATH AHEAD

#### 9.1 Summary

The research focused on manipulation of micro-environment of enzymes for development of novel interfacial biocatalysis and sensitive biosensors. Based on concepts from membrane bound cellular systems a unique interfacial enzymatic catalysis was developed for industrial biotransformations. The stability and catalytic efficiency of the interface-assembled enzymes were investigated and enhanced by employing tools from different fields like reaction engineering, nanotechnology, chemistry, electrical and interfacial science. In another effort, a novel highly sensitive biosensor was developed by utilizing the unique opportunities available from interaction between diverse fields like enzyme technology and nanotechnology.

The interfacial enzyme catalysis achieved by conjugation of polymers to enzymes enabled simultaneous access of enzymes to reactants dissolved in both the phases. The factors like the surface packing, assembly morphology, and interfacial mobility of the interface-assembled enzyme, mass transfer of substrates and products to the interface and interfacial interaction of these molecules that influence efficient interfacial enzyme catalysis were investigated. The specific conclusions are:

(I) This project is the first in-depth analysis on enzyme assembling and motion behaviors at organic - aqueous interface. A surface pressure analysis was carried out in a

Langmuir film balance to characterize the surface assembly morphology of the interface-assembled enzyme and the results were interpreted in terms of phase behavior, aggregation and intramolecular rearrangement of the interface-assembled enzymes. The response of the interfacial enzyme layer to the change in their molecular areas by compression and expansion is an important characterization tool in assessing the phase behavior of the enzyme monolayer. The Langmuir film balance study with the repeatable surface pressure isotherm clearly indicated a monolayer assembly at the interface with little or no aggregation formation of interface-assembled enzymes and exhibited phase transition behavior with a plateau region in the isotherm. However, it is difficult to suggest the exact molecular structural reasons for the observation of plateau region due to the large size of polymer-enzyme conjugate molecule for this transition. One possibility is that the modified enzyme may be lying about its axis at the interface but on further compression the polymer is pushed out of the interface forcing the modified enzyme to take a more upright configuration at the interface. Fluorescence recovery after photobleaching technique was used to evaluate the interfacial two-dimensional mobility of interface-assembled enzyme. The mobility evaluated in terms of diffusion coefficient,  $6.7 \times 10^{-10} \text{ cm}^2/\text{sec}$ , is comparable to membrane binding proteins in natural systems but was found to be three orders of magnitude less than that of native enzyme in bulk solutions due to interfacial constraints of two dimensional diffusion and surface packing of the modified enzyme at the interface.

**(II)** It was found that the conjugation of hydrophobic polymers protected the enzymes from interfacial denaturation while assembled at the interface. The polymer stabilized the three dimensional structure of the enzyme by shielding the hydrophobic portions of the enzymes from the interface. This was particularly evident with chloroperoxidase that was used for epoxidation of styrene, the operational stability of CPO improved by 2 folds, when assembled at the interface. The interfacial assembly of enzymes like chloroperoxidase at the interface also offered a unique opportunity to enhance the stability of the enzyme against the deactivation effect of its reactants like hydrogen peroxide ( $H_2O_2$ ) in bulk phase. Presence of excess  $H_2O_2$  irreversibly oxidizes the active site of CPO, porphyrin ring, to a superoxide form rendering it unusable for subsequent reaction. Therefore, denaturation by  $H_2O_2$  was prevented by low level of  $H_2O_2$  exposure to the enzyme at the interface. The stability of an interface-binding CPO against the deactivation effect of  $H_2O_2$  was further enhanced by two different approaches.

In one approach, several chemical stabilizers including polymers, sugars and surfactants were used to either protect the enzyme by forming a solvent layer around it or by interacting with the oxidative intermediates and preventing it from oxidizing the porphyrin ring. Polyethylene glycol proved to be a good stabilizer for both operational and storage stability of interface-assembled CPO. PEG improved the operational stability of interface-assembled CPO by almost 2 folds and retained 60% of the activity even after incubation with 1 mM  $H_2O_2$  for 24 hours. This is considered to be a consequence of the modified distribution of  $H_2O_2$  in the reaction system. PEG can form hydrogen bonds and forms a solvent layer at the enzyme surface exposed to the aqueous phase and may also

reduce the interfacial tension, which stabilized the interface-assembled CPO from both interfacial and H<sub>2</sub>O<sub>2</sub> denaturation. In the second approach for stabilizing the interface-assembled CPO, *in situ* generation of hydrogen peroxide (H<sub>2</sub>O<sub>2</sub>) from glucose and oxygen by using glucose oxidase (GOx) was employed. This maintained the local concentration of H<sub>2</sub>O<sub>2</sub> low at the CPO surface and extended operational stability by 2 folds for interface-assembled CPO. The stabilizing effect of *in situ* generation H<sub>2</sub>O<sub>2</sub> is due to stabilization by glucose and lowered concentration of H<sub>2</sub>O<sub>2</sub>.

**(III)** It was discovered that balanced hydrophobic-hydrophilic structural manipulation of cofactors with proteins and polymers resulted in a novel interface assembled cofactor. To achieve cell like complexities with interfacial enzyme catalysis, multienzyme-cofactor systems were investigated as a starting point. In an interfacial enzymatic reaction system involving multienzymes and cofactors, localization of the cofactor at the interface, apart from improving the process economy, will lead to easy scale-up off the reaction system with minimum downstream operations. Therefore, interface-assembled nicotinamide cofactors like NAD(P)H were synthesized by derivatizing cofactors with macromolecules. N<sup>6</sup> and C8 positions on the adenine ring for NAD(P)H are among the few functional groups available for structural manipulation for cofactor modification. The carbon atom at C8 position of the adenine ring has the highest electron density that makes it the ideal position for electrophilic substitution but N<sup>6</sup> modified NAD(P)H derivatives interact better with dehydrogenases because of more favorable access to the adenine binding site in the enzyme is maintained. Therefore, N<sup>6</sup> position was used for

modification to yield macromolecular derivatives of cofactor that self-assembled at oil-water interface. A stable and active interface-assembled cofactor was synthesized by functionalizing the N<sup>6</sup> position by 1-(3-Dimethyl-aminopropyl)-3-ethylcarbodiimide hydrochloride and subsequent stabilization by N-hydroxysuccinimide of the amine reactive O-acylisourea intermediate. The combined effect of stabilization of intermediate and ease of purification by interface assembly resulted in a high yield of 67%, higher than most of the studies for synthesis of macromolecular derivatives of cofactor. Both NADH and NADPH were modified for interfacial assembly, and their activities were evaluated with multienzyme reaction systems with *in situ* regeneration of cofactor. The interface-binding cofactor was active at the interface even after multiple reaction cycles at room temperature with a total turnover number that was almost twice to that of free cofactor and exhibited an extended stability at the oil-water interface with a continuous operation for 2150 hours for the multienzyme reaction system that involved alcohol dehydrogenase from *Lactobacillus brevis* and glucose dehydrogenase with NADPH as cofactor for reduction of acetophenone in organic phase with simultaneous oxidation of glucose in aqueous phase respectively.

A kinetic analysis for different configuration of cofactors provided the dominant resistance towards interfacial reaction. Damkohler numbers for different form of the cofactors indicated that the productivity with interface assembled cofactor will be 730 times lower than that with free cofactor for a single reaction cycle. However, this limitation was offset by the remarkable stability of interface assembled cofactor that can be reused for more than 3 months without appreciable loss of activity. The binding

resistance of enzyme-cofactor,  $K_c$ , was found to be 6 times higher with interface assembled cofactor than free cofactor in solution. This kinetic study revealed that the mobility and interfacial interaction of the molecules at the interface may be the dominant resistance towards interfacial reaction.

**(IV)** A novel mechanism of nanostirring was developed by magnetically stirring the interface-assembled enzymes at the interface with nanoparticles, which acted as nanoscale stirrers. The nanostirring improved the interfacial interaction between different molecules and the mass transfer of substrates/products near the boundary layer at the interface. Iron oxide superparamagnetic nanoparticles embedded in the polymer-enzyme conjugate at oil-water interface were used as a nanoscale stirrer and the nanostirring was realized by employing an external alternating magnetic field generator outside the reactor. The mobility improvement of enzymes due to nanostirring improved the reaction rate by over 600% for interface assembled enzymes with both single enzyme reaction system involving CPO and multienzymes reaction system with NADPH as cofactor. However, with native enzymes due to surface spreading of enzymes on nanoparticles, the activity dropped with nanostirring. This difference between native and interface assembled enzymes was due to the presence of polymer that protected the interface-assembled enzymes from hydrophobic surface spreading at the nanoparticles surface. A direct correlation was observed between the improvements in the observed reaction rate to the mobility change of enzymes at the interface at different frequencies of nanostirring, which was visualized and quantified through fluorescence microscopy.



(V) The interfacial interaction of interface-assembled enzymes and interface assembled cofactor was realized with multiple interfacial cofactor turnovers achieved by employing a fast multienzyme reaction system with shear resistant dehydrogenases. The realization of interfacial interaction of different enzymes and cofactors is an essential step towards fabrication of artificial cell for efficient and economic biotransformations. As seen from the kinetic analysis and the diffusion coefficient estimation through FRAP for interface-assembled enzymes, the interfacial mobility and the interaction of molecules at the interface is limited by the interfacial constraints and this in turn results in slower reactions. The bottlenecks of slow reaction coupled with quick denaturation of dehydrogenases due to stirring, possessed a challenging problem to carry out reaction with interface-assembled enzyme and interface-assembled cofactor. To overcome this limitation a multienzyme reaction system that involved ADH RS1, which is relatively stable on stirring coupled with GluDH that gave a faster turnover for the NADH regeneration was employed. It was demonstrated that an interfacial reaction with interface-assembled enzyme and interface-assembled cofactor can be achieved by this reaction system. The reaction optimized with respect to polymer modifier, substrate concentration and enzyme ratio exhibited multiple turnovers of interface assembled cofactor at the interface, which in turn indicated an interfacial interaction between interface-assembled enzyme and interface-assembled cofactor. However, further systematic and detailed analysis of this reaction system with both cofactor and enzymes assembled at the interface is required for better understanding of interfacial interaction between these molecules.

(VI) Highly sensitive, stable and reproducible biosensors were developed with organic soluble enzymes. The enhanced hydrophobicity of enzymes achieved by its microenvironment manipulation with surfactant was used to develop organic soluble enzymes. The organic- soluble enzymes were electrospun with polymer to form bioactive nanofibers that were employed for the fabrication of glucose biosensor. Most of the previous studies for electrospinning polymer-enzyme solution, involved water soluble polymers. This led to loss of catalyst in aqueous solutions, which severely limited the use of these biocatalytic nanofibers as glucose sensors. To overcome this limitation, a novel method of electrospinning polymer-enzyme solution in organic solvent was developed. Prior to electrospinning, the enzymes were ion paired with surfactant and was thus made soluble in organic phase. When examined for glucose sensor applications, the nanofibers exhibited a 100 fold improvement of sensitivity compared to previous studies. The high specific surface area of the nanofibers combined with high enzyme loading resulted faster reaction that made the enzyme carrying nanofibrous material ideal for biosensing applications at low analyte concentration.

## **9.2 Future work**

To improve the performance of interface-assembled multienzyme system, further study of the interfacial system is needed. The reactions with both enzymes and cofactor assembled at the interface has to be optimized with respect to surface pressure isotherm, studying the form or phase of enzyme assembly morphology that is optimum for interfacial interaction of enzyme at cofactor. Quantitative correlations between the

interfacial enzyme properties and the activity of the enzymes at the interface have to be developed to improve the production efficiency, product quality and stability. Strategies based on the knowledge gained by this study, has to be developed for scale up of multistep reactions at the interface involving dehydrogenases and cofactor

All these advances will make enzymatic process a promising alternative to traditional chemical routes in that the operation is easy and simple and the product obtained is usually of high purity. The interfacial multienzyme reaction strategy is expected to enhance the potential of enzymes for wide range of applications including organic synthesis, pollutant degradation, fuel processing, food technology, detergency, cosmetics, coating processes, pharmaceuticals, and biotechnology. The synergistic use of multiple enzymes in nontraditional environments like oil-water interface and in functional materials will eventually lead to fabrication of artificial cells.

## BIBLIOGRAPHY

1. Lodish, H., Berk, A., Matsudaira, P., Kaiser, C.A., Krieger, M., Scott, M.P., Zipursky, L., and Darnell, J., *Molecular cell biology*. 5 ed. 2003, New York: W. H. Freeman and Company.
2. Johnson, J.E. and Cornell, R.B., *Amphitropic proteins: Regulation by reversible membrane interactions (review)*. *Molecular Membrane Biology*, 1999. 16(3): p. 217-235.
3. Dill, K.A., *Dominant forces in protein folding*. *Biochemistry*, 1990. 29(31): p. 7133-7155.
4. Pace, C.N., Fisher, L.M., and Cupo, J.F., *Globular protein stability: Aspects of interest in protein turnover*. *Acta Biologica et Medica Germanica*, 1981. 40(10-11): p. 1385-92.
5. Ponnuswamy, P.K., *Hydrophobic characteristics of folded proteins*. *Progress in Biophysics and Molecular Biology*, 1993. 59(1): p. 57-103.
6. Privalov, P.L. and Gill, S.J., *Stability of protein structure and hydrophobic interaction*. *Advances in Protein Chemistry*, 1988. 39: p. 191-234.
7. Prime, K.L. and Whitesides, G.M., *Self-assembled organic monolayers: Model systems for studying adsorption of proteins at surfaces*. *Science*, 1991. 252(5009): p. 1164-1167.
8. Piéroni, G., Gargouri, Y., Sarda, L., and Verger, R., *Interactions of lipases with lipid monolayers : Facts and questions*. *Advances in Colloid and Interface Science*, 1990. 32(4): p. 341-378.
9. Verger, R. and Pattus, F., *Lipid-protein interactions in monolayers*. *Chemistry and Physics of Lipids*, 1982. 30(2-3): p. 189-227.
10. Zaks, A. and Klibanov, A.M., *Enzymatic catalysis in organic media at 100oc*. *Science*, 1984. 22(224): p. 1249-1251.
11. Bommarius, A.S. and Riebel, B.R., *Biocatalysis*. 1994, New York: Wiley-VCH Verlag GmbH & Co.
12. Izmailova, V.N. and Yampolskaya, G.P., *Properties of protein interfacial layers at liquid-fluid interfaces*. *Studies in Interface Science*, 1998. 7(Proteins at Liquid Interfaces): p. 103-147.

13. Derewenda, U., Brzozowski, A.M., Lawson, D.M., and Derewenda, Z.S., *Catalysis at the interface: The anatomy of a conformational change in a triglyceride lipase*. *Biochemistry*, 1992. 31(5): p. 1532-1541.
14. Louwrier, A., Drtina, G.J., and Klibanov, A.M., *On the issue of interfacial activation of lipase in nonaqueous media*. *Biotechnol. Bioeng.*, 1996. 50(1): p. 1-5.
15. Lee, D., et al., *Simple fabrication of a highly sensitive and fast glucose biosensor using enzymes immobilized in mesocellular carbon foam*. *Advanced Materials*, 2005. 17(23): p. 2828-2833.
16. Wong, C.H. and Whitesides, G.M., *Enzymes in synthetic organic chemistry*. 1994, Oxford, U.K.: Elsevier Science.
17. Robertson, D.E. and Steer, B.A., *Recent progress in biocatalyst discovery and optimization*. *Current Opinion in Chemical Biology*, 2004. 8(2): p. 141-149.
18. van den Burg, B. and Eijssink, V.G.H., *Selection of mutations for increased protein stability*. *Current Opinion in Biotechnology*, 2002. 13(4): p. 333-337.
19. Caussette, M., Gaunand, A., Planche, H., Colombie, S., Monsan, P., and Lindet, B., *Pectinmethylesterase inactivation by bubbling with n<sub>2</sub>*. *Biotechnology Techniques*, 1998. 12(7): p. 561-564.
20. Caussette, M., Gaunand, A., Planche, H., Monsan, P., and Lindet, B., *Inactivation of enzymes by inert gas bubbling: A kinetic study*. *Annals of the New York Academy of Sciences*, 1998. 864(Enzyme Engineering XIV): p. 228-233.
21. Caussette, M., Planche, H., Delepine, S., Monsan, P., Gaunand, A., and Lindet, B., *The self catalytic enzyme inactivation induced by solvent stirring: A new example of protein conformational change induction*. *Protein Engineering*, 1997. 10(10): p. 1235-1240.
22. Illanes, A.s. and Wilson, L., *Enzyme reactor design under thermal inactivation*. *Critical Reviews in Biotechnology*, 2003. 23(1): p. 61.
23. Rosell, C.M., Terreni, M., Fernandez-Lafuente, R., and Guisan, J.M., *A criterion for the selection of monophasic solvents for enzymatic synthesis*. *Enzyme and Microbial Technology*, 1998. 23(1-2): p. 64-69.
24. Spieß, A., Schlothauer, R.C., Hinrichs, J., Scheidat, B., and Kasche, V., *Ph gradients in immobilized amidases and their influence on rates and yields of beta-lactam hydrolysis*. *Biotechnol. Bioeng.*, 1999. 62(3): p. 267-277.

25. Klibanov, A.M., *Improving enzymes by using them in organic solvents*. Nature, 2001. 409: p. 246.
26. Koskinen, A.M.P. and Klibanov, A.M., *Enzymatic reactions in organic media*. 1st ed. 1996, London: Blackie academic & Professional: Chapman & Hall.
27. Wang, P., Dai, S., Waezsada, S.D., Tsao, A., and Davison, B.H., *Enzyme stabilization by covalent binding in nanoporous sol-gel glass for nonaqueous biocatalysis*. Biotech. Bioeng., 2001. 74(3): p. 249-255.
28. Zacchigna, M., Luca, G.D., Lassiani, L., Varnavas, A., and Boccu, E., *Properties of methoxy(polyethylene glycol)-lipase from candida rugosa in organic solvents*. IL Farmaco, 1998. 53: p. 758-763.
29. Castro, G.R. and Knubovets, T., *Homogeneous biocatalysis in organic solvents and water-organic mixtures*. Critical Reviews in Biotechnology 2003. 23: p. 195-231.
30. Drauz, K. and Waldmann, H., *Enzyme catalysis in organic synthesis: A comprehensive handbook*. 1995, New York: VCH.
31. Loughlin, W.A., *Biotransformation in organic synthesis*. Bioresource Technology, 2000. 74: p. 49-62.
32. Reslow, M., Adlercreutz, P., and Mattiasson, B., *On the importance of the support material for bioorganic synthesis*. Eur. J. Biochem., 1988. 172: p. 573-578.
33. Antczak, T., Mrowiec-Bialon, J., Bielecki, S., Jarzebski, A.B., Malinowski, J., Lachowski, A., and Galas, E.P., *Thermostability and esterification activity of mucor javanicus lipase entrapped in silica aerogel matrix and in organic solvents*. Biotech. Tech., 1997. 11(1): p. 9-11.
34. Koops, B.C., Verheij, H.M., Slotboom, A.J., and Egmond, M.R., *Effect of chemical modification on the activity of lipases in organic solvents*. Enzyme and Microbial Technology, 1999. 25: p. 622-631.
35. Ujang, Z., Al-Sharbati, N., and Vaidya, A.M., *Organic-phase enzymatic esterification in a hollow fiber membrane reactor with in situ gas-phase water activity control*. Biotech. Progr, 1997. 13: p. 39-42.
36. Garcia-Garibay, M., Lopez-Munguia, A., and Barzana, E., *Alcoholysis and reverse hydrolysis reaction in organic one-phase system with a hyperthermophilic b-glycosidase*. Biotechnology and Bioengineering, 2000. 69(6): p. 627-632.

37. Daubresse, C., Grandfils, C., Jerome, R., and Teyssie, P., *Enzyme immobilization in reactive nanoparticles produced by inverse microemulsion polymerization*. Colloid Polym. Sci., 1996. 274(5): p. 482-489.
38. DeSantis, G. and Jones, J.B., *Probing the altered specificity and catalytic properties of mutant subtilisin chemically modified at position s156c and s166c in the s1 pocket*. Bioorg. Med Chem, 1999. 7: p. 2293-2301.
39. Hiroto, M., Ymada, M., and Inada, Y., *Stabilization of trypsin by modification with comb-shaped copolymers of poly(ethylene glycol) derivative and maleic anhydride*. Biotech. Tech., 1995. 9(2 (Feb.,95)): p. 105-110.
40. Mohapatra, S.C. and Hsu, J.T., *Immobilization of  $\alpha$ -chymotrypsin for use in batch and continuous reactors*. Journal of Chemical Technology and Biotechnology, 2000. 75: p. 519-525.
41. Oh, J.-T. and Jung-Hyun Kim, *Preparation and properties of immobilized amyloglucosidase on nonporous ps/pnass microspheres*. Enzyme and Microbial Technology, 2000(27): p. 356-361.
42. Parthasarathy, R. and Martin, C.R., *Synthesis of polymeric microcapsule arrays and their use for enzyme immobilization*. Nature, 1994. 369(May 26): p. 298-301.
43. Takahashi, K., Ajima, A., Yoshimoto, T., Okada, M., Matsushima, A., Tamaura, Y., and Inada, Y., *Chemical reactions by polyethylene glycol-modified enzymes in chlorinated hydrocarbons*. Journal of Organic Chemistry, 1985. 50: p. 3414-3415.
44. Okahata, Y. and Mori, T., *Lipid-coated enzymes as efficient catalysts in organic media*. Trends Biotechnol., 1997. 15: p. 50-54.
45. Naidja, A., Huang, P.M., and Bollag, J.M., *Activity of tyrosinase immobilized on hydroxyaluminum-montmorillonite complexes*. Journal of Molecular Catalysis A: Chemical, 1997. 115(2): p. 305-316.
46. Gill, I. and Ballesteros, A., *Encapsulation of biologicals within silicate, siloxane, and hybrid sol-gel polymers: An efficient and generic approach*. Journal of the American Chemical Society, 1998. 120(34): p. 8587-8598.
47. Schuleit, M. and Luisi, P.L., *Enzyme immobilization in silica-hardened organogels*. Biotechnology and Bioengineering, 2001. 72(2): p. 249-253.
48. Govardhan, C.P., *Crosslinking of enzymes for improved stability and performance*. Current opinion in biotechnology 1999. 10(4): p. 331-5.

49. Kazan, D., Ertan, H., and Erarslan, A., *Stabilization of escherichia coli penicillin g acylase against thermal inactivation by crosslinking with dextran dialdehyde polymers*. Applied Microbiology and Biotechnology, 1997. 48(2): p. 191-197.
50. Parrado, J. and Bautista, J., *Immobilization-stabilization of kerase, a serine protease from streptomyces fradiae, by covalent attachment to porous glass*. Bioscience, Biotechnology, and Biochemistry, 1995. 59(5): p. 906-7.
51. Parrado, J., Millan, F., and Bautista, J., *Kerose immobilization by covalent attachment to porous glass*. Process Biochemistry (Oxford), 1995. 30(8): p. 735-41.
52. Arroyo, M., *Immobilized enzymes: Theory, methods of study and applications*. Ars Pharmaceutica, 1998. 39(2): p. 111-127.
53. Nakamura, S., *Biocatalysts*. Gurin Kemisutori, 2001: p. 144-158.
54. Somers, W.A.C., Van Hartingsveldt, W., Stigter, E.C.A., and Van Der Lugt, J.P., *Bio-electrochemistry: A powerful tool for the production of ingredients in the food industry*. Agro-Food-Industry Hi-Tech, 1997. 8(2): p. 32-35.
55. Stambolieva, N.A., *Use of immobilized enzymes in food technology*. Nauchni Trudove - Vissh Institut po Khranitelna i Vkusova Promishlenost, Plovdiv, 1998. 43: p. 199-204.
56. Trevan, M., *Techniques of immobilization*. In: *Immobilized enzymes. An introduction and applications in biotechnology*, M. Trevan, Editor. 1980, Wiley: Chichester-New York. p. 1-9.
57. Tosa, T.M., Takao; Fuse, Noriko; Chibata, Ichiro., *Continuous enzyme reactions. I. Screening of carriers for preparation of water-insoluble aminoacylase*. Enzymologia, 1966. 31(4): p. 214-224.
58. Brodelius, P. and Mosbach, K., *Immobilization techniques for cells/organelles*, in *Methods in enzymology*, M. K., Editor. 1987, Academic Press: London. p. 173-454.
59. Swaisgood, H.E., *Immobilization of enzymes and some applications in food industry*, in *Enzymes and immobilized cells in biotechnology*, A. Laskin, Editor. 1985, Benjamin Cummins: London. p. 1-24.
60. Itozawa, T. and Kise, H., *Immobilization of hldh on polymer materials for reduction of cyclohexanone with nadh regeneration under two-phase conditions*. Journal of Fermentation and Bioengineering, 1995. 80: p. 30-34.



61. El-Zahab, B., Jia, H., and Wang, P., *Enabling multienzyme biocatalysis using nanoporous materials*. *Biotechnology and Bioengineering*, 2004. 87(2): p. 178-183.
62. Jia, H., Zhu, G., and Wang, P., *Catalytic behaviors of enzymes attached to nanoparticles: The effect of particle mobility*. *Biotechnology and Bioengineering* 2003. 84(4): p. 406-414.
63. Davis, B.G., *Chemical modification of biocatalysts*. *Current opinion in Biotechnology*, 2003(14): p. 379-386.
64. Tann, C.M., Qi, D., and Distefano, M.D., *Enzyme design by chemical modification of protein scaffolds*. *Current opinion in chemical biology*, 2001. 5(6): p. 696-704. .
65. Eyzaguirre, J., ed. *Chemical modification of enzymes*. Ellis horwood series in biochemistry and biotechnology, ed. A. Wiseman. 1987, John Wiley & Sons: NY. 187p.
66. Ethtezazi, T., Melia, C.D., and Washington, C., *Obtaining pore size distributions within porous microspheres using stereological methods*. *Proceedings of the International Symposium on Controlled Release of Bioactive Materials*, 1997. 24th: p. 629-630.
67. Ueji, S.-I., Tanaka, H., Hanaoka, T., Ueda, A., Watanabe, K., Kaihatsu, K., and Ebara, Y., *Effects of chemical modification of lipase on its enantioselectivity in organic solvents*. *Chem Lett*, 2001: p. 1066-1067.
68. Vinogradov, A., Kudryashova, E., Grinberg, V., Grinberg, N., Burova, T., and Levashov Andrey, V., *The chemical modification of  $\alpha$ -chymotrypsin with both hydrophobic and hydrophilic compounds stabilizes the enzyme against denaturation in water-organic media*. *Protein Engineering*, 2001. 14: p. 683-689.
69. DeSantis, G., Berglund, P., Stabile, M., Gold, M., and Jones, J.B., *Site-directed mutagenesis combined with chemical modification as a strategy for altering the specificity of the  $s1$  and  $s1'$  pockets of subtilisin bacillus lentus*. *Biochemistry*, 1998. 37: p. 5968-5973.
70. DeSantis, G. and Jones, J.B., *Chemical modification of enzymes for enhanced functionality*. *Current Opinion in Biotechnology*, 1999. 10: p. 324-330.
71. Quioco, F.A. and Richards, F.M., *Intermolecular cross linking of a protein in the crystalline state: Carboxypeptidase-a*. *Proceedings of the National Academy of Sciences of the United States of America*, 1964. 52: p. 833-839.

72. Hernaiz, M.J., Sanchez-Montero, J.M., and Sinisterra, J.V.S., *Modification of purified lipases from candida rugosa with polyethylene glycol: A systematic study*. *Enz. Micro. Tech.*, 1999. 24: p. 181-190.
73. Khmel'nitsky, Y.L., Belova, A.B., Levashov, A.V., and Mozhaev, V.V., *Relationship between surface hydrophilicity of a protein and its stability against denaturation by organic solvents*. *Federatn. Europ. Biochm. Soc.*, 1991. 284(2): p. 267-269.
74. Kwon, O., Imanishi, Y., and Ito, Y., *Catalytic activity and conformation of chemically modified subtilisin carlsberg in organic media*. *Biotech. Bioeng.*, 1999. 66(4): p. 265-270.
75. Pina, C., Clark, D.S., and Blanch, H.W., *The activity of peg-modified chymotrypsin in aqueous and organic media*. *Biotech. Tech.*, 1989. 3(5): p. 333-338.
76. Scott, C., Scott, T., and Woodward, C.O., *The chemical modification of enzymes to enhance solubilization in organic solvents for interaction with coal*. *Fuel*, 1993. 72(12): p. 1695-1700.
77. Tinoco, R. and Vazquez-Duhalt, R., *Chemical modification of cytochrome c improves their catalytic properties in oxidation of polycyclic aromatic hydrocarbons*. *Enz. Micro. Tech.*, 1998. 22: p. 8-12.
78. Vazquez-Duhalt, R., Fedorak, P.M., and Westlake, D.W.S., *Role of enzyme hydrophobicity in biocatalysis in organic solvents*. *Enz. Micro. Tech.*, 1992. 14(October): p. 837-841.
79. Haring, D. and Schreier, P., *Cross-linked enzyme crystals*. *Current Opinion in Chemical Biology*, 1999. 3: p. 35-38.
80. Persichetti, R.A., St. Clair, N.L., Griffith, J.P., Navia, M.A., and Margolin, A.L., *Cross-linked enzyme crystals (clecs) of thermolysin in the synthesis of peptides*. *J. Am. Chem. Soc.*, 1995. 117: p. 2732-2737.
81. Dordick, J.S., Khmel'nitsky, Y.L., and Serfeeva, M.V., *The evolution of biotransformation technologies*. *Current Opinion in Microbiology*, 1998. 1(2): p. 311-318.
82. Miyanaga, M., Ohmori, M., Imamura, K., Sakiyama, T., and Nakanishi, K., *Stability of immobilized thermolysin in organic solvents*. *J. Bioscience and Bioengineering*, 1999. 87(4): p. 463-472.

83. Wang, P., Sergeeva, M.V., Lim, L., and Dordick, J.S., *Biocatalytic plastics as active and stable materials for biotransformations*. Nature Biotechnology, 1997. 15(8): p. 789-793.
84. Yang, Z., Mesiano, A.J., Venkatasubramanian, S., Gross, S.H., Harris, J.M., and Russell, A.J., *Activity and stability of enzymes incorporated into acrylic polymers*. J. Am. Chem. Soc., 1995. 117: p. 4843-4850.
85. Paradkar, V.M. and Dordick, J.S., *Aqueous-like activity of .Alpha.-chymotrypsin dissolved in nearly anhydrous organic solvents*. J. Am. Chem. Soc., 1994. 116(11): p. 5009-5010.
86. Ljunger, G., Adlercreutz, P., and Mattiasson, B., *Reactions catalyzed by peg-modified a-chymotrypsin in organic solvents. Influence of water content and degree of modification*. Biocatalysis, 1993. 7: p. 279-288.
87. Takahashi, K., Nishimura, H., Yoshimoto, T., Saito, Y., and Inada, Y., *A chemical modification to make horseradish peroxidase soluble and active in benzene*. Biochem. Biophys. Res. Commun., 1984. 121(1): p. 261-265.
88. Yang, Z., Domach, M., Auger, R., Yang, F.X., and Russell, A.J., *Polyethylene glycol-induced stabilization of subtilisin*. Enz. Micro. Tech., 1996. 18: p. 82-89.
89. Chandy, T., Mooradian, D.L., and Rao, G.H.R., *Chitosan/polyethylene glycol-alginate microcapsules for oral delivery of hirudin*. Journal of Applied Polymer Science, 1998. 70: p. 2143-2153.
90. Chae, H.J. and Yoo, Y.J., *Mathematical analysis of an enzymatic reaction in an aqueous/organic two-phase system: Tyrosinase-catalysed hydroxylation of phenol*. J. Chem. Tech. Biotechnol., 1997. 70: p. 163-170.
91. Antonini, E., Carrea, G., and Cremonesi, P., *Enzyme catalyzed-reactions in water-organic solvent 2-phase systems*. Enz. Micro. Tech., 1981. 3: p. 291-296.
92. Hickel, A., Radke, C.J., and Blanch, H.W., *Hydroxynitrile lyase at the diisopropyl ether/water interface: Evidence for interfacial enzyme activity*. Biotechnol. Bioeng., 1999. 65(4): p. 425-436.
93. Baldascini, H., Ganzeveld, K.J., Janssen, D.B., and Beenackers, A.A.C.M., *Effect of mass transfer limitations on the enzymatic kinetic resolution of epoxides in a two liquid phase system*. Biotechnol. Bioeng., 2001. 73(1): p. 44-54.
94. Gargouri, M., *Biocatalysis in liquid-liquid biphasic media: Coupled mass transfer and chemical reactions*, in *Liquid interfaces in chemical, biological, and*

- pharmaceutical applications*, A.G. Volkov, Editor. 2001, Marcel Dekker, Inc.: NY. p. 553-584.
95. Gelb, M.H., Min, J.-H., and Jain, M.K., *Do membrane-bound enzymes access their substrates from the membrane or aqueous phase: Interfacial versus non-interfacial enzymes*. *Biochimica et Biophysica Acta*, 2000. 1488: p. 20-27.
  96. Volkov, A.G., *Redox reactions at liquid hydrocarbon/water interfaces: Biophysical aspects*. *Electrochimica Acta*, 1998. 44(1): p. 139-153.
  97. Hernandez-Justiz, O., Fernandez-Lafuente, R., Terreni, M., and Guisan, J.M., *Use of aqueous two-phase systems for in situ extraction of water soluble antibiotics during their synthesis by enzymes immobilized on porous supports*. *Biotechnol. Bioeng.*, 1998. 59(1): p. 73-79.
  98. Khmelnitsky, Y.L., Gladilin, A.K., Roubailo, V.L., Martinek, K., and Levashov, A.V., *Reversed micelles of polymeric surfactants in nonpolar organic solvents. A new microheterogeneous medium for enzymatic reactions*. *Eur. J. Biochem.*, 1992. 206(3): p. 737-745.
  99. Luisi, P.L., *Enzymes hosted in reverse micelles in hydrocarbon solution*. *Angew. Chem. Int. Ed.*, 1985. 24: p. 439-450.
  100. Cascao-Pereira, L.G. and A., H., *Interfacial versus homogeneous enzymatic cleavage of mandelonitrile by hydroxynitrile lyase in a biphasic system*. *Biotechnol. Bioeng.*, 2003. 83: p. 498-501.
  101. Straathof, A.J.J., *Enzymatic catalysis via liquid - liquid interfaces*. *Biotechnol. Bioeng.*, 2003. 83(4): p. 371-375.
  102. Duinhoven, S., Poort, R., Voet, G.V.d., Agterof, W.G.M., Norde, W., and Lyklema, J., *Driving forces for enzyme adsorption at solid-liquid interfaces 2. The fungal lipase lipolase*. *Journal of Colloid and Interface Science*, 1995. 170: p. 351-357.
  103. Miller, R., Aksenenko, E.V., Fainerman, V.B., and Pison, U., *Kinetics of adsorption of globular proteins at liquid/fluid interfaces*. *Colloids and Surfaces A: Physicochemical and Engineering Aspects*, 2001. 183-185: p. 381-390.
  104. Tsung, E.F. and Tilton, R.D., *Measurement of catalytic reaction kinetics for adsorbed enzyme monolayers*. *Journal of Colloid and Interface Science*, 1999. 213: p. 208-217.
  105. Gennis, R.B., *Biomembranes*. 1989: New York: Springer-Verlag.

106. Balashev, K., Jensen, T.R., Kjaer, K., and Bjornholm, T., *Novel methods for studying lipids and lipases and their mutual interaction at interfaces. Part i. Atomic force microscopy*. Biochimie, 2001. 83: p. 387-397.
107. Marangoni, A.G., *Enzyme kinetics of lipolysis revisited: The role of lipase interfacial binding*. Biochemical and Biophysical Research Communications, 1994. 200(No. 3): p. 1321-1328.
108. Mori, T., Fujita, S., and Okahata, Y., *Transglycosylation in a two-phase aqueous-organic system with catalysis by a lipid-coated b-d-galactosidase*. Carbohydrate Research, 1997. 298: p. 65-73.
109. Soler, G., Bastida, A., Blanco, R.M., Fernandez-Lafuente, R., and Guisan, J.M., *Reactivation strategies by unfolding/refolding of chymotrypsin derivatives after inactivation by organic solvents*. Biochimica et Biophysica Acta - Protein Struct. & Mol. Enzymol. , 1997. 1339(1): p. 167-175.
110. Husain, s., Jafri, F., and Saleemuddin, M., *Effects of chemical modification on the stability of invertase before and after immobilization*. Enz. Micro. Tech., 1997. 18: p. 275-280.
111. Qi, D., Tann, C.-M., Haring, D., and Distefano, M.D., *Generation of new enzymes via covalent modification of existing proteins*. Chem. Rev., 2001. 101: p. 3081-3111.
112. Zhu, G. and Wang, P., *Polymer-enzyme conjugates can self-assemble at oil/water interfaces and effect interfacial biotransformations*. Journal of the American Chemical Society, 2004. 126(36): p. 11132-11133.
113. Nnanna, I.A. and Xia, J., *Protein-based surfactants: Synthesis, physicochemical properties, and applications*. Science series ed. A.T. Hubbard. Vol. 101. 2001: New York: Marcel Dekker, Inc.
114. Daines, A.M., Maltmann, B.A., Filtsch, S.L., *Synthesis and modifications of carbohydrates, using biotransformations*. Current Opinion in Chemical Biology, 2004. 8: p. 106-113.
115. Steckhan, E., *Electroenzymatic synthesis*. Electrochemistry V, 1994. 170: p. 83-111.
116. Baughn, R.L., Adalsteinsson, O., and Whitesides, G.M., *Large scale enzyme catalyzed synthesis of atp from adenosine and acetyl phosphate: Regeneration of atp from amp*. J. Am. Chem. Soc., 1978. 100(1): p. 304-306.

117. Lee, M. and Means, G.E., *Nad<sup>+</sup>/nadh recycling by coimmobilized lactate dehydrogenase and glutamate dehydrogenase*. *Enz. Micro. Tech.* , 1998. 23: p. 49-57.
118. Seelbach, K. and Kragl, U., *Nanofiltration membranes for cofactor retention in continuous enzymatic synthesis*. *Enz. Micro. Tech.*, 1997. 20(5): p. 389-392.
119. Legoy, M.D., Garde, V.L., Lemoullec, J.M., Ergan, F., and Thomas, D., *Cofactor regeneration in immobilized enzyme systems: Chemical grafting of functional nad in the active site of dehydrogenase*. *Biochimie*, 1980. 62(5-6): p. 341-345.
120. Yamazaki, Y. and Maeda, H., *The co-immobilization of nad and dehydrogenase and its application to bioreactors for synthesis and analysis*. *Agric. Biol. Chem.* , 1982. 46(6): p. 1571-1581.
121. Liao, L., *Novel multi-enzymatic biocatalysis involving cofactor regeneration: A study of interface-self-assembled and microcapsules-encapsulated systems*, in *Chemical Engineering*. 2005, University of Akron: Akron.
122. Bardea, A., Katz, E., Bueckmann, A.F., and Willner, I., *Nad<sup>+</sup>-dependent enzyme electrodes: Electrical contact of cofactor-dependent enzymes and electrodes*. *J. Am. Chem. Soc.*, 1997. 119: p. 9114-9119.
123. Kim, J., Grate, J.W., and Wang, P., *Nanostructures for enzyme stabilization*. *Chemical Engineering Science*, 2006. 61(3): p. 1017-1026.
124. Livage, J., Coradin, T., and Roux, C., *Encapsulation of biomolecules in silica gels*. *Journal of Physics: Condensed Matter*, 2001. 13(33): p. R673-R691.
125. Tischer, W. and Kasche, V., *Immobilized enzymes: Crystals or carriers?* *Trends in Biotechnology*, 1999. 17(8): p. 326-335.
126. De Jong, K. and Geus, J., *Carbon nanofibers: Catalytic synthesis and applications*. *Catalysis Reviews: Science & Engineering*, 2000. 42(4): p. 481.
127. Ogihara, H., Takenaka, S., Yamanaka, I., and Otsuka, K., *Reduction of no with the carbon nanofibers formed by methane decomposition*. *Carbon*, 2004. 42(8-9): p. 1609-1617.
128. Baker, R.T.K., Laubernds, K., Wootsch, A., and Paál, Z., *Pt/graphite nanofiber catalyst in n-hexane test reaction*. *Journal of Catalysis*, 2000. 193(1): p. 165-167.
129. Park, C. and Baker, R.T.K., *Catalytic behavior of graphite nanofiber supported nickel particles. 2. The influence of the nanofiber structure*. *Journal of Physical Chemistry B*, 1998. 102(26): p. 5168-5177.

130. Gao, R., Tan, C.D., and Baker, R.T.K., *Ethylene hydroformylation on graphite nanofiber supported rhodium catalysts*. *Catalysis Today*, 2001. 65(1): p. 19-29.
131. Bessel, C.A., Laubernds, K., Rodriguez, N.M., and Baker, R.T.K., *Graphite nanofibers as an electrode for fuel cell applications*. *Journal of Physical Chemistry B*, 2001. 105(6): p. 1115-1118.
132. Jia, H., Zhu, G., Vugrinovich, B., Kataphinan, W., Reneker, D.H., and Wang, P., *Enzyme-carrying polymeric nanofibers prepared via electrospinning for use as unique biocatalysts*. *Biotechnology Progress*, 2002. 18(5): p. 1027-1032.
133. Doshi, J. and Reneker, D.H., *Electrospinning process and applications of electrospun fibers*. *Journal of Electrostatics*, 1995. 32(2&3): p. 151-160.
134. Theron, A., Zussman, E., and Yarin, A.L., *Electrostatic field-assisted alignment of electrospun nanofibres*. *Nanotechnology*, 2001. 12(3): p. 384.
135. Reneker, D.H., Yarin, A.L., Fong, H., and Koombhongse, S., *Bending instability of electrically charged liquid jets of polymer solutions in electrospinning*. *Journal of Applied Physics*, 2000. 87(9): p. 4531-4547.
136. Sawickaa, K., Goumab, P., and Simon, S., *Electrospun biocomposite nanofibers for urea biosensing*. *Sensors and Actuators B*, 2005. 108: p. 585-588.
137. Xie, J. and Hsieh, Y.-L., *Ultra-high surface fibrous membranes from electrospinning of natural proteins: Casein and lipase enzyme*. *J. Mater. Sci.*, 2003. 38: p. 2125 – 2133.
138. Herricks, T.E., Kim, S.-H., Kim, J., Li, D., Kwak, J.H., Grate, J.W., Kim, S.H., and Xia, Y., *Direct fabrication of enzyme-carrying polymer nanofibers by electrospinning*. *Journal of materials chemistry*, 2005. 15: p. 3241-3245.
139. Zhang, Y., Lim, C., Ramakrishna, S., and Huang, Z.-M., *Recent development of polymer nanofibers for biomedical and biotechnological applications*. *Journal of Materials Science: Materials in Medicine*, 2005. 16(10): p. 933-946.
140. Wang, X., Kim, Y.-G., Drew, C., Ku, B.-C., Kumar, J., and Samuelson, L.A., *Electrostatic assembly of conjugated polymer thin layers on electrospun nanofibrous membranes for biosensors*. *Nano Lett.*, 2004. 4(2): p. 331-334.
141. Clark, L.C., Jr. and Lyons, C., *Electrode systems for continuous monitoring in cardiovascular surgery*. *Annals of the New York Academy of Sciences* 1962. 102(Art. 1): p. 29-45.

142. Guilbault, G.G. and Lubrano, G.J., *An enzyme electrode for the amperometric determination of glucose*. *Analytica Chimica Acta*, 1973. 64(3): p. 439-455.
143. Shichiri, M., Kawamori, R., Yamasaki, Y., Hakui, N., and Abe, H., *Wearable artificial endocrine pancreas with needle-type glucose sensor*. *Lancet* 1982. 2(8308): p. 1129-31.
144. Cass, A.E.G., Davis, G., Francis, G.D., Hill, H.A.O., Aston, W.J., Higgins, I.J., Plotkin, E.V., Scott, L.D.L., and Turner, A.P.F., *Ferrocene-mediated enzyme electrode for amperometric determination of glucose*. *Analytical Chemistry*, 1984. 56(4): p. 667-671.
145. Degani, Y. and Heller, A., *Direct electrical communication between chemically modified enzymes and metal electrodes. I. Electron transfer from glucose oxidase to metal electrodes via electron relays, bound covalently to the enzyme*. *Journal of Physical Chemistry*, 1987. 91(6): p. 1285-1289.
146. Bradford, M.M., *A rapid and sensitive method for the quantitation of microgram quantities of protein utilizing the principle of protein-dye binding*. *Analytical Biochemistry*, 1976. 72: p. 248-254.
147. Matsushita, M., Irino, T., Komoda, T., and Sakagishi, Y., *Determination of proteins by a reverse biuret method combined with the copper-bathocuproine chelate reaction*. *Clinica Chimica Acta*, 1993. 216(1-2): p. 103-111.
148. Brzozowski, A.M., et al., *A model for interfacial activation in lipases from the structure of a fungal lipase-inhibitor complex*. *Nature*, 1991. 351(6326): p. 491-494.
149. Bates, I.R., Wiseman, P.W., and Hanrahan, J.W., *Investigating membrane protein dynamics in living cells*. *Biochemistry & Cell Biology*, 2006. 84(6): p. 825-831.
150. Poo, M.-m. and Cone, R.A., *Lateral diffusion of rhodopsin in the photoreceptor membrane*. *Nature*, 1974. 247(5441): p. 438-441.
151. Chen, Y., Lagerholm, B.C., Yang, B., and Jacobson, K., *Methods to measure the lateral diffusion of membrane lipids and proteins*. *Methods*, 2006. 39(2): p. 147-153.
152. Adkins, E.M., Samuvel, D.J., Fog, J.U., Eriksen, J., Jayanthi, L.D., Vaegter, C.B., Ramamoorthy, S., and Gether, U., *Membrane mobility and microdomain association of the dopamine transporter studied with fluorescence correlation spectroscopy and fluorescence recovery after photobleaching*. *Biochemistry*, 2007. 46(37): p. 10484-10497.



153. Axelrod, D., Koppel, D.E., Schlessinger, J., Elson, E., and Webb, W.W., *Mobility measurement by analysis of fluorescence photobleaching recovery kinetics*. Biophysical Journal, 1976. 16(9): p. 1055-1069.
154. Soumpasis, D.M., *Theoretical analysis of fluorescence photobleaching recovery experiments*. Biophysical Journal, 1983. 41(1): p. 95-97.
155. Young, M.E., Carroad, P.A., and Bell, R.L., *Estimation of diffusion coefficients of proteins*. Biotechnol. Bioeng., 1980. 22(5): p. 947-955.
156. Kitani, K., Tanaka, S., and Zs.-Nagy, I., *Age-dependence of the lateral diffusion coefficient of lipids and proteins in the hepatocyte plasma membrane of bn/birijhsd rats as revealed by the smear-frap technique*. Archives of Gerontology and Geriatrics, 1998. 26(3): p. 257-273.
157. Allain, E.J., Hager, L.P., Deng, L., and Jacobsen, E.N., *Highly enantioselective epoxidation of disubstituted alkenes with hydrogen peroxide catalyzed by chloroperoxidase*. J. Am. Chem. Soc., 1993. 115: p. 4415-4416.
158. Colonna, S., Gaggero, N., Richelmi, C., and Pasta, P., *Recent biotechnological developments in the use of peroxidases*. Trends Biotechnol., 1999. 17(4): p. 163-168.
159. Dexter, A.F., Lakner, F.J., Campbell, R.A., and Hager, L.P., *Highly enantioselective epoxidation of 1,1-disubstituted alkenes catalyzed by chloroperoxidase*. J. Am. Chem. Soc., 1995. 117: p. 6412-6413.
160. Sariaslani, F.S., *Microbial enzymes for oxidation of organic molecules*. Critic. Rev. Biotechnol., 1989. 9(3): p. 171-257.
161. Trevisan, V., Signoretto, M., Colonna, S., Pironti, V., and Strukul, G., *Microencapsulated chloroperoxidase as a recyclable catalyst for the enantioselective oxidation of sulfides with hydrogen peroxide*. Angewandte Chemie International Edition, 2004. 43: p. 4097-4099.
162. Smith, G., *Synthetically useful reactions of epoxides*. Synthesis, 1984. 8: p. 629-656.
163. Santhanam, L. and Dordick, J.S., *Chloroperoxidase-catalyzed epoxidation of styrene in aqueous and nonaqueous media*. Biocat. Biotransform., 2002. 20(4): p. 265-274.
164. Pereira, L.G.C., Hickel, A., Radke, C.J., and Blanch, H.W., *A kinetic model for enzyme interfacial activity and stability: Pa-hydroxynitrile lyase at the diisopropyl ether/water interface*. Biotechnol. Bioeng., 2002. 78(6): p. 595-605.

165. Zhu, G. and Wang, P., *Novel interface-binding chloroperoxidase for interfacial epoxidation of styrene*. J. Biotechnol., 2005. 117(2): p. 137-213.
166. Van Deurzen, M.P.J., Seelbach, K., Van Rantwijk, F., Kargl, U., and Sheldon, R.A., *Chloroperoxidase: Use of hydrogen peroxide-stat for controlling reactions and improving enzyme performance*. Biocat. Biotransform., 1997. 15: p. 1-16.
167. Velde, F.V.D., Lourenco, N.D., M., B., Rantwijk, F.V., and Sheldon, R.A., *Improved operational stability of peroxidases by coimmobilization with glucose oxidase*. Biotechnol. Bioeng., 2000. 69: p. 286-291.
168. Borole, A.P., Dai, S., Cheng, C.L., Rodrigues, M.J., and Davison, B.H., *Performance of chloroperoxidase stabilization in mesoporous sol-gel glass using in situ glucose oxidase peroxide generation*. Appl. Biochem. Biotechnol., 2004. 113-116: p. 273-285.
169. Andersson, M., Andersson, M.M., and Adlercreutz, P., *Stabilisation of chloroperoxidase towards peroxide dependent inactivation*. Biocat. Biotransform., 2000. 18(6): p. 457-469.
170. Dawson, J.H. and Sono, M., *Cytochrome p-450 and chloroperoxidase: Thiolate-ligated heme enzymes. Spectroscopic determination of their active site structures and mechanistic implication of thiolate ligation*. Chem. Rev., 1987. 87: p. 1255-1276.
171. Zaks, A. and Dodds, D.R., *Chloroperoxidase-catalyzed asymmetric oxidations: Substrate specificity and mechanistic study*. J. Am. Chem. Soc., 1995. 117(42): p. 10419-10424.
172. Krix, G., Bommarius, A.S., Drauz, K., Kottenhahn, M., Schwarm, M., and Kula, M.R., *Enzymatic reduction of [alpha]-keto acids leading to -amino acids, - or -hydroxy acids*. Journal of Biotechnology, 1997. 53(1): p. 29-39.
173. Riebel, Bettina R., Gibbs, Phillip R., Wellborn, William B., and Bommarius, Andreas S., *Cofactor regeneration of nad<sup>+</sup> from nadh: Novel water-forming nadh oxidases*. Advanced Synthesis & Catalysis, 2002. 344(10): p. 1156-1168.
174. Zhang, M., Mullens, C., and Gorski, W., *Coimmobilization of dehydrogenases and their cofactors in electrochemical biosensors*. Analytical Chemistry, 2007. 79(6): p. 2446-2450.
175. Forde, J., Oakey, L., Jennings, L., and Mulcahy, P., *Fundamental differences in bioaffinity of amino acid dehydrogenases for n6- and s6-linked immobilized cofactors using kinetic-based enzyme-capture strategies*. Analytical Biochemistry, 2005. 338(1): p. 102-112.

176. Raitman, O.A., Katz, E., Buckmann, A.F., and Willner, I., *Integration of polyaniline/poly(acrylic acid) films and redox enzymes on electrode supports: An in situ electrochemical/surface plasmon resonance study of the bioelectrocatalyzed oxidation of glucose or lactate in the integrated bioelectrocatalytic systems*. Journal of the American Chemical Society, 2002. 124(22): p. 6487-6496.
177. Yan, Y., Zheng, W., Su, L., and Mao, L., *Carbon-nanotube-based glucose biofuel cells*. Advanced Materials, 2006. 18(19): p. 2639-2643.
178. Hassler, B.L., Kohli, N., Zeikus, J.G., Lee, I., and Worden, R.M., *Renewable dehydrogenase-based interfaces for bioelectronic applications*. Langmuir, 2007. 23(13): p. 7127-7133.
179. Temiño, D.M.-R.D., Hartmeier, W., and Ansorge-Schumacher, M.B., *Entrapment of the alcohol dehydrogenase from lactobacillus kefir in polyvinyl alcohol for the synthesis of chiral hydrophobic alcohols in organic solvents*. Enzyme and Microbial Technology, 2005. 36(1): p. 3-9.
180. Fukuzumi, S., Inada, O., Satoh, N., Suenobu, T., and Imahori, H., *Significant enhancement of electron transfer reduction of nad<sup>+</sup> analogues by complexation with scandium ion and the detection of the radical intermediate-scandium ion complex*. Journal of the American Chemical Society, 2002. 124(31): p. 9181-9188.
181. Kotlyar, A.B. and Borovok, N., *Nadh oxidation and nad<sup>+</sup> reduction catalysed by tightly coupled inside-out vesicles from paracoccus denitrificans*. European Journal of Biochemistry, 2002. 269(16): p. 4020-4024.
182. Song, H.-K., Lee, Sahng H., Won, K., Park, Je H., Kim, Joa K., Lee, H., Moon, S.-J., Kim, Do K., and Park, Chan B., *Electrochemical regeneration of nadh enhanced by platinum nanoparticles*. Angewandte Chemie, 2008. 47(9): p. 1749-1752.
183. Chang, T. and Prakash, S., *Procedures for microencapsulation of enzymes, cells and genetically engineered microorganisms*. Molecular Biotechnology, 2001. 17(3): p. 249-260.
184. Katz, E., Lioubashevski, O., and Willner, I., *Magnetic field effects on bioelectrocatalytic reactions of surface-confined enzyme systems: Enhanced performance of biofuel cells*. Journal of the American Chemical Society, 2005. 127(11): p. 3979-3988.

185. Pollard, D., Truppo, M., Pollard, J., Chen, C.-y., and Moore, J., *Effective synthesis of (s)-3,5-bis(trifluoromethyl)phenyl ethanol by asymmetric enzymatic reduction*. Tetrahedron: Asymmetry, 2006. 17(4): p. 554-559.
186. Grunwald, J., Wirz, B., Scollar, M.P., and Klivanov, A.M., *Asymmetric oxidoreductions catalyzed by alcohol dehydrogenase in organic solvents*. Journal of the American Chemical Society, 1986. 108(21): p. 6732-6734.
187. Lortie, R., Villaume, I., Legoy, M.D., and Thomas, D., *Enzymatic production of long-chain aldehydes in a fixed bed reactor using organic solvents and cofactor regeneration*. Biotechnology and Bioengineering, 1989. 33(2): p. 229-232.
188. Mano, N., Mao, F., and Heller, A., *Characteristics of a miniature compartmentless glucose-o<sub>2</sub> biofuel cell and its operation in a living plant*. Journal of the American Chemical Society, 2003. 125(21): p. 6588-6594.
189. Okuda, K., Urabe, I., and Okada, H., *Synthesis of poly(ethylene glycol)-bound nadp by selective modification at the 6-amino group of nadp*. European Journal of Biochemistry, 1985. 151(1): p. 33-38.
190. Zayats, M., Katz, E., Baron, R., and Willner, I., *Reconstitution of apo-glucose dehydrogenase on pyrroloquinoline quinone-functionalized au nanoparticles yields an electrically contacted biocatalyst*. Journal of the American Chemical Society, 2005. 127(35): p. 12400-12406.
191. Narayanan, R., Zhu, G., and Wang, P., *Stabilization of interface-binding chloroperoxidase for interfacial biotransformation*. Journal of Biotechnology, 2007. 128(1): p. 86-92.
192. Adams, M.J., et al., *Structure-function relationships in lactate dehydrogenase*. Proceedings of the National Academy of Sciences of the United States of America, 1973. 70(7): p. 1968-1972.
193. Zappelli, P., Rossodivita, A., Prosperi, G., Pappa, R., and Re, L., *New coenzymically-active soluble and insoluble macromolecular nad<sup>+</sup> derivatives*. European Journal of Biochemistry, 1976. 62(1): p. 211-215.
194. Bückmann, A. and Carrea, G., *Synthesis and application of water-soluble macromolecular derivatives of the redox coenzymes nad(h), nadp(h) and fad, in Vertebrate cell culture ii and enzyme technology*. 1989. p. 97-152.
195. Pullman, M.E., Colowick, S.P., and Kaplan, N.O., *Comparison of diphosphopyridine nucleotide with its deaminated derivative in various enzyme systems*. Journal of Biological Chemistry, 1952. 194(2): p. 593-602.

196. Lowe, C.R. and Mosbach, K., *Synthesis of adenine-substituted derivatives of nadp and their potential as active coenzymes and affinity adsorbents*. European Journal of Biochemistry, 1974. 49(3): p. 511-520.
197. Sakamoto, H., Nakamura, A., Urabe, I., Yamada, Y., and Okada, H., *Analysis of improvement of the synthesis of n6-(2-carboxyethyl)-nad*. Journal of Fermentation Technology, 1986. 64(6): p. 511-516.
198. Kishimoto, T., Itami, M., Yomo, T., Urabe, I., Yamada, Y., and Okada, H., *Improved methods for the preparation of n6-(2-carboxyethyl)-nad and poly(ethylene glycol)-bound nad(h)*. Journal of Fermentation and Bioengineering, 1991. 71(6): p. 447-449.
199. Schmidt, H.-L. and Grenner, G., *Coenzyme properties of nad<sup>+</sup> bound to different matrices through the amino group in the 6-position*. European Journal of Biochemistry, 1976. 67(1): p. 295-302.
200. Zappelli, P., Rossodivita, A., and Re, L., *Synthesis of coenzymically active soluble and insoluble macromolecularized nad<sup>+</sup> derivatives*. European Journal of Biochemistry, 1975. 54(2): p. 475-482.
201. Chenault, H.K. and Whitesides, G.M., *Regeneration of nicotinamide cofactors for use in organic synthesis*. Applied Biochemistry and Biotechnology, 1987. 14(2): p. 147-197.
202. Ikemi, M., Ishimatsu, Y., and Kise, S., *Sorbitol production in charged membrane bioreactor with coenzyme regeneration system: Ii. Theoretical analysis of a continuous reaction with retained and regenerated nadph*. Biotechnology and Bioengineering, 1990. 36(2): p. 155-165.
203. Rover, L., Fernandes, J.C.B., Neto, G.d.O., Kubota, L.T., Katekawa, E., and Serrano, S.H.P., *Study of nadh stability using ultraviolet-visible spectrophotometric analysis and factorial design*. Analytical Biochemistry, 1998. 260(1): p. 50-55.
204. Wu, J.T., Wu, L.H., and Knight, J.A., *Stability of nadph: Effect of various factors on the kinetics of degradation [published erratum appears in clin chem 1987 may;33(5):724]*. Clinical Chemistry, 1986. 32(2): p. 314-319.
205. Alberty, R.A., *Thermodynamics of reactions of nicotinamide adenine dinucleotide and nicotinamide adenine dinucleotide phosphate*. Archives of Biochemistry and Biophysics, 1993. 307(1): p. 8-14.

206. Ghomashchi, F., O'Hare, T., Clary, D., and Gelb, M.H., *Interfacial catalysis by phospholipase a2: Evaluation of the interfacial rate constants by steady-state isotope effect studies*. *Biochemistry*, 1991. 30(29): p. 7298-7305.
207. Yu, B.Z., Rogers, J., Nicol, G.R., Theopold, K.H., Seshadri, K., Vishweshwara, S., and Jain, M.K., *Catalytic significance of the specificity of divalent cations as  $k_s^*$  and  $k_{cat}^*$  cofactors for secreted phospholipase a2*. *Biochemistry*, 1998. 37(36): p. 12576-12587.
208. Jain, M.K., Yu, B.Z., Rogers, J., Gelb, M.H., Tsai, M.D., Hendrickson, E.K., and Hendrickson, H.S., *Interfacial catalysis by phospholipase a2: The rate-limiting step for enzymic turnover*. *Biochemistry*, 1992. 31(34): p. 7841-7847.
209. Tyrakowska, B., Verhaert, R.M.D., Hilhorst, R., and Veeger, C., *Enzyme kinetics in reversed micelles*. 1990. 187(1): p. 81-88.
210. Verhaert, R.M.D., Tyrakowska, B.C., Hilhorst, R., Schaafsma, T.J., and Veeger, C., *Enzyme kinetics in reversed micelles*. *Eur. J. Biochem.*, 1990. 187(1): p. 73-79.
211. Vogel, P.D., *Nature's design of nanomotors*. *European Journal of Pharmaceutics and Biopharmaceutics*, 2005. 60(2): p. 267-277.
212. Abrahams, J.P., Leslie, A.G.W., Lutter, R., and Walker, J.E., *Structure at 2.8 Å resolution of *f1*-atpase from bovine heart mitochondria*. *Nature*, 1994. 370(6491): p. 621-628.
213. Noji, H., Yasuda, R., Yoshida, M., and Kinosita, K., *Direct observation of the rotation of *f1*-atpase*. *Nature*, 1997. 386(6622): p. 299-302.
214. Weber, J., *Atp synthase: Subunit-subunit interactions in the stator stalk*. *Biochimica et Biophysica Acta (BBA) - Bioenergetics*, 2006. 1757(9-10): p. 1162-1170.
215. Weber, J. and Senior, A.E., *Atp synthesis driven by proton transport in *f1f0*-atp synthase*. *FEBS Letters*, 2003. 545(1): p. 61-70.
216. Adachi, K., Oiwa, K., Nishizaka, T., Furuike, S., Noji, H., Itoh, H., Yoshida, M., and Kinosita Jr, K., *Coupling of rotation and catalysis in *f1*-atpase revealed by single-molecule imaging and manipulation*. *Cell*, 2007. 130(2): p. 309-321.
217. Halling, P., *Biocatalysis in multi-phase reaction mixtures containing organic liquids*. *Biotech. Adv.*, 1987. 5: p. 47-84.

218. Asuri, P., Karajanagi, S.S., Dordick, J.S., and Kane, R.S., *Directed assembly of carbon nanotubes at liquid-liquid interfaces: Nanoscale conveyors for interfacial biocatalysis*. Journal of the American Chemical Society, 2006. 128(4): p. 1046-1047.
219. Willner, I., Basnar, B., and Willner, B., *Nanoparticle-enzyme hybrid systems for nanobiotechnology*. FEBS journal, 2007. 274(2): p. 302-309.
220. Xu, C. and Sun, S., *Monodisperse magnetic nanoparticles for biomedical applications*. Polymer International, 2007. 56(7): p. 821-826.
221. Yoshino, T., Tanaka, T., Takeyama, H., and Matsunaga, T., *Single nucleotide polymorphism genotyping of aldehyde dehydrogenase 2 gene using a single bacterial magnetic particle*. Biosensors and Bioelectronics, 2003. 18(5-6): p. 661-666.
222. Gazeau, F., Baravian, C., Bacri, J.C., Perzynski, R., and Shliomis, M.I., *Energy conversion in ferrofluids: Magnetic nanoparticles as motors or generators*. Physical Review E, 1997. 56(1): p. 614.
223. Brigger, I., Dubernet, C., and Couvreur, P., *Nanoparticles in cancer therapy and diagnosis*. Advanced Drug Delivery Reviews, 2002. 54(5): p. 631-651.
224. Cyril, A., Ulf, S., Lydie, A., Philipp, Z., Ralf, T., C, T.J., and Stefan, M., *Hybrids of silver nanoparticles with amphiphilic hyperbranched macromolecules exhibiting antimicrobial properties*. Chemical communications (Cambridge, England), 2002. 24: p. 3018.
225. Tkachenko, A.G., Xie, H., Coleman, D., Glomm, W., Ryan, J., Anderson, M.F., Franzen, S., and Feldheim, D.L., *Multifunctional gold nanoparticle-peptide complexes for nuclear targeting*. Journal of the American Chemical Society, 2003. 125(16): p. 4700-4701.
226. Narayanan, R., Wu, S., Reneker, D.H., and Wang, P., *Electrospun enzyme-carrying polyurethane nanofibers for use in biosensors*. PMSE Preprints, 2007. 97: p. 769.
227. Hamley, I.W., *Nanotechnology with soft materials*. Angewandte chemie, 2003. 42(15): p. 1692-1712.
228. Cölfen, H. and Mann, S., *Higher-order organization by mesoscale self-assembly and transformation of hybrid nanostructures*. Angewandte Chemie, 2003. 42(21): p. 2350-2365.

229. Bommel, K.J.C.v., Friggeri, A., and Shinkai, S., *Organic templates for the generation of inorganic materials*. *Angewandte Chemie*, 2003. 42(9): p. 980-999.
230. Vijayalakshmi, A., Tarunashree, Y., Baruwati, B., Manorama, S.V., Narayana, B.L., Johnson, R.E.C., and Rao, N.M., *Enzyme field effect transistor (enfet) for estimation of triglycerides using magnetic nanoparticles*. *Biosensors and Bioelectronics*, 2008. 23(11): p. 1708-1714.
231. Holligan, D.L., Gillies, G.T., and Dailey, J.P., *Magnetic guidance of ferrofluidic nanoparticles in an in vitro model of intraocular retinal repair*. *Nanotechnology*, 2003. 6: p. 661.
232. Jain, T.K., Morales, M.A., Sahoo, S.K., Leslie-Pelecky, D.L., and Labhasetwar, V., *Iron oxide nanoparticles for sustained delivery of anticancer agents*. *Molecular Pharmaceutics*, 2005. 2(3): p. 194-205.
233. Kuhn, S.J., Finch, S.K., Hallahan, D.E., and Giorgio, T.D., *Proteolytic surface functionalization enhances in vitro magnetic nanoparticle mobility through extracellular matrix*. *Nano Letters*, 2006. 6(2): p. 306-312.
234. Siffalovic, P., Majkova, E., Chitu, L., Jergel, M., Luby, S., Satka, A., and Roth, S.V., *Self-assembly of iron oxide nanoparticles studied by time-resolved grazing-incidence small-angle x-ray scattering*. *Physical Review B (Condensed Matter and Materials Physics)*, 2007. 76(19): p. 195432-8.
235. Bresme, F. and Oettel, M., *Nanoparticles at fluid interfaces*. *Journal of Physics: Condensed Matter*, 2007. 19(41): p. 413101.
236. Willner, I. and Katz, E., *Controlling chemical reactivity at solid-solution interfaces by means of hydrophobic magnetic nanoparticles*. *Langmuir*, 2006. 22(4): p. 1409-1419.
237. Karajanagi, S.S., Vertegel, A.A., Kane, R.S., and Dordick, J.S., *Structure and function of enzymes adsorbed onto single-walled carbon nanotubes*. *Langmuir*, 2004. 20(26): p. 11594-11599.
238. Koeller, K.M. and Wong, C.-H., *Enzymes for chemical synthesis*. *Nature*, 2001. 409(6817): p. 232.
239. Devaux-Basséguy, R. and Bergel, P.G.A., *Electroenzymatic processes: A clean technology alternative for highly selective synthesis?* *Journal of Chemical Technology & Biotechnology* 1997. 68(4): p. 389-396.
240. Nidetzky, B., Haltrich, D., and Kulbe, K.D., *Carry out coenzyme conversions economically*. *CHEMTECH*, 1996. 26(1): p. 31-36.



241. MacDiarmid, A.G., et al., *Electrostatically-generated nanofibers of electronic polymers*. Synthetic Metals, 2001. 119(1-3): p. 27-30.
242. Matthews, J.A., Wnek, G.E., Simpson, D.G., and Bowlin, G.L., *Electrospinning of collagen nanofibers*. Biomacromolecules, 2002. 3(2): p. 232-238.
243. Fong, H., Liu, W., Wang, C.-S., and Vaia, R.A., *Generation of electrospun fibers of nylon 6 and nylon 6-montmorillonite nanocomposite*. Polymer, 2002. 43(3): p. 775-780.
244. Shin, C. and Chase, G.G., *Water-in-oil coalescence in micro-nanofiber composite filters*. AIChE Journal, 2004. 50(2): p. 343-350.
245. Wu, L., Yuan, X., and Sheng, J., *Immobilization of cellulase in nanofibrous pva membranes by electrospinning*. Journal of Membrane Science, 2005. 250: p. 167-173.
246. Patel, A.C., Li, S., Yuan, J.-M., and Wei, Y., *In situ encapsulation of horseradish peroxidase in electrospun porous silica fibers for potential biosensor applications*. Nano Lett., 2006. 6(5): p. 1042-1046.
247. Lee, S.-W. and Belcher, A.M., *Virus-based fabrication of micro- and nanofibers using electrospinning*. Nano Lett., 2004. 4(3): p. 387-390.
248. Manesh, K.M., Santhosh, P., Gopalan, A., and Lee, K.-P., *Electrospun poly(vinylidene fluoride)/poly aminophenylboronic acid) composite nanofibrous membrane as a novel glucose sensor*. Analytical Biochemistry, 2007. 360: p. 189-195.
249. Wu, S., Ju, H.X., and Liu, Y., *Conductive mesocellular silica-carbon nanocomposite foams for immobilization, direct electrochemistry, and biosensing of proteins*. Advanced Functional Materials, 2007. 17(4): p. 585-592.
250. Lin, Y., Lu, F., Tu, Y., and Ren, Z., *Glucose biosensors based on carbon nanotube nanoelectrode ensembles*. Nano Letters, 2004. 4(2): p. 191-195.
251. Newman, J.D. and Setford, S.J., *Enzymatic biosensors*. Molecular Biotechnology, 2006. 32.
252. Distel, K.A., Zhu, G., and Wang, P., *Biocatalysis using an organic-soluble enzyme for the preparation of poly(lactic acid) in organic solvents*. Bioresource Technology, 2005. 96(5): p. 617-623.

253. Wang, P., Woodward, C.A., and Kaufman, E.N., *Poly(ethylene glycol)-modified ligninase enhances pentachlorophenol biodegradation in water-solvent mixtures*. Biotechnology and Bioengineering, 1999. 64(3): p. 290-297.
254. Veronese, F.M., *Peptide and protein pegylation: A review of problems and solutions*. Biomaterials, 2001. 22(5): p. 405-417.
255. Mori, T. and Okahata, Y., *A variety of lipid-coated glycoside hydrolases as effective glycosyl transfer catalysts in homogeneous organic solvents*. Tetrahedron Letters, 1997. 38(11): p. 1971-1974.
256. Bindhu, L.V. and Emilia Abraham, T., *Preparation and kinetic studies of surfactant-horseradish peroxidase ion paired complex in organic media*. Biochemical Engineering Journal, 2003. 15(1): p. 47-57.
257. Baszkin, A., Boissonade, M.M., Rosilio, V., Kamyshny, A., and Magdassi, S., *Adsorption of hydrophobized glucose oxidase at solution/air interface*. Journal of Colloid and Interface Science, 1997. 190(2): p. 313-317.
258. Shipovskov, S., Trofimova, D., Saprykin, E., Christenson, A., Ruzgas, T., Levashov, A.V., and Ferapontova, E.E., *Spraying enzymes in microemulsions of aot in nonpolar organic solvents for fabrication of enzyme electrodes*. Anal. Chem., 2005. 77(21): p. 7074-7079.
259. Kamyshny, A., Trofimova, D., Magdassi, S., and Levashov, A., *Native and modified glucose oxidase in reversed micelles*. Colloids and Surfaces B: Biointerfaces, 2002. 24(3-4): p. 177-183.
260. Mehta, S.K., Bhasin, K.K., Chauhan, R., and Dham, S., *Effect of temperature on critical micelle concentration and thermodynamic behavior of dodecyldimethylethylammonium bromide and dodecyltrimethylammonium chloride in aqueous media*. Colloids and Surfaces A: Physicochem. Eng. Aspects, 2005. 255: p. 153-157.
261. Wu, J.C., Chua, P.S., Chow, Y., Li, R., Carpenter, K., and Yu, H., *Extraction of candida rugosa lipase from aqueous solutions into organic solvents by forming an ion-paired complex with aot*. Journal of Chemical Technology & Biotechnology, 2006. 81(6): p. 1003-1008.
262. Wang, J., Llu, J., Chen, L., and Lu, F., *Highly selective membrane-free, mediator-free glucose biosensor*. Anal. Chem., 1994. 66: p. 3600-3603.
263. Vamvakaki, V., Tsagaraki, K., and Chaniotakis, N., *Carbon nanofiber-based glucose biosensor*. Anal. Chem., 2006. 78: p. 5538-5542.

264. Karyakin, A.A., Kotel'nikova, E.A., Lukachova, L.V., Karyakina, E.E., and Wang, J., *Optimal environment for glucose oxidase in perfluorosulfonated ionomer membranes: Improvement of first-generation biosensors*. *Anal. Chem.*, 2002. 74(7): p. 1597-1603.

## APPENDIX

### Nomenclature

Symbol	Explanation	Unit
$[..]$	Square brackets denote a concentration in moles per bulk solution volume	moles/volume
$[C]$	Concentration of cofactor at the interface	moles/volume
$[E]$	Concentration of cofactor bound active enzyme at interface	moles/volume
$[E_{inactive}]$	Concentration of inactive form of enzyme at interface	moles/volume
$D_a$	Damkohler number	
$D_L$	Diffusion coefficient for substrate to diffuse from bulk to interface	Length $s^{-1}$
$j$	Product flux per enzyme molecule	Molecules $s^{-1}$
$k_{-1}, k_3$	Dissociation rate constants for $E-S \rightarrow E+S$ and $E-P \rightarrow E+P$	$s^{-1}$
$k_1, k_3$	Association rate constants for $E + S \rightarrow E-S$ and $E + P \rightarrow E-P$	(mole fraction) $^{-1}s^{-1}$
$k_2, k_2$	Rate constants for chemical changes $E-S \rightarrow E-P$ and $E-P \rightarrow E-S$	$s^{-1}$
$K_c$	Dissociation constant for $E-C \rightarrow E + C$	Moles/volume
$k_{cats}$	Catalytic rate for enzyme at the interface	$s^{-1}$
$k_D$	Apparent rate constant for diffusion limited reactions	Length $^2 s^{-1}$
$k_f$	Mass transfer coefficient	$s^{-1}$
$k_i$	Relaxation rate for the integrated Michaelis Menten equation at the interface	$s^{-1}$
$K_{MP}$	Michaelis constant for product and enzyme at the interface	mole fraction
$K_{MS}$	Michaelis constant for substrate and enzyme at the interface	mole fraction
$X_A$	Mole fraction of species A at the interface	mole fraction